The role and expression of TFEB in contracting skeletal muscle myotubes

Diane M. Brownlee

A THESIS SUBMITTED TO THE FACULTY OF GRADUATE STUDIES IN PARTIAL FULFILLMENT OF THE REQUIREMENTS FOR THE DEGREE OF

MASTER OF SCIENCE

Graduate Program in
Biology
York University
Toronto, Ontario

October 2015

Abstract:

The maintenance of the mitochondrial pool is essential for the beneficial effects that are seen following an acute bout of contractile activity. Mitochondrial quality control consists of two pathways, mitochondrial biogenesis and mitochondrial autophagy, termed mitophagy. However, the mechanisms and activation of mitophagy in skeletal muscle remain generally elusive. Specifically, we are interested in mitophagy that occurs during or immediately following exercise in skeletal muscle. Recently, transcription factor EB (TFEB) has been identified as a key player as the master regulator of lysosomal biogenesis. To identify the unknown role that TFEB plays in mitophagy, we utilized a cell culture model of skeletal muscle myotubes. We examined the transcription and activation of TFEB and its downstream targets following acute exercise and recovery and following chronic exercise. We found that TFEB is activated following exercise and that it plays an important role in the transcription of mitophagy genes.

Acknowledgements:

There are many people I need to thank for the completion of this thesis,

To Dave, whose expertise, understanding, and patience, added considerably to my graduate experience. I appreciate his vast knowledge and skill in many areas and his assistance in writing reports. Thank you for being there to answer even the smallest question, preparing me for every step though out this process, you've been a great supervisor and a great leader.

To my friends and family, for their never ending support and encouragement throughout the length of this thesis. To my family, you have always been there for me and supported and guided me through all of my endeavors. Dommie, for being undeniably my greatest friend and role model, for never giving up on me and keeping my spirits up. Nothing can be accomplished alone and therefore I owe this success to the people who have never let me down or faltered in the confidence they held in me. You all make me stronger every day.

To my lab mates, I could not have asked for better teammates and friends to spend the last two years with. I appreciate every piece of advice, guidance and laughs over the years.

And to J.K. Rowling, whose books have guided me though every single day of my masters. Teaching me lessons of friendship and bravery and offering adventure even in the depths of cell culture.

Table of Contents

List of Tables

List of Figures

Review of Literature

Manuscript

Appendix B: Additional Data

LIST OF ABBREVIATIONS

ADP	Adenosine diphosphate
AMP	Adenosine monophosphate
AMPK	AMP-activated protein kinase
ATG	Autophagy related gene
ATP	Adenosine triphosphate
bHLH	Basic helix-loop-helix
BNIP	BCL2 and E1B 19 kDa interacting proteins
CamK	Calcium/Calmodulin-dependnt kinase
CCA	Chronic contractile activity
CLEAR	Coordinated Lysosomal Expression and Regulation
COX	Cytochrome *c* oxidase
DMEM	Dulbecco's modified eagle medium
DNA	Deoxyribonucleic acid
DRP1	Dynamin related protein 1
ERK 1/2	Extracellular-signal-regulated kinases 1 and 2
ERRα	Estrogen-related receptor alpha
ETC	Electron Transport Chain
FOXO3a	Forkhead box O3
GAA	Glucosidase, alpha; acid
GCN5L1	General control of amino acid synthesis 5-like 1
GTPase	Guanosine triphosphate
LAMP 1/2	Lysosomal associated membrane proteins 1 and 2

LC3	Microtubule-associated proteins 1A-1B light chain 3A
LIR	LC3-interacting region
LSD	Lysosomal Storage disorder
MCOLN1	Mucolipin 1
MFN1/2	Mitofusin 1/2
MIRO	Mitochondrial RHO GTPase
MiT/TFE	Microthalmia-transcription factor E
mRNA	messenger ribonucleic acid
mtDNA	mitochondrial DNA
mTORC1	mammalian target of rapamycin complex 1
NIX	Bcl2/E1B 19 kDa-interacting protein 3-like protein
NRF1	Nuclear respiratory factor 1
NUGEMP	Nuclear gene-encoded mitochondrial protein
p38 MAPK	p38 mitogen-activated protein kinase
PGC-1a	Peroxisome proliferator-activated receptor-γ coactivator-1α
PINK1	Phosphatase and tensin homolog-induced putative kinase 1
PolyQ-AR	Polyglutamine-expanded androgen receptor
RANKL	Receptor activator of nuclear factor kappa-B ligand
ROS	Reactive oxygen species
SBMA	Spinal and bulbar muscular atrophy
Tfam	Mitochondrial transcription factor-A
TFEB	Transcritpion factor EB
v-ATPase	Vacuolar-type H+ATPase

VDAC	Voltage Dependant anion channels
$\Delta\psi_m$	Mitochondrial membrane potential

REVIEW OF LITERATURE

1.0 **Mitochondrial Turnover**

Mitochondria are essential organelles responsible for aerobic respiration in eukaryotic cells. The majority of the energy that eukaryotes rely on is obtained through the use of mitochondria, thus emphasizing the importance of these dynamic organelles. Due to the requirement for aerobic respiration, mitochondria are found in high abundance in oxidative tissues such as heart, kidney, and the brain (23, 87, 125). The inner mitochondrial membrane plays host to a collection of enzyme complexes termed the electron transport chain (ETC) that are the source of adenosine triphosphate (ATP) generation (16, 125). Mitochondria play an important role, it is essential that the mitochondrial pool in cells is healthy and is maintained. This is done through two antagonistic processes, mitochondrial biogenesis and mitochondrial autophagy. Mitochondrial biogenesis is the synthesis of mitochondria whereas the opposing pathway is the degradation of damaged mitochondria through macro-autophagy, hereafter known as mitophagy. In diseases where the maintenance of the mitochondrial pool is inhibited or limited, such as in Parkinson's disease, Alzheimer's disease or Pompe disease, the regulation of mitochondrial turnover is observed to be essential for whole body health (81, 96, 103, 120). Small alterations in the functionality of the turnover pathways can have such a startling and drastic effect on the health of the cell and the organism.

1.1 **Mitochondrial Biogenesis**

Mitochondrial biogenesis is the creation of new mitochondria. The process of biogenesis involves the activation of the transcription of various nuclear genes encoding

mitochondrial proteins (NUGEMPS). Pathways that are triggered by numerous stimuli, including cell stress or environmental triggers, can activate mitochondrial biogenesis. Biogenesis pathways rely on the transcription and translation of genes encoded not only by the nuclear genome, but also by mitochondrial DNA (mtDNA). Expanding the mitochondrial network additionally augments enzymatic activity. Various stimuli can activate the cascades that will enhance the mitochondrial reticulum, and an important stimulus to note is contractile activity (39, 40). It has long been established that contractile activity induces aerobic metabolism and an increase in mitochondrial content (38, 122). The extent of the mitochondrial modifications is dependent on the type and length of contractile activity. During an acute bout of exercise, mitochondrial biogenesis will be initiated by putative signals that are activated by contractile activity such as cytosolic calcium levels, oxygen consumption, ROS production and ATP turnover (11, 40). Following the activation of these pathways, signaling cascades will commence due to the phosphorylation of kinases such as calcium /calmodulin- dependent kinase (CaMK), p38 mitogen-activated protein kinase (MAPK) and AMP-activated protein kinase (AMPK). These kinases will inaugurate the activation and induction of mitochondrial biogenesis transcription factors and co-activators. Peroxisome-proliferator activated receptor gamma co-activator (PGC-1α) is a co activator involved in the activation of the transcription of many essential mitochondrial biogenesis genes (143).

1.1.1 **Regulation of biogenesis: PGC-1α**

Mitochondrial biogenesis is dependent on the coordination of the expression of many nuclear and mitochondrial-encoded genes. PGC-1α is known as the master regulator of mitochondrial biogenesis, a member of the peroxisome proliferator activated receptor (PPAR) family (92, 144). First discovered for its transcriptional activation with thermogenesis, PGC-1α and its family of transcriptional co-activators are responsible for the assembly of macrocomplexes of the transcriptional machinery (92). PGC-1α co-activates nuclear respiratory factors 1 and 2 (NRF-1 and NRF-2), which can upregulate the transcription of mitochondrial transcription factor A (TFAM) (91, 136). TFAM plays an imperative role in mitochondrial biogenesis by regulating mitochondrial-encoded genes including the 13 subunits of the respiratory chain (48, 49). Several studies have examined the importance of PGC-1α in response to various external stimuli. Initially, PGC-1α was investigated with its relationship to mitochondrial biogenesis in response to cold (92). In skeletal muscles where PGC-1α mRNA was undetectable at ambient temperatures, cold exposure for 12 hours induced PGC-1α mRNA (77, 92). Furthermore, upregulation of PGC-1α is paralleled by an increase in ATP-synthase proteins and cytochrome-c oxidase subunits (92, 146). Following an acute bout of exercise, not only was PGC-1α transcription was significantly elevated, but downstream targets of PGC-1α were also increased significantly (2, 11, 77, 131). Early *in vitro* studies investigating the overexpression of PGC-1α found a dramatic 2-3 fold amplification in subunits of the respiratory chain components COX IV, COX II and cytochrome c, in addition to an

enhancement in respiratory capabilities (5, 143). Lin et al. explored the effects of PGC-1α overexpression by utilizing PGC-1α transgenic mice and showed an increased drive for oxidative metabolism and mitochondrial gene expression in skeletal muscles (63).

Specifically when discussing PGC-1α induction following contractile activity it is important to understand the mechanism in which the co-activator is stimulated (5). AMPK, an energy-sensitive kinase, in activated following the hydrolysis of ATP and the formation of AMP by myokinases resulting in AMP accumulation in cytosol. Increased levels of AMP will activate AMPK upstream of PGC-1α. Interestingly, AMPK acts on both the biogenesis and autophagy pathways in order to restore energy levels in the cell (64, 99, 102). These pathways have been demonstrated using *in vitro* methods that provided evidence that following contractile activity, the chemical activation of AMPK will cause PGC-1α induction (42). This important pathway drives the increases in mitochondrial quality through the activation of PGC-1α following exercise, or other various cellular stresses.

1.2 **Mitophagy**

Efficient removal of damaged or dysfunctional mitochondria in response to environmental or molecular cues is essential for maintaining an overall healthy pool of mitochondria. This mechanism is initiated by the selection of dysfunctional mitochondrion, differentiated by their decrease in membrane potential ($\Delta\Psi$) and an increase in reactive oxygen species (ROS) production (Fig. 1) (45, 72, 82, 116). There are

many known stimuli that can trigger this process of mitophagy, including hypoxia (147), ischemia (57, 115) and mtDNA damage (58). Mitophagy plays a crucial role in the health of the cell. When the process is dysfunctional or impaired, issues can result linked to apoptosis, cancer and many muscular and neurodegenerative disorders (3, 10, 29, 72). Until recently, autophagic processes were considered nonselective degradation pathway, however, recent studies have revealed that autophagy can selectively target and degrade nonfunctional organelles in the cell (79). Evidence specifically for mitochondrial targeting for degradation was demonstrated by Schweers et al. (2007) (105). Authors provided novel evidence of mitochondrial flagging for degradation when they observed extreme loss of erythroid cell mitochondria during the process of cell maturation (105). Physiological stimuli, such as cold and dietary restriction, have been shown to enhance mitochondrial turnover rate (3, 66, 87, 92). Following caloric restriction, mitochondria have been demonstrated to have a decreased membrane potential in addition to decreased oxygen consumption activating mitochondrial turnover (3, 66, 139). It is essential to recall that mitophagy should not be considered a catabolic process under the effects of stressors. Mitophagy and mitochondrial biogenesis can be stimulated by the same environmental effects, which in turn induces "quality control" (3). If the damaged mitochondria are not sequestered and degraded it is proposed that the organelle will produce damaging ROS and cause deleterious effects to the mtDNA, as well and the surrounding cell organelles (103).

1.2.1 **Mitophagy pathways**

When a mitochondrion is damaged, it releases warning signals that alert the cell that the organelle is no longer functioning at its optimal state. One of the major pathways in mitophagy is PINK1/Parkin pathway; PTEN-induced putative kinase 1 (PINK1) and parkin E3 ubiquitin ligase work together to flag and target mitochondria for degradation. Extensive work has looked into the mechanisms of this important mitophagy pathway elucidating the way that PINK1 and parkin act to mediate the removal of the mitochondrion (32, 36, 80, 140). It has been proposed that PINK1 acts as a stress sensor. In normal functioning mitochondria, PINK1 will be imported and rapidly degraded by proteases (127, 137). However, in unhealthy mitochondria, the import system is compromised due to the depolarization of the organelle and PINK1 cannot be imported. PINK1 will then accumulate on the outer mitochondrial membrane, where it can be activated and stabilized by phosphorylation on multiple sites (Fig.1) (82, 137). Recent publications have strengthened this fact by demonstrating that one of the phosphorylation sites of PINK1 that activate and stabilize it is Thr257, which in turn, allows it to phosphorylate and activate the E3 ubiquitin ligase parkin on Ser65 (53). In addition to phosphorylating parkin, PINK1 will also phosphorylate and activate ubiquitin which can act to activate parkin as well (47, 55). Consequent to the activation of parkin, it has been demonstrated that parkin will go on to ubiquitinate various outer mitochondrial membrane proteins, such as Voltage-dependent anion channels (VDAC), Mitofusin 1/2 (MFN1/2) (123), Mitochondrial RHO GTPase (Miro) (65), 70 kDa mitochondrial outer

membrane protein (TOM70) (81) and dynamin related protein-1 (DRP1) (138). Once these outer mitochondrial proteins are flagged, adaptor protein p62 can commence to tag the mitochondrion for sequestration and degradation. Following the flagging of the mitochondrion, optineurin, an autophagy receptor that contains an ubiquitin binding domain and an LC3-interacting region (LIR) will be activated and will facilitate the sequestering of damaged mitochondria (141). An autophagic vesicle will be formed following the lipidation of Microtubule-associated protein 1 light chain 3 (LC3I) to LC3II with the aid of several autophagy related genes (ATG) (83, 124). LC3II can commence the formation of the autophagosomal vesicle by binding with adaptor proteins, such as, p62, and guide the vesicle around the organelle. Once engulfed completely, the autophagosome will be transported to the lysosome where the autophagosome and the lysosome will fuse with the aid of lysosomal associated membrane proteins 1 and 2 (LAMP1 and LAMP2) (21, 25). The lysosome can then degrade the contents of the autophagosome and the resulting amino acids can be recycled by the cell and used to create new organelles and proteins.

Many pathways regulate mitochondrial clearance in order to ensure the effective removal of dysfunctional organelles. An additional pathway involved in the selective removal of mitochondria is BNIP and NIX selective flagging. BCL-2 related protein, NIX, and BNIP3 will localize to damaged mitochondria to tag the organelle for degradation (36, 140, 147). Initially only associated with cell death and apoptosis, these families of proteins also associate with LC3 family proteins to aid in the formation of

autophagosomal membrane (15, 86). Studies have demonstrated that NIX contains an LIR linear binding sequence, solidifying the suggestions that NIX can selectively flag mitochondria for degradation and aid in the autophagosomal recruitment (51, 115). In addition to the binding sequence, Novark et al. explored the relation of NIX and LC3 in cells treated with the mitochondrial uncoupler CCCP, and they discovered an enhanced co-localization of NIX and LC3 (86). This ability to bind to LC3 in combination with evidence of binding to damaged mitochondria plays an important role in identifying and flagging mitochondria for degradation.

1.2.2 **Mitophagy signaling**

Mitophagy can be initiated as a result of many cellular stressors that can activate pathways resulting in mitochondrial clearance to maintain the health of the cell. There are many stress sensors present in the cell that will activate cellular clearance pathways (139). It is well established that mitochondria are a main producer for ROS as a by product of respiration in the cells, it is also well known that ROS have the capability to cause oxidative damage to mitochondrial DNA, and potentially the nuclear DNA if the damaged organelle is not degraded (117, 145). Furthermore, if respiration is damaged or inhibited, ROS production of the mitochondrion will increase (130). Additionally, the decreased membrane potential of the mitochondrion will inhibit import of proteins into the organelle (59). Following inhibition of oxidative phosphorylation (OXPHOS) and dissipation of the mitochondrial membrane potential with CCCP, this treatment was demonstrated to inhibit nutrient sensing kinase mammalian target of rapamycin complex

1 (mTORC1) and initiate mitophagy (46, 59). Furthermore, AMPK has been identified as an inhibitor of mTORC1 to activate mitophagy pathways (50). Authors discovered that, following starvation, AMPK will inhibit mTORC1 leading to a UNC-51-like kinase 1 (Ulk1)-AMPK interaction. This interaction will activate Ulk1 through phosphorylation and lead to induction of various mitophagy and autophagy pathways (7, 50, 62).

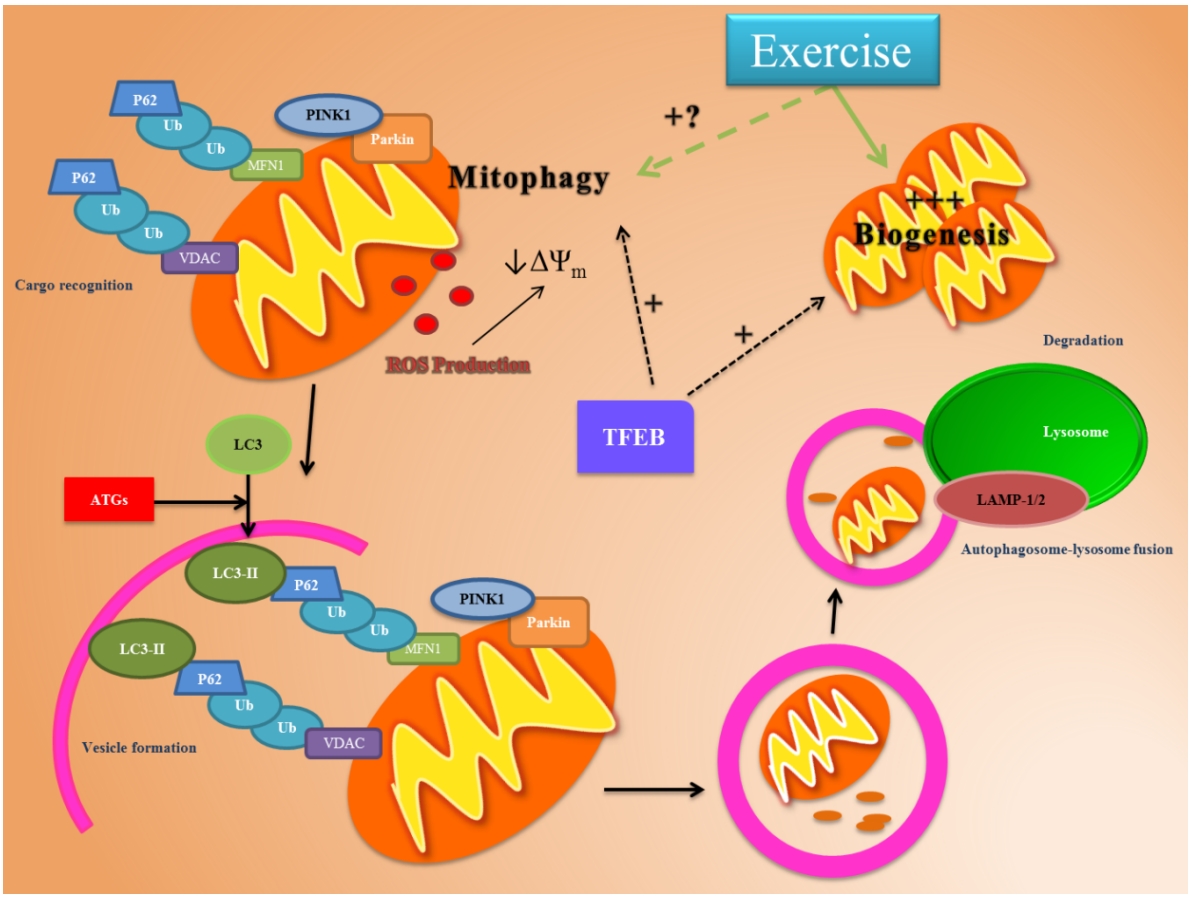

Figure 1: Mitochondria are an invaluable and essential organelle. In order to ensure an optimal quality of the mitochondria is maintained, cellular quality control pathways are activated to remove damaged or dysfunctional organelles. This process is termed mitophagy. When a mitochondrion is dysfunctional, the electron transport chain (ETC) will produce an excess of reactive oxygen species (ROS). Increased levels of ROS will contribute to oxidative damage of the mitochondrial DNA (mtDNA) and decrease the membrane potential ($\Delta\Psi_m$). Normal functioning mitochondria will import PINK1 into the inner membrane where it is cleaved, yet when the membrane potential is compromised PINK1 is unable to be imported and accumulates on the outer mitochondrial membrane (OMM). Membrane bound PINK1 recruits and activates Parkin, an E3-ubiquitin ligase, to the OMM. Activated Parkin will flag the mitochondrion for degradation by ubiquiting OMM proteins such as MFN1 and VDAC. Following ubiquitination, adapter protein p62 will bind to ubiquitin while LC3-I is lipidated by various autophagy related genes (ATG) into LC3-II. LC3-II binds to p62 to aid in the elongation of the pre-autophagosomal membrane. The double membrane vesicle will be formed around the targeted mitochondria. Once fully engulfed, it will be transported to the lysosome where the autophagosome and lysosome will fuse, assisted by lysosomal membrane proteins 1 and 2 (LAMP1 and LAMP2), and the contents can be degraded. Transcription factor EB (TFEB), known as the master regulator of lysosomal biogenesis is involved in the transcription of many genes involved in steps of mitophagy. TFEB is important for organelle targeting, vesicle formation, autophagosomal and lysosomal fusion and cargo degradation. Additionally, exercise has been established to activate the process of mitochondrial biogenesis, however the activation of mitophagy following exercise has not been fully investigated.

1.2.3 **Pathology of dysfunctional mitophagy**

Pathologies characterized by dysfunctional aggregates due to improper mitophagy have long been established in the literature. Small alterations in any of the essential mitophagy proteins could lead to harmful and detrimental results. Parkinson's disease patients have been recently demonstrated to be linked to irregular function or absence of PINK1 and parkin (72, 80, 82, 140). Mutations in Park2, the gene encoding parkin caused a significant increase in early onset Parkinson's disease. Patients that possessed a mutation in park2 demonstrated swollen, damaged and dysfunctional mitochondria along with muscle loss revealing that parkin recruitment to the damaged mitochondria is essential for the maintenance of the mitochondrial pool and muscle health. Vincow et al., explored the parkin-PINK1 pathway by selectively knocking out parkin and PINK1 separately in Drosophila and measuring basal mitophagy levels. Though mitophagy levels were not inhibited as greatly as in ATG7 knockout Drosophila, they were significantly impaired compared to levels of control flies (135).

Another neurodegenerative disease that has been related to dysfunctions in mitophagy pathways is Alzheimer's disease. This neurodegenerative condition is characterized by the extracellular deposition of amyloid β (Aβ). This accumulation over time leads to loss of synapses and neuronal death in the brain (41). Following this increase in Aβ deposition, the fragments disrupt mitochondrial activity leading to the characteristic features found in Alzheimer's disease patients (24). Studies have unveiled the underlying mechanisms of these dysfunctional mitochondria utilizing a transgenic

mouse model overexpressing the mutant amyloid precursor. These authors found that, over time Aβ would build up in the mitochondria and caused a decrease in mitochondrial oxygen consumption and enzymatic activity of ETC complexes III and IV (12). Manczak et al., investigated further and found the mitochondria to produce significantly more ROS compared to the wild type controls (69). These studies, and many more, have emphasized the significance of mitochondrial functionality in healthy cells, and pinpoint targets for therapeutic interventions.

An additional noteworthy disease that causes devastating effects due to defective mitophagy is Huntington's disease. This disease is caused by a CAG repeat expansion in the huntington protein which leads to accumulation of intercellular protein aggregates. Recent evidence has shown that the mitochondria impairment caused with mutant huntingtons protein plays a key part in the pathology of the disease (8). It has been demonstrated that a mutation in the huntingtons protein will cause inhibition of PGC-1α transcription which in turn, causes a decrease in NUGEMPs leading to decreased mitochondrial function and neurodegeneration (14, 17). Huntingtons mice cross bred with PGC-1α KO mice showed an increase in neurodegeneration compared to huntingtons and control mice (20, 121). It is important to note that inducing the expression of PGC-1α has the ability to partially reverse the toxic effects caused by mutant huntingtons (129). Moreover, the importance of PGC-1α induction and its role in mitochondrial health are demonstrated to play an essential part in the mechanism driving this detrimental disease.

These examples of impaired autophagy and dysfunctional mitochondria prove the balance that is required for the maintenance of our cells.

1.3 **Exercise and mitophagy**

The beneficial health effects of exercise have been well documented in the literature. When engaging in physical, exercise many molecular signaling pathways are activated that will result in increases in mitochondrial content and quality. During contractile activity it is well known that mitochondria release ROS that can initiate mitochondrial turnover, mitochondrial biogenesis and mitophagy (4). If dysfunctional mitochondria are not removed efficiently via mitophagy, an accumulation of harmful organelles will result (54). Recent studies have demonstrated that mitophagy is initiated following an acute bout of exercise (5, 34, 37, 43, 44, 134). Studies from our laboratory and others, indicate exercise-induced increases in mitochondrially-localized mitophagy markers, p62, parkin and ubiquitin (43), demonstrating the initiation of mitophagy following exercise (133, 134). Furthermore, the impact of exercise on mitophagy activation can be observed following a recovery period. He et al. (2012), demonstrated a significant increase in GFP-LC3 puncta in both cardiac and skeletal muscles following a recovery period of 30 minutes to 110 minutes (37). This effect was mimicked by starvation, a well established autophagy stimulus (29, 37, 107, 110). Jamart et al. (2013) additionally investigated the additive effect of endurance exercise and starvation on autophagy. Following exercise, they discovered that in combination with starvation there was a greater initiation of autophagy markers LC3-II and p62 in the fasted and exercised

mice than mice in the exercised or nutrient deprived treatment groups alone (44). Additionally, fasted and exercised mice demonstrated and increase in pathways that are activated with exercise, such as an increase in phosphorylated form of p38 MAP kinase. However, there are many studies that emphasized essential pathways with mandatory players for the beneficial effects of exercise. Vainshtein et al. (2014) presented studies that observed that PGC-1α is required for the phenotypic adaptations and substrate utilization following exercise. PGC-1α is required for mitochondrial biogenesis, angiogenesis and metabolic adaptations following a bout of exercise (134). Furthermore, Grumati et al. determined that collagen VI deficient mice cannot achieve the beneficial adaptations of exercise due to their dystrophic phenotype. Interestingly, they indicated that the phenotype in combination with exercise caused detrimental effects to autophagy flux resulting in more muscle wasting and apoptosis (33, 34). In contrast, prolonged muscle disuse, such as denervation or prolonged inactivity, will also initiate mitophagy pathways. Denervation-induced mitophagy is marked by increases in mitochondrially-localized p62, LC3-II, parkin and ubiquitin (133). Recall, that all these markers are essential steps in the selective degradation process.

1.3.1 **Muscle cell culture model of exercise**

C2C12 cells are a murine muscle cell line that has been used for a wide-range of skeletal muscles studies, since differentiated myotubes have contractile elements that are found in skeletal muscle. When stimulated, C2C12 myotubes contract and can demonstrate similar adaptations to those found in exercising skeletal muscle (1, 30, 84).

Following electric pulse stimulation (EPS) it was shown that the resulting biochemical response was comparable to that of *in vivo* stimulation. In terms of excitation-induced contractile activity, C2C12 cells demonstrated comparable adaptations resulting in sarcomere formation, activation of kinases such as AMP kinase and MAP kinase cascades, and improved insulin responses (84) (30) (9). Furthermore, transcriptional activation that can be observed following acute or repeated bouts of exercise have been replicated in myotubes with EPS (9). Following contractile activity, comparable results to those observed in exercised mice were seen in the induction of mitochondrial regulators such as mitochondrial transcription factor A (TFAM), PGC-1α, nuclear respiratory factor 2a (NRF2) and estrogen-related receptor α (ERRα) (9, 89). Previous work from our laboratory has also demonstrated that this method of *in vitro* stimulation is successful in activating mitochondrial biogenesis by demonstrating an increased enzymatic activity of cytochrome oxidase (COX) and an increase in mitochondrial markers, TFAM and COXIV (11, 78, 131). Therefore the use of C2C12 myotubes as an *in vitro* method to examine the effects of contractile activity on skeletal muscle has proven to be invaluable, and comparable to the effects that can be seen following exercise.

2.0 **TFEB**

2.1 **Role of TFEB**

Microthalmia-transcription factor E (MiT/TFE) is a basic helix-loop-helix (bHLH) transcriptional subfamily of proteins known to bind to E-box sequences. This E-box binding motif is similar to that of the Coordinated Lysosomal Expression and

Regulation (CLEAR) consensus sequence (104). The MiT/TFE transcription factor subfamily contains four members that control various lysosomal genes in addition to the other regulatory pathways they play a role in, including MITF, TFE3, TFEB and TFEC (98, 104). Transcription factor EB (TFEB) is known as the master regulator of lysosomal biogenesis. The activation and role of TFEB are essential for the transcription of many downstream targets involved in cargo recognition, autophagosome formation, autophagosomal and lysosomal fusion and cargo degradation (112). TFEB specifically activates autophagy genes by upregulating the transcription of genes belonging to the CLEAR network genes that also regulate the process of autophagy (112). Members of the CLEAR network that are directly targeted by TFEB fall into five categories, including lysosomal hydrolases and accessory proteins, lysosomal membrane, lysosomal acidification, non-lysosomal proteins involved in lysosomal biogenesis and autophagy (88). Inactive TFEB is kept phosphorylated and sequestered in the cytosol under normal nutrient conditions (Fig. 2). However, following low nutrient conditions or cellular stress, TFEB can be dephosphorylated into its active form and translocated to the nucleus where it will upregulate these crucial genes required for lysosomal biogenesis. One interesting point is that the important genes regulated by TFEB do not significantly overlap with the genes regulated by FOXO3a, suggesting that they act in parallel to regulate autophagy pathways (101, 107).

The protective and beneficial role that TFEB plays in regulating cell autophagy has been demonstrated in many studies. Adenoviral overexpression of TFEB in mice

caused protection against obesity and diabetes (111). Interestingly overexpression also allowed the mice to utilize their fat more effectively. Furthermore, the authors found that when knocking out PGC-1α, the effects of the overexpression of TFEB were inhibited. This emphasized the connection between the two transcriptional regulators through the autoregulatory feedback loop controlling PGC-1α and TFEB (67, 98, 111).

2.1.1 **Targets of TFEB**

The role of TFEB in lysosomal and autophagosomal regulation has been demonstrated to be well conserved throughout evolution. Authors have investigated the relationship between TFEB and its *C. Elegans* orthologue HLH-30 and discovered that this gene shares many of the essential roles that TFEB plays in mammals (28, 61). Furthermore, TFEB has also been shown to be conserved in *Drosophila* models (35). To date, more than 400 genes have been identified as direct targets of TFEB. Following TFEB activation through a starvation-induced autoregulatory feedback loop, multiple genes were demonstrated to be upregulated by TFEB. These were involved in ATPase pumps, proteases, lipid metabolism, membrane proteins, fusion proteins, lysosomal membrane proteins, and autophagy proteins (88, 111). Genes such as Cathepsin D, LAMP1, p62 where all shown to significantly increase with TFEB activation (104, 111, 113). The activation of TFEB has been actively investigated following starvation. Following 24 hours of starvation, TFEB mRNA levels were significantly increased in the liver, muscle and kidney (111) (106). Moreover, TFEB overexpression exhibited beneficial effects through regulation of lipid catabolism under high fat diet condition, as

the lipid content of muscles and body weight were both rescued by the effects of TFEB overexpression. The contrary was seen with a TFEB knockout model (111).

An essential gene that is regulated by TFEB activation is the mitochondrial biogenesis regulator PGC-1α. Following starvation, PGC-1α luciferase activity was increased significantly in addition to the increase seen with TFEB dose overexpression (111). Similar results have been exhibited with denervation-induced mitophagy, as a correlated increase in both PGC-1α and TFEB was observed following denervation (133). Likewise, recent studies have discovered GCN5-like protein 1 (GCN5L1), the controls both mitochondrial biogenesis and degradation through the interdependent regulation of both TFEB and PGC-1α (106). The investigators extensively demonstrated the role of GCN5L1 by investigating a GCN5L1 knockout model and observing that both TFEB and PGC-1α expression was increased, along with their downstream targets (106). However, when the GCN5L1 knockout model was paired with either silenced TFEB or PGC-1α, the expression of both TFEB and PGC-1α was also decreased, indicating that the two transcriptional proteins play a role in the regulation of each other. These results show that there is a link between the two master regulators of opposing processes, mitochondrial biogenesis and lysosomal biogenesis, emphasizing the quality control mechanisms that are required in stress responses.

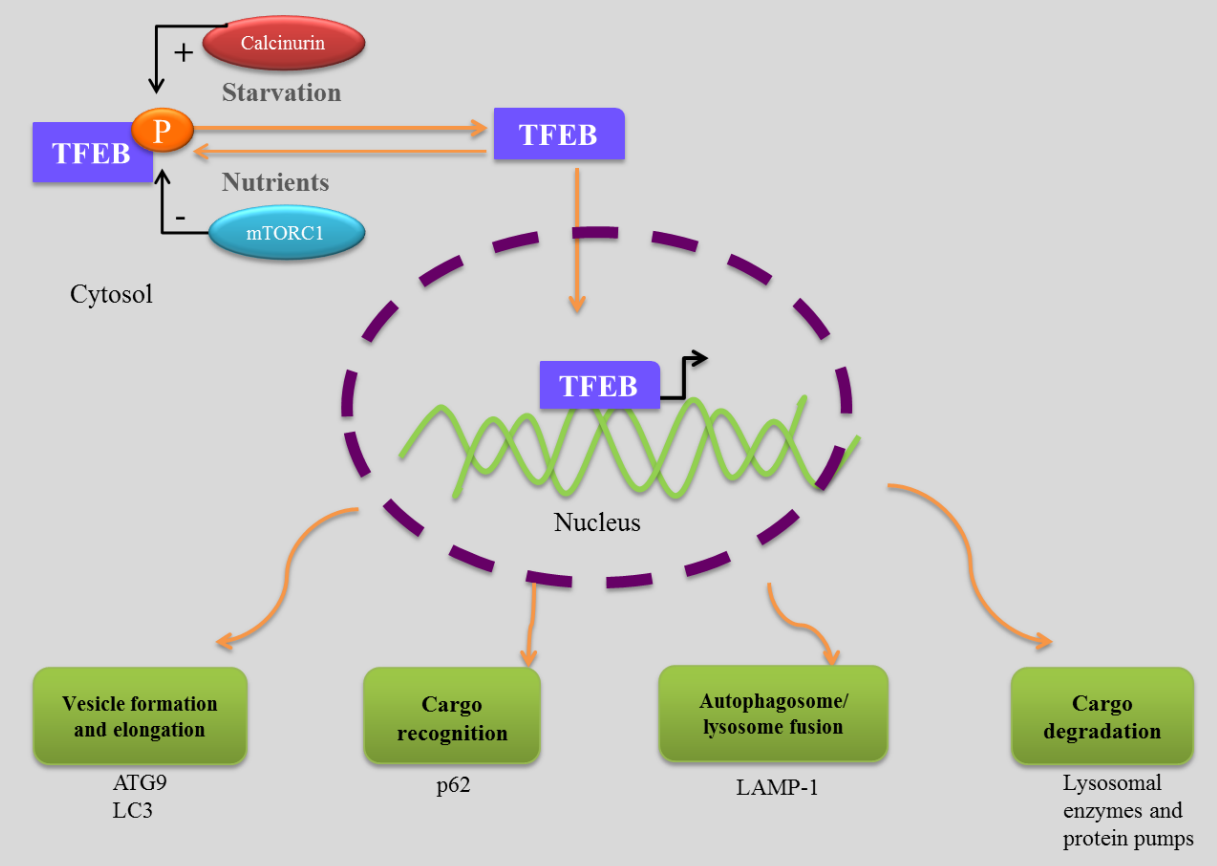

Figure 2 : Transcription factor EB (TFEB) is known as the master regulator of lysosomal biogenesis. Under normal cellular conditions, TFEB is sequestered in the cytosol and inactive via phosphorylation by ERK2 or mTORC1. However, following conditions of low nutrients or cellular stress, mTORC1 and ERK2 release their inhibition on TFEB and it is dephosphorylated into its active form by calcinurin. TFEB translocations to the nucleus where it can upregulate many essential genes involved In autophagy. These include but are not limited to genes involved in vesicle formation and elongation, cargo recognition, autophagosomal and lysosomal fusion and cargo degradation.

2.2 **Activation and regulation of TFEB**

In order to completely understand a transcription factor it first is important to understand how it is regulated, and previously mentioned investigations have examined the external stimuli that can activate TFEB. Studies have shown that stimuli such as

starvation is one of the main activators of TFEB (75, 105, 109). It is now well known that TFEB is regulated through protein phosphorylation that regulates its localization in the cell. When inactive, the transcription factor will be phosphorylated and kept localized in the cytosol. However following activation through dephosphorylation, TFEB will be translocated to the nucleus. Once translocated, TFEB will be capable of upregulating a plethora of autophagy and lysosomal genes (Fig. 2). This, in turn, will increase the ability of the cell to respond to the need for degradation.

2.2.1 **Activators and inhibitors**

TFEB is a target of mTORC1, a nutrient sensitive kinase and the key negative regulator of TFEB. Considering that mTORC1 is deactivated following a bout of starvation, mTORC1 would no longer be able to phosphorylate and inhibit the activation of TFEB (109, 114). Once released of the selective inhibition of this nutrient sensitive kinase, TFEB can be dephosphorylated by calcineurin and it can translocate to the nucleus (75). Studies have solidified these mechanisms for TFEB deactivation by mTORC1. By inhibiting mTORC1 activity with various inhibitors such as, PP242 or Torin 1, researchers confirmed that mTORC1 had a inhibiting effect on the activation of TFEB (71, 149). Following inhibition of mTORC1 autophagy flux was significantly increased following starvation (149). mTORC1, a growth regulator, responds to amino acid levels in the cytosol. When amino acids are released from the lysosome they activate Rag GTPases. Rag proteins interact with a complex that contains MAPSP1, ROBLD3 and c11orf59, combined in a complex which is defined as Ragulator (100). The Rag-

Ragulator complex in turn will promote the translocation of mTORC1 to the lysosomal surface where it will be activated. This complete complex is sufficient to regulate the starvation-induced activation of TFEB (71, 114, 150). Lysosomal membrane proteins regulate the interactions of the lysosome with other cellular structures. One of these is the vacuolar H^+-ATPase (v-ATPase) complex which is also involved in lysosomal acidification (88, 104). TFEB is recruited to the lysosome by the Rag complex and phosphorylated by the mTORC1 complex on Ser211 and Ser142 (71). Phosphorylated TFEB will bind with 14-3-3 protein that will prevent its nuclear translocation (71, 97). However, mTORC1 is not the only kinase involved in the regulation of TFEB, as extracellular signal-regulated kinase (ERK)2 and PKCβ are active in the regulation of the transcription factor (27, 112). ERK2 plays a similar role as mTORC1 and phosphorylates TFEB on Ser142. Furthermore, PKCβ acts in osteoclasts and is activated by nuclear factor κ-B ligand (RANKL), which is an important regulator of differentiation in osteoclasts. It acts to enhance transcriptional activity of TFEB through the phosphorylation of three serine residues (27). Recent studies have also indicated ZKSCAN3 as a regulator or TFEB activity. Studies showed that the silencing of ZKSCAN3 induced TFEB activity and the transcription of its downstream targets in addition to autophagic flux. The mechanisms of this inhibition of TFEB through ZKSCAN3 activation remains to be investigated further (18).

Though studies have thoroughly investigated the inhibition of TFEB, pathways involved in TFEB activation and translocation to the nucleus have only recently been

studied. Mendia et at., discovered that the two serine sites involved in the inhibition of TFEB activity interact with calcineurin (73, 75). Additionally, energy-demanding states such as starvation and physical exercise promote TFEB translocation, which was diminished with the inhibition of calcineurin, indicating that TFEB activity is mediated by calcineurin. Furthermore, inhibition of mTORC1 in cells that have calcineurin silenced had significantly decreased TFEB translocation. Authors have also investigated the role of lysosomal Ca^{2+} release through mucolipin 1 (MCOLN1) and the activation of TFEB, and found that lysosomal calcium signaling plays an essential role in the activation of TFEB (75, 128). This provides novel insight into the regulation and activation of TFEB, and in turn, the regulation of lysosomal biogenesis and autophagy.

2.2.2 **TFEB and exercise**

The activation of TFEB following exercise has been scarcely investigated, but considering the well-documented activation of this protein following low nutrient condition and calcium increase, it would be logical to speculate that TFEB would be activated following exercise. Calcium levels are known to increase following acute contractile activity, and this signaling mechanism is essential for mitochondrial biogenesis (13, 70, 148). In combination with what is known about the pathways activated with exercise and what we appreciate about the activation of TFEB, it is reasonable to surmise that TFEB is activated with exercise. Recently, a study by Mendia et al. has investigated the role of TFEB following a bout of exercise (75). The authors investigated what signaling mechanisms are acting on TFEB to initiate its activation and

translocation following exercise. The investigators observed TFEB translocation to the nucleus following one bout of exhaustive exercise, and this effect was abolished with the inhibition of calcineurin (75). This is supported by the literature, it has been well documented that calcineurin activity is known to increase following exercise (68, 142). This knowledge that TFEB translocation can be activated by exercise is important in therapeutic studies, as well as to expand the network of knowledge about this incredible transcription factor. However, very little else is known about TFEB activation following exercise.

2.3 **Role of TFEB in lysosomal therapies**

Lysosomal storage disorders (LSD) are a collection of diseases that are characterized by the accumulation of waste products that cannot be degraded by the lysosomes. Investigation of the therapeutic approach for these diseases has been a growing problem due to the increasing prevalence of the diseases. One of these detrimental diseases, Pompe disease, is a metabolic myopathy caused by a deficiency in acid alpha-glucosidase (GAA). This enzyme is responsible for the breakdown of glycogen to glucose in the lysosomes. Patients with Pompe disease have an accumulation of glycogen in the lysosomes (56, 90). Furthermore, this build up of autophagic byproducts collect in skeletal muscle fibers causing hypertrophy (94, 95). Recent therapies for these storage disorder diseases involve enzyme replacement therapy (ERT), but a major issue in such diseases is that the therapy cannot reach the target tissues such as skeletal muscles (60, 132). The resistance that skeletal muscle has to ERT has been

speculated to be due to the mass of the tissue, the low density of receptors responsible for the uptake of GAA, and poor trafficking of GAA to the lysosomes inside the muscle tissue (6, 52, 93). Due to the impact that TFEB has had, the researchers sought to investigate its role as a therapeutic target for Pompe disease (74, 120). Authors have found that *in vitro* and *in vivo* TFEB induction was sufficient in inducing exocytosis driven lysosomal clearance that would improve the aggregation accumulation that is the driving muscular issue in Pompe disease (26, 120). These investigations of the therapeutic potential of TFEB in Pompe disease are novel and require more investigation before being applied to patients.

Recent research involving TFEB has begun to look at more beneficial effects that the induction of the transcription factor can have. Studies have investigated Huntington's disease in relation to TFEB. In combination with PGC-1α, a transcriptional co-activator that is inhibited by mutant huntington protein, these two transcriptional regulators can induce the removal of aggregates (129). The PGC-1α-induced induction of TFEB can eradicate protein aggregates in the brain of Huntington diseased mice (31, 111, 119, 129). This pathway is critical for understanding therapeutics for this disease. It is essential to note that PGC-1α activation of TFEB promotes protostasis, causing a balance between the pathways regulated by these transcriptional regulators (119).

The important role of TFEB is emphasized in the increased examination of TFEB as a therapeutic target. Another neurodegenerative disease that has been investigated with TFEB regulation is spinal and bulbar muscular atrophy (SBMA). SBMA is caused by a

polygluatamine expansion of the androgen receptor gene product (polyQ-AR), which will result in a complete loss or alteration of protein function (22, 126). PolyQ-AR reduces protein turnover and autophagic flux in motor neurons (19). Furthermore, when investigating autophagy regulation in neurons, it was found that AR physically interacts with and co-activates TFEB, and in SBMA mice the activity of TFEB is inhibited by mutant AR (19, 118). This gives novel information regarding the large impact that TFEB has on the transcription of autophagy proteins through protein-protein interactions and activation. AR function is not completely known, but recent studies show that its dysfunction to have the ability to cause neurotoxicity (85). Further investigation of this pathway remains to be investigated as a potential use as a therapeutic target.

3.0 **Study Objectives**

Though much is known about the regulation and control of mitochondrial biogenesis, the opposing pathway, mitophagy, is more elusive in its understanding. Additionally research on TFEB is in its infancy, and its effects on skeletal muscle have not been thoroughly examined. Research in this area could provide new insight into mitochondrial-lysosomal interactions in response to exercise. Furthermore, it would be intriguing to see how this transcription factor is activated in response to contractile activity. It has well been established in various cell lines that TFEB is activated under stress conditions such as starvation (108, 111), but the roles of TFEB in skeletal muscle under the effects of exercise remains generally unknown. Therefore based on my literature review, the purposes of this thesis were: 1) to determine the effect of acute

contractile activity and recovery on short term TFEB activation and expression, 2) to determine how chronic contractile activity will induce adaptations of TFEB expression and its downstream targets, and 3) to clarify the pathways that TFEB is involved in by utilizing a TFEB overexpression model. These objectives will provide useful insight to the unknown roles of TFEB in skeletal muscle.

Hypotheses

Recent previous studies have examined the effect of nutrient deprivation on TFEB. Activators of TFEB, such as, calcinerin are activated by exercise resulting in TFEB translocation and induction. However, the mechanisms are not completely clear. We hypothesize that TFEB will be activated following an acute bout of exercise and upregulate the transcription of various lysosomal biogenesis genes. Furthermore, we hypothesize that the adenoviral overexpression of TFEB will cause an abundance of protein and induce an increased transcripton of TFEB target genes and further increase their transcription following exercise. If TFEB is activated following one bout of acute contractile activity we hypothesize that following 4 days of chronic contractile activity there will be an increase in TFEB downstream targets.

Literature Review Reference List

1. **Ahadian S, Ostrovidov S, Hosseini V, Kaji H, Ramalingam M, Bae H, Khademhosseini A**. Electrical stimulation as a biomimicry tool for regulating muscle cell behavior. *Organogenesis* 9: 87–92.

2. **Akimoto T, Pohnert SC, Li P, Zhang M, Gumbs C, Rosenberg PB, Williams RS, Yan Z**. Exercise stimulates Pgc-1alpha transcription in skeletal muscle through activation of the p38 MAPK pathway. *J Biol Chem* 280: 19587–93, 2005.

3. **Amigo I, Kowaltowski AJ**. Dietary restriction in cerebral bioenergetics and redox state. *Redox Biol* 2: 296–304, 2014.

4. **Anderson EJ, Lustig ME, Boyle KE, Woodlief TL, Kane DA, Lin C-T, Price JW, Kang L, Rabinovitch PS, Szeto HH, Houmard JA, Cortright RN, Wasserman DH, Neufer PD**. Mitochondrial H2O2 emission and cellular redox state link excess fat intake to insulin resistance in both rodents and humans. *J Clin Invest* 119: 573–81, 2009.

5. **Baar K, Wende AR, Jones TE, Marison M, Nolte LA, Chen M, Kelly DP, Holloszy JO**. Adaptations of skeletal muscle to exercise: rapid increase in the transcriptional coactivator PGC-1. *FASEB J* 16: 1879–86, 2002.

6. **Banugaria SG, Prater SN, Ng Y-K, Kobori JA, Finkel RS, Ladda RL, Chen Y-T, Rosenberg AS, Kishnani PS**. The impact of antibodies on clinical outcomes in diseases treated with therapeutic protein: lessons learned from infantile Pompe disease. *Genet Med* 13: 729–36, 2011.

7. **Behrends C, Sowa ME, Gygi SP, Harper JW**. Network organization of the human autophagy system. *Nature* 466: 68–76, 2010.

8. **Bossy-Wetzel E, Petrilli A, Knott AB**. Mutant huntingtin and mitochondrial dysfunction. *Trends Neurosci* 31: 609–16, 2008.

9. **Burch N, Arnold A-S, Item F, Summermatter S, Brochmann Santana Santos G, Christe M, Boutellier U, Toigo M, Handschin C**. Electric pulse stimulation of cultured murine muscle cells reproduces gene expression changes of trained mouse muscle. *PLoS One* 5: e10970, 2010.

10. **Carter HN, Chen CCW, Hood DA**. Mitochondria, Muscle Health, and Exercise with Advancing Age. *Physiology (Bethesda)* 30: 208–223, 2015.

11. **Carter HN, Hood DA**. Contractile activity-induced mitochondrial biogenesis and mTORC1. *Am J Physiol Cell Physiol* 303: C540–7, 2012.

12. **Caspersen C, Wang N, Yao J, Sosunov A, Chen X, Lustbader JW, Xu HW, Stern D, McKhann G, Yan S Du**. Mitochondrial Abeta: a potential focal point for neuronal metabolic dysfunction in Alzheimer's disease. *FASEB J* 19: 2040–1, 2005.

13. **Chabi B, Adhihetty PJ, Ljubicic V, Hood DA**. How is mitochondrial biogenesis affected in mitochondrial disease? [Online]. *Med Sci Sports Exerc* 37: 2102–10, 2005. http://www.ncbi.nlm.nih.gov/pubmed/16331136 [22 Jun. 2015].

14. **Chaturvedi RK, Adhihetty P, Shukla S, Hennessy T, Calingasan N, Yang L, Starkov A, Kiaei M, Cannella M, Sassone J, Ciammola A, Squitieri F, Beal MF**. Impaired PGC-1 function in muscle in Huntington's disease. *Hum Mol Genet* 18: 3048–3065, 2009.

15. **Chen G, Cizeau J, Vande Velde C, Park JH, Bozek G, Bolton J, Shi L, Dubik D, Greenberg A**. Nix and Nip3 Form a Subfamily of Pro-apoptotic Mitochondrial Proteins. *J Biol Chem* 274: 7–10, 1999.

16. **Chinnery PF**. Mitochondria. *J Neurol Neurosurg Psychiatry* 74: 1188–1199, 2003.

17. **Choo YS, Johnson GVW, MacDonald M, Detloff PJ, Lesort M**. Mutant huntingtin directly increases susceptibility of mitochondria to the calcium-induced permeability transition and cytochrome c release. *Hum Mol Genet* 13: 1407–20, 2004.

18. **Chua JP, Reddy SL, Merry DE, Adachi H, Katsuno M, Sobue G, Robins DM, Lieberman AP**. Transcriptional activation of TFEB/ZKSCAN3 target genes underlies enhanced autophagy in spinobulbar muscular atrophy. *Hum Mol Genet* 23: 1376–86, 2014.

19. **Cortes CJ, Miranda HC, Frankowski H, Batlevi Y, Young JE, Le A, Ivanov N, Sopher BL, Carromeu C, Muotri AR, Garden GA, La Spada AR**. Polyglutamine-expanded androgen receptor interferes with TFEB to elicit autophagy defects in SBMA. *Nat Neurosci* 17: 1180–9, 2014.

20. **Cui L, Jeong H, Borovecki F, Parkhurst CN, Tanese N, Krainc D**. Transcriptional repression of PGC-1alpha by mutant huntingtin leads to mitochondrial dysfunction and neurodegeneration. *Cell* 127: 59–69, 2006.

21. **Dahlgren C, Carlsson SR, Karlsson A, Lundqvist H, Sjölin C**. The lysosomal membrane glycoproteins Lamp-1 and Lamp-2 are present in mobilizable organelles, but are absent from the azurophil granules of human neutrophils. [Online]. *Biochem J* 311 (Pt 2: 667–74, 1995. http://www.pubmedcentral.nih.gov/articlerender.fcgi?artid=1136051&tool=pmcentrez&rendertype=abstract [10 Jun. 2015].

22. **Dejager S, Bry-Gauillard H, Bruckert E, Eymard B, Salachas F, LeGuern E, Tardieu S, Chadarevian R, Giral P, Turpin G**. A comprehensive endocrine description of Kennedy's disease revealing androgen insensitivity linked to CAG repeat length. *J Clin Endocrinol Metab* 87: 3893–901, 2002.

23. **DEMPSEY EW**. Variations in the structure of mitochondria. [Online]. *J Biophys Biochem Cytol* 2: 305–12, 1956. http://www.pubmedcentral.nih.gov/articlerender.fcgi?artid=2229743&tool=pmcentrez&rendertype=abstract [7 Jun. 2015].

24. **Du H, Guo L, Fang F, Chen D, Sosunov AA, McKhann GM, Yan Y, Wang C, Zhang H, Molkentin JD, Gunn-Moore FJ, Vonsattel JP, Arancio O, Chen JX, Yan S Du**. Cyclophilin D deficiency attenuates mitochondrial and neuronal perturbation and ameliorates learning and memory in Alzheimer's disease. *Nat Med* 14: 1097–105, 2008.

25. **Eskelinen E-L**. Roles of LAMP-1 and LAMP-2 in lysosome biogenesis and autophagy. *Mol Aspects Med* 27: 495–502, 2006.

26. **Feeney EJ, Spampanato C, Puertollano R, Ballabio A, Parenti G, Raben N**. What else is in store for autophagy? Exocytosis of autolysosomes as a mechanism of TFEB-mediated cellular clearance in Pompe disease. *Autophagy* 9: 1117–8, 2013.

27. **Ferron M, Settembre C, Shimazu J, Lacombe J, Kato S, Rawlings DJ, Ballabio A, Karsenty G**. A RANKL-PKCβ-TFEB signaling cascade is necessary for lysosomal biogenesis in osteoclasts. *Genes Dev* 27: 955–69, 2013.

28. **Fisher DE, Carr CS, Parent LA, Sharp PA**. TFEB has DNA-binding and oligomerization properties of a unique helix-loop-helix/leucine-zipper family. [Online]. *Genes Dev* 5: 2342–52, 1991. http://www.ncbi.nlm.nih.gov/pubmed/1748288 [18 Jun. 2015].

29. **Frank M, Duvezin-Caubet S, Koob S, Occhipinti A, Jagasia R, Petcherski A, Ruonala MO, Priault M, Salin B, Reichert AS**. Mitophagy is triggered by mild

oxidative stress in a mitochondrial fission dependent manner. *Biochim Biophys Acta* 1823: 2297–310, 2012.

30. **Fujita H, Nedachi T, Kanzaki M**. Accelerated de novo sarcomere assembly by electric pulse stimulation in C2C12 myotubes. *Exp Cell Res* 313: 1853–65, 2007.

31. **Ghosh A, Jana M, Modi K, Gonzalez FJ, Sims KB, Berry-Kravis E, Pahan K**. Activation of Peroxisome Proliferator-activated Receptor α Induces Lysosomal Biogenesis in Brain Cells: IMPLICATIONS FOR LYSOSOMAL STORAGE DISORDERS. *J Biol Chem* 290: 10309–24, 2015.

32. **Giordano S, Darley-Usmar V, Zhang J**. Autophagy as an essential cellular antioxidant pathway in neurodegenerative disease. *Redox Biol* 2: 82–90, 2014.

33. **Grumati P, Bonaldo P**. Autophagy in skeletal muscle homeostasis and in muscular dystrophies. *Cells* 1: 325–45, 2012.

34. **Grumati P, Coletto L, Schiavinato A, Castagnaro S, Bertaggia E, Sandri M, Bonaldo P**. Physical exercise stimulates autophagy in normal skeletal muscles but is detrimental for collagen VI-deficient muscles. [Online]. *Autophagy* 7: 1415–23, 2011. http://www.pubmedcentral.nih.gov/articlerender.fcgi?artid=3288016&tool=pmcentrez&rendertype=abstract [20 Jul. 2015].

35. **Hallsson JH**. The Basic Helix-Loop-Helix Leucine Zipper Transcription Factor Mitf Is Conserved in Drosophila and Functions in Eye Development. *Genetics* 167: 233–241, 2004.

36. **Hattori N, Saiki S, Imai Y**. Regulation by mitophagy. *Int J Biochem Cell Biol* 53: 147–50, 2014.

37. **He C, Bassik MC, Moresi V, Sun K, Wei Y, Zou Z, An Z, Loh J, Fisher J, Sun Q, Korsmeyer S, Packer M, May HI, Hill JA, Virgin HW, Gilpin C, Xiao G, Bassel-Duby R, Scherer PE, Levine B**. Exercise-induced BCL2-regulated autophagy is required for muscle glucose homeostasis. *Nature* 481: 511–5, 2012.

38. **Holloszy JO, Booth FW**. Biochemical adaptations to endurance exercise in muscle. *Annu Rev Physiol* 38: 273–91, 1976.

39. **Hood DA, Irrcher I, Ljubicic V, Joseph A-M**. Coordination of metabolic plasticity in skeletal muscle. *J Exp Biol* 209: 2265–75, 2006.

40. **Hood DA, Uguccioni G, Vainshtein A, D'souza D**. Mechanisms of exercise-induced mitochondrial biogenesis in skeletal muscle: implications for health and disease. *Compr Physiol* 1: 1119–34, 2011.

41. **Huang Y, Mucke L**. Alzheimer mechanisms and therapeutic strategies. *Cell* 148: 1204–22, 2012.

42. **Jäger S, Handschin C, St-Pierre J, Spiegelman BM**. AMP-activated protein kinase (AMPK) action in skeletal muscle via direct phosphorylation of PGC-1alpha. *Proc Natl Acad Sci U S A* 104: 12017–22, 2007.

43. **Jamart C, Benoit N, Raymackers J-M, Kim HJ, Kim CK, Francaux M**. Autophagy-related and autophagy-regulatory genes are induced in human muscle after ultraendurance exercise. *Eur J Appl Physiol* 112: 3173–7, 2012.

44. **Jamart C, Naslain D, Gilson H, Francaux M**. Higher activation of autophagy in skeletal muscle of mice during endurance exercise in the fasted state. *Am J Physiol Endocrinol Metab* 305: E964–74, 2013.

45. **Jin SM, Youle RJ**. The accumulation of misfolded proteins in the mitochondrial matrix is sensed by PINK1 to induce PARK2/Parkin-mediated mitophagy of polarized mitochondria. *Autophagy* 9: 1750–7, 2013.

46. **Jung CH, Ro S-H, Cao J, Otto NM, Kim D-H**. mTOR regulation of autophagy. *FEBS Lett* 584: 1287–95, 2010.

47. **Kane LA, Lazarou M, Fogel AI, Li Y, Yamano K, Sarraf SA, Banerjee S, Youle RJ**. PINK1 phosphorylates ubiquitin to activate Parkin E3 ubiquitin ligase activity. *J Cell Biol* 205: 143–53, 2014.

48. **Kang D, Hamasaki N**. Maintenance of mitochondrial DNA integrity: repair and degradation. *Curr Genet* 41: 311–22, 2002.

49. **Kang D, Kim SH, Hamasaki N**. Mitochondrial transcription factor A (TFAM): roles in maintenance of mtDNA and cellular functions. *Mitochondrion* 7: 39–44.

50. **Kim J, Kundu M, Viollet B, Guan K-L**. AMPK and mTOR regulate autophagy through direct phosphorylation of Ulk1. *Nat Cell Biol* 13: 132–41, 2011.

51. **Kirkin V, McEwan DG, Novak I, Dikic I**. A role for ubiquitin in selective autophagy. *Mol Cell* 34: 259–69, 2009.

52. **Koeberl DD, Li S, Dai J, Thurberg BL, Bali D, Kishnani PS**. β2 Agonists enhance the efficacy of simultaneous enzyme replacement therapy in murine Pompe disease. *Mol Genet Metab* 105: 221–7, 2012.

53. **Kondapalli C, Kazlauskaite A, Zhang N, Woodroof HI, Campbell DG, Gourlay R, Burchell L, Walden H, Macartney TJ, Deak M, Knebel A, Alessi DR, Muqit MMK**. PINK1 is activated by mitochondrial membrane potential depolarization and stimulates Parkin E3 ligase activity by phosphorylating Serine 65. *Open Biol* 2: 120080, 2012.

54. **Koves TR, Ussher JR, Noland RC, Slentz D, Mosedale M, Ilkayeva O, Bain J, Stevens R, Dyck JRB, Newgard CB, Lopaschuk GD, Muoio DM**. Mitochondrial overload and incomplete fatty acid oxidation contribute to skeletal muscle insulin resistance. *Cell Metab* 7: 45–56, 2008.

55. **Koyano F, Okatsu K, Kosako H, Tamura Y, Go E, Kimura M, Kimura Y, Tsuchiya H, Yoshihara H, Hirokawa T, Endo T, Fon EA, Trempe J-F, Saeki Y, Tanaka K, Matsuda N**. Ubiquitin is phosphorylated by PINK1 to activate parkin. *Nature* 510: 162–6, 2014.

56. **Kroos M, Hoogeveen-Westerveld M, van der Ploeg A, Reuser AJJ**. The genotype-phenotype correlation in Pompe disease. *Am J Med Genet C Semin Med Genet* 160C: 59–68, 2012.

57. **Kubli DA, Quinsay MN, Huang C, Lee Y, Gustafsson AB**. Bnip3 functions as a mitochondrial sensor of oxidative stress during myocardial ischemia and reperfusion. *Am J Physiol Heart Circ Physiol* 295: H2025–31, 2008.

58. **Kurihara Y, Kanki T, Aoki Y, Hirota Y, Saigusa T, Uchiumi T, Kang D**. Mitophagy plays an essential role in reducing mitochondrial production of reactive oxygen species and mutation of mitochondrial DNA by maintaining mitochondrial quantity and quality in yeast. *J Biol Chem* 287: 3265–72, 2012.

59. **Kwon K-Y, Viollet B, Yoo OJ**. CCCP induces autophagy in an AMPK-independent manner. *Biochem Biophys Res Commun* 416: 343–8, 2011.

60. **Lachmann RH**. Enzyme replacement therapy for lysosomal storage diseases. *Curr Opin Pediatr* 23: 588–93, 2011.

61. **Lapierre LR, De Magalhaes Filho CD, McQuary PR, Chu C-C, Visvikis O, Chang JT, Gelino S, Ong B, Davis AE, Irazoqui JE, Dillin A, Hansen M**. The

TFEB orthologue HLH-30 regulates autophagy and modulates longevity in Caenorhabditis elegans. *Nat Commun* 4: 2267, 2013.

62. **Lee JW, Park S, Takahashi Y, Wang H-G**. The association of AMPK with ULK1 regulates autophagy. *PLoS One* 5: e15394, 2010.

63. **Lin J, Wu H, Tarr PT, Zhang C-Y, Wu Z, Boss O, Michael LF, Puigserver P, Isotani E, Olson EN, Lowell BB, Bassel-Duby R, Spiegelman BM**. Transcriptional co-activator PGC-1 alpha drives the formation of slow-twitch muscle fibres. *Nature* 418: 797–801, 2002.

64. **Lira VA, Benton CR, Yan Z, Bonen A**. PGC-1alpha regulation by exercise training and its influences on muscle function and insulin sensitivity. *Am J Physiol Endocrinol Metab* 299: E145–61, 2010.

65. **Liu S, Sawada T, Lee S, Yu W, Silverio G, Alapatt P, Millan I, Shen A, Saxton W, Kanao T, Takahashi R, Hattori N, Imai Y, Lu B**. Parkinson's disease-associated kinase PINK1 regulates Miro protein level and axonal transport of mitochondria. *PLoS Genet* 8: e1002537, 2012.

66. **López-Lluch G, Hunt N, Jones B, Zhu M, Jamieson H, Hilmer S, Cascajo M V, Allard J, Ingram DK, Navas P, de Cabo R**. Calorie restriction induces mitochondrial biogenesis and bioenergetic efficiency. *Proc Natl Acad Sci U S A* 103: 1768–73, 2006.

67. **Ma X, Liu H, Murphy JT, Foyil SR, Godar RJ, Abuirqeba H, Weinheimer CJ, Barger PM, Diwan A**. Regulation of the Transcription Factor EB-PGC1α Axis by Beclin-1 Controls Mitochondrial Quality and Cardiomyocyte Death under Stress. *Mol Cell Biol* 35: 956–976, 2015.

68. **Mammucari C, Milan G, Romanello V, Masiero E, Rudolf R, Del Piccolo P, Burden SJ, Di Lisi R, Sandri C, Zhao J, Goldberg AL, Schiaffino S, Sandri M**. FoxO3 controls autophagy in skeletal muscle in vivo. *Cell Metab* 6: 458–71, 2007.

69. **Manczak M, Anekonda TS, Henson E, Park BS, Quinn J, Reddy PH**. Mitochondria are a direct site of A beta accumulation in Alzheimer's disease neurons: implications for free radical generation and oxidative damage in disease progression. *Hum Mol Genet* 15: 1437–49, 2006.

70. **Marcil M, Bourduas K, Ascah A, Burelle Y**. Exercise training induces respiratory substrate-specific decrease in Ca2+-induced permeability transition

pore opening in heart mitochondria. *Am J Physiol Heart Circ Physiol* 290: H1549–57, 2006.

71. **Martina JA, Chen Y, Gucek M, Puertollano R**. MTORC1 functions as a transcriptional regulator of autophagy by preventing nuclear transport of TFEB. *Autophagy* 8: 903–14, 2012.

72. **Matsuda N, Sato S, Shiba K, Okatsu K, Saisho K, Gautier CA, Sou Y-S, Saiki S, Kawajiri S, Sato F, Kimura M, Komatsu M, Hattori N, Tanaka K**. PINK1 stabilized by mitochondrial depolarization recruits Parkin to damaged mitochondria and activates latent Parkin for mitophagy. *J Cell Biol* 189: 211–21, 2010.

73. **Medina DL, Ballabio A**. Lysosomal calcium regulates autophagy. *Autophagy* (May 22, 2015). doi: 10.1080/15548627.2015.1047130.

74. **Medina DL, Fraldi A, Bouche V, Annunziata F, Mansueto G, Spampanato C, Puri C, Pignata A, Martina JA, Sardiello M, Palmieri M, Polishchuk R, Puertollano R, Ballabio A**. Transcriptional activation of lysosomal exocytosis promotes cellular clearance. *Dev Cell* 21: 421–30, 2011.

75. **Medina DL, Di Paola S, Peluso I, Armani A, De Stefani D, Venditti R, Montefusco S, Scotto-Rosato A, Prezioso C, Forrester A, Settembre C, Wang W, Gao Q, Xu H, Sandri M, Rizzuto R, De Matteis MA, Ballabio A**. Lysosomal calcium signalling regulates autophagy through calcineurin and TFEB. *Nat Cell Biol* 17: 288–299, 2015.

76. **Medina DL, Di Paola S, Peluso I, Armani A, De Stefani D, Venditti R, Montefusco S, Scotto-Rosato A, Prezioso C, Forrester A, Settembre C, Wang W, Gao Q, Xu H, Sandri M, Rizzuto R, De Matteis MA, Ballabio A**. Lysosomal calcium signalling regulates autophagy through calcineurin and TFEB. *Nat Cell Biol* 17: 288–299, 2015.

77. **Meirhaeghe A, Crowley V, Lenaghan C, Lelliott C, Green K, Stewart A, Hart K, Schinner S, Sethi JK, Yeo G, Brand MD, Cortright RN, O'Rahilly S, Montague C, Vidal-Puig AJ**. Characterization of the human, mouse and rat PGC1 beta (peroxisome-proliferator-activated receptor-gamma co-activator 1 beta) gene in vitro and in vivo. *Biochem J* 373: 155–65, 2003.

78. **Menzies KJ, Singh K, Saleem A, Hood DA**. Sirtuin 1-mediated effects of exercise and resveratrol on mitochondrial biogenesis. *J Biol Chem* 288: 6968–79, 2013.

79. **Mizushima N**. Autophagy in protein and organelle turnover. *Cold Spring Harb Symp Quant Biol* 76: 397–402, 2011.

80. **Narendra D, Tanaka A, Suen D-F, Youle RJ**. Parkin is recruited selectively to impaired mitochondria and promotes their autophagy. *J Cell Biol* 183: 795–803, 2008.

81. **Narendra D, Walker JE, Youle R**. Mitochondrial quality control mediated by PINK1 and Parkin: links to parkinsonism. *Cold Spring Harb Perspect Biol* 4, 2012.

82. **Narendra DP, Jin SM, Tanaka A, Suen D-F, Gautier CA, Shen J, Cookson MR, Youle RJ**. PINK1 is selectively stabilized on impaired mitochondria to activate Parkin. *PLoS Biol* 8: e1000298, 2010.

83. **Nath S, Dancourt J, Shteyn V, Puente G, Fong WM, Nag S, Bewersdorf J, Yamamoto A, Antonny B, Melia TJ**. Lipidation of the LC3/GABARAP family of autophagy proteins relies on a membrane-curvature-sensing domain in Atg3. *Nat Cell Biol* 16: 415–24, 2014.

84. **Nedachi T, Fujita H, Kanzaki M**. Contractile C2C12 myotube model for studying exercise-inducible responses in skeletal muscle. *Am J Physiol Endocrinol Metab* 295: E1191–204, 2008.

85. **Nedelsky NB, Pennuto M, Smith RB, Palazzolo I, Moore J, Nie Z, Neale G, Taylor JP**. Native functions of the androgen receptor are essential to pathogenesis in a Drosophila model of spinobulbar muscular atrophy. *Neuron* 67: 936–52, 2010.

86. **Novak I, Kirkin V, McEwan DG, Zhang J, Wild P, Rozenknop A, Rogov V, Löhr F, Popovic D, Occhipinti A, Reichert AS, Terzic J, Dötsch V, Ney PA, Dikic I**. Nix is a selective autophagy receptor for mitochondrial clearance. *EMBO Rep* 11: 45–51, 2010.

87. **Owen OE, Felig P, Morgan AP, Wahren J, Cahill GF**. Liver and kidney metabolism during prolonged starvation. *J Clin Invest* 48: 574–83, 1969.

88. **Palmieri M, Impey S, Kang H, di Ronza A, Pelz C, Sardiello M, Ballabio A**. Characterization of the CLEAR network reveals an integrated control of cellular clearance pathways. *Hum Mol Genet* 20: 3852–66, 2011.

89. **Philp A, Belew MY, Evans A, Pham D, Sivia I, Chen A, Schenk S, Baar K**. The PGC-1α-related coactivator promotes mitochondrial and myogenic

adaptations in C2C12 myotubes. *Am J Physiol Regul Integr Comp Physiol* 301: R864–72, 2011.

90. **Van der Ploeg AT, Reuser AJJ**. Pompe's disease. *Lancet* 372: 1342–53, 2008.

91. **Puigserver P, Adelmant G, Wu Z, Fan M, Xu J, O'Malley B, Spiegelman BM**. Activation of PPARgamma coactivator-1 through transcription factor docking. [Online]. *Science* 286: 1368–71, 1999. http://www.ncbi.nlm.nih.gov/pubmed/10558993 [21 May 2015].

92. **Puigserver P, Wu Z, Park CW, Graves R, Wright M, Spiegelman BM**. A cold-inducible coactivator of nuclear receptors linked to adaptive thermogenesis. [Online]. *Cell* 92: 829–39, 1998. http://www.ncbi.nlm.nih.gov/pubmed/9529258 [16 Mar. 2015].

93. **Raben N, Jatkar T, Lee A, Lu N, Dwivedi S, Nagaraju K, Plotz PH**. Glycogen stored in skeletal but not in cardiac muscle in acid alpha-glucosidase mutant (Pompe) mice is highly resistant to transgene-encoded human enzyme. [Online]. *Mol Ther* 6: 601–8, 2002. http://www.ncbi.nlm.nih.gov/pubmed/12409258 [25 Jun. 2015].

94. **Raben N, Roberts A, Plotz PH**. Role of autophagy in the pathogenesis of Pompe disease. [Online]. *Acta Myol* 26: 45–8, 2007. http://www.pubmedcentral.nih.gov/articlerender.fcgi?artid=2949326&tool=pmcentrez&rendertype=abstract [25 Jun. 2015].

95. **Raben N, Schreiner C, Baum R, Takikita S, Xu S, Xie T, Myerowitz R, Komatsu M, Van der Meulen JH, Nagaraju K, Ralston E, Plotz PH**. Suppression of autophagy permits successful enzyme replacement therapy in a lysosomal storage disorder--murine Pompe disease. *Autophagy* 6: 1078–89, 2010.

96. **Redmann M, Dodson M, Boyer-Guittaut M, Darley-Usmar V, Zhang J**. Mitophagy mechanisms and role in human diseases. *Int J Biochem Cell Biol* 53: 127–33, 2014.

97. **Roczniak-Ferguson A, Petit CS, Froehlich F, Qian S, Ky J, Angarola B, Walther TC, Ferguson SM**. The transcription factor TFEB links mTORC1 signaling to transcriptional control of lysosome homeostasis. *Sci Signal* 5: ra42, 2012.

98. **Salma N, Song JS, Arany Z, Fisher DE**. Transcription Factor Tfe3 Directly Regulates Pgc-1Alpha in Muscle. *J. Cell. Physiol.* (March 3, 2015). doi: 10.1002/jcp.24978.

99. **Salt IP, Johnson G, Ashcroft SJ, Hardie DG**. AMP-activated protein kinase is activated by low glucose in cell lines derived from pancreatic beta cells, and may regulate insulin release. [Online]. *Biochem J* 335 (Pt 3: 533–9, 1998. http://www.pubmedcentral.nih.gov/articlerender.fcgi?artid=1219813&tool=pmcentrez&rendertype=abstract [29 Jul. 2015].

100. **Sancak Y, Bar-Peled L, Zoncu R, Markhard AL, Nada S, Sabatini DM**. Ragulator-Rag complex targets mTORC1 to the lysosomal surface and is necessary for its activation by amino acids. *Cell* 141: 290–303, 2010.

101. **Sanchez AMJ, Bernardi H, Py G, Candau RB**. Autophagy is essential to support skeletal muscle plasticity in response to endurance exercise. *Am J Physiol Regul Integr Comp Physiol* 307: R956–69, 2014.

102. **Sanchez AMJ, Candau RB, Csibi A, Pagano AF, Raibon A, Bernardi H**. The role of AMP-activated protein kinase in the coordination of skeletal muscle turnover and energy homeostasis. *Am J Physiol Cell Physiol* 303: C475–85, 2012.

103. **Santos RX, Correia SC, Wang X, Perry G, Smith MA, Moreira PI, Zhu X**. A synergistic dysfunction of mitochondrial fission/fusion dynamics and mitophagy in Alzheimer's disease. *J Alzheimers Dis* 20 Suppl 2: S401–12, 2010.

104. **Sardiello M, Palmieri M, di Ronza A, Medina DL, Valenza M, Gennarino VA, Di Malta C, Donaudy F, Embrione V, Polishchuk RS, Banfi S, Parenti G, Cattaneo E, Ballabio A**. A gene network regulating lysosomal biogenesis and function. *Science* 325: 473–7, 2009.

105. **Schweers RL, Zhang J, Randall MS, Loyd MR, Li W, Dorsey FC, Kundu M, Opferman JT, Cleveland JL, Miller JL, Ney PA**. NIX is required for programmed mitochondrial clearance during reticulocyte maturation. *Proc Natl Acad Sci U S A* 104: 19500–5, 2007.

106. **Scott I, Webster BR, Chan CK, Okonkwo JU, Han K, Sack MN**. GCN5-like protein 1 (GCN5L1) controls mitochondrial content through coordinated regulation of mitochondrial biogenesis and mitophagy. *J Biol Chem* 289: 2864–72, 2014.

107. **Settembre C, Ballabio A**. TFEB regulates autophagy: an integrated coordination of cellular degradation and recycling processes. *Autophagy* 7: 1379–81, 2011.

108. **Settembre C, Ballabio A**. TFEB regulates autophagy: an integrated coordination of cellular degradation and recycling processes. *Autophagy* 7: 1379–81, 2011.

109. **Settembre C, Ballabio A**. Lysosomal adaptation: how the lysosome responds to external cues. *Cold Spring Harb Perspect Biol* 6, 2014.

110. **Settembre C, De Cegli R, Mansueto G, Saha PK, Vetrini F, Visvikis O, Huynh T, Carissimo A, Palmer D, Klisch TJ, Wollenberg AC, Di Bernardo D, Chan L, Irazoqui JE, Ballabio A**. TFEB controls cellular lipid metabolism through a starvation-induced autoregulatory loop. *Nat Cell Biol* 15: 647–58, 2013.

111. **Settembre C, De Cegli R, Mansueto G, Saha PK, Vetrini F, Visvikis O, Huynh T, Carissimo A, Palmer D, Klisch TJ, Wollenberg AC, Di Bernardo D, Chan L, Irazoqui JE, Ballabio A**. TFEB controls cellular lipid metabolism through a starvation-induced autoregulatory loop. *Nat Cell Biol* 15: 647–58, 2013.

112. **Settembre C, Di Malta C, Polito VA, Garcia Arencibia M, Vetrini F, Erdin S, Erdin SU, Huynh T, Medina D, Colella P, Sardiello M, Rubinsztein DC, Ballabio A**. TFEB links autophagy to lysosomal biogenesis. *Science* 332: 1429–33, 2011.

113. **Settembre C, Medina DL**. TFEB and the CLEAR network. *Methods Cell Biol* 126: 45–62, 2015.

114. **Settembre C, Zoncu R, Medina DL, Vetrini F, Erdin S, Erdin S, Huynh T, Ferron M, Karsenty G, Vellard MC, Facchinetti V, Sabatini DM, Ballabio A**. A lysosome-to-nucleus signalling mechanism senses and regulates the lysosome via mTOR and TFEB. *EMBO J* 31: 1095–108, 2012.

115. **Shi R-Y, Zhu S-H, Li V, Gibson SB, Xu X-S, Kong J-M**. BNIP3 interacting with LC3 triggers excessive mitophagy in delayed neuronal death in stroke. *CNS Neurosci Ther* 20: 1045–55, 2014.

116. **Shirihai OS, Song M, Dorn GW**. How Mitochondrial Dynamism Orchestrates Mitophagy. *Circ Res* 116: 1835–1849, 2015.

117. **Simon H-U, Haj-Yehia A, Levi-Schaffer F**. Role of reactive oxygen species (ROS) in apoptosis induction. *Apoptosis* 5: 415–418, [date unknown].

118. **La Spada AR, Taylor JP**. Repeat expansion disease: progress and puzzles in disease pathogenesis. *Nat Rev Genet* 11: 247–58, 2010.

119. **La Spada AR**. PPARGC1A/PGC-1α, TFEB and enhanced proteostasis in Huntington disease: defining regulatory linkages between energy production and protein-organelle quality control. *Autophagy* 8: 1845–7, 2012.

120. **Spampanato C, Feeney E, Li L, Cardone M, Lim J-A, Annunziata F, Zare H, Polishchuk R, Puertollano R, Parenti G, Ballabio A, Raben N**. Transcription factor EB (TFEB) is a new therapeutic target for Pompe disease. *EMBO Mol Med* 5: 691–706, 2013.

121. **St-Pierre J, Drori S, Uldry M, Silvaggi JM, Rhee J, Jäger S, Handschin C, Zheng K, Lin J, Yang W, Simon DK, Bachoo R, Spiegelman BM**. Suppression of reactive oxygen species and neurodegeneration by the PGC-1 transcriptional coactivators. *Cell* 127: 397–408, 2006.

122. **Takahashi M, Hood DA**. Chronic stimulation-induced changes in mitochondria and performance in rat skeletal muscle. [Online]. *J Appl Physiol* 74: 934–41, 1993. http://www.ncbi.nlm.nih.gov/pubmed/8458817 [11 May 2015].

123. **Tanaka A, Cleland MM, Xu S, Narendra DP, Suen D-F, Karbowski M, Youle RJ**. Proteasome and p97 mediate mitophagy and degradation of mitofusins induced by Parkin. *J Cell Biol* 191: 1367–80, 2010.

124. **Tanida I, Ueno T, Kominami E**. LC3 conjugation system in mammalian autophagy. *Int J Biochem Cell Biol* 36: 2503–18, 2004.

125. **Tao M, You C-P, Zhao R-R, Liu S-J, Zhang Z-H, Zhang C, Liu Y**. Animal mitochondria: evolution, function, and disease. [Online]. *Curr Mol Med* 14: 115–24, 2014. http://www.ncbi.nlm.nih.gov/pubmed/24195633 [7 Jun. 2015].

126. **Thomas PS**. Loss of endogenous androgen receptor protein accelerates motor neuron degeneration and accentuates androgen insensitivity in a mouse model of X-linked spinal and bulbar muscular atrophy. *Hum Mol Genet* 15: 2225–2238, 2006.

127. **Thomas RE, Andrews LA, Burman JL, Lin W-Y, Pallanck LJ**. PINK1-Parkin pathway activity is regulated by degradation of PINK1 in the mitochondrial matrix. *PLoS Genet* 10: e1004279, 2014.

128. **Tong Y, Song F**. Intracellular calcium signaling regulates autophagy via calcineurin-mediated TFEB dephosphorylation. *Autophagy* (June 4, 2015). doi: 10.1080/15548627.2015.1054594.

129. **Tsunemi T, Ashe TD, Morrison BE, Soriano KR, Au J, Roque RAV, Lazarowski ER, Damian VA, Masliah E, La Spada AR**. PGC-1α rescues Huntington's disease proteotoxicity by preventing oxidative stress and promoting TFEB function. *Sci Transl Med* 4: 142ra97, 2012.

130. **Turrens JF, Alexandre A, Lehninger AL**. Ubisemiquinone is the electron donor for superoxide formation by complex III of heart mitochondria. [Online]. *Arch Biochem Biophys* 237: 408–14, 1985. http://www.ncbi.nlm.nih.gov/pubmed/2983613 [11 Jun. 2015].

131. **Uguccioni G, Hood DA**. The importance of PGC-1α in contractile activity-induced mitochondrial adaptations. *Am J Physiol Endocrinol Metab* 300: E361–71, 2011.

132. **Urbanelli L, Magini A, Polchi A, Polidoro M, Emiliani C**. Recent developments in therapeutic approaches for lysosomal storage diseases. [Online]. *Recent Pat CNS Drug Discov* 6: 1–19, 2011. http://www.ncbi.nlm.nih.gov/pubmed/21073432 [25 Jun. 2015].

133. **Vainshtein A, Desjardins EM, Armani A, Sandri M, Hood DA**. PGC-1α modulates denervation-induced mitophagy in skeletal muscle. *Skelet Muscle* 5: 9, 2015.

134. **Vainshtein A, Tryon LD, Pauly M, Hood DA**. Role of PGC-1α during acute exercise-induced autophagy and mitophagy in skeletal muscle. *Am J Physiol Cell Physiol* 308: C710–9, 2015.

135. **Vincow ES, Merrihew G, Thomas RE, Shulman NJ, Beyer RP, MacCoss MJ, Pallanck LJ**. The PINK1-Parkin pathway promotes both mitophagy and selective respiratory chain turnover in vivo. *Proc Natl Acad Sci U S A* 110: 6400–5, 2013.

136. **Virbasius J V, Scarpulla RC**. Activation of the human mitochondrial transcription factor A gene by nuclear respiratory factors: a potential regulatory link between nuclear and mitochondrial gene expression in organelle biogenesis. [Online]. *Proc Natl Acad Sci U S A* 91: 1309–13, 1994. http://www.pubmedcentral.nih.gov/articlerender.fcgi?artid=43147&tool=pmcentrez&rendertype=abstract [9 Jun. 2015].

137. **Vives-Bauza C, Zhou C, Huang Y, Cui M, de Vries RLA, Kim J, May J, Tocilescu MA, Liu W, Ko HS, Magrané J, Moore DJ, Dawson VL, Grailhe R, Dawson TM, Li C, Tieu K, Przedborski S**. PINK1-dependent recruitment of Parkin to mitochondria in mitophagy. *Proc Natl Acad Sci U S A* 107: 378–83, 2010.

138. **Wang H, Song P, Du L, Tian W, Yue W, Liu M, Li D, Wang B, Zhu Y, Cao C, Zhou J, Chen Q**. Parkin ubiquitinates Drp1 for proteasome-dependent degradation: implication of dysregulated mitochondrial dynamics in Parkinson disease. *J Biol Chem* 286: 11649–58, 2011.

139. **Webster BR, Scott I, Traba J, Han K, Sack MN**. Regulation of autophagy and mitophagy by nutrient availability and acetylation. *Biochim Biophys Acta* 1841: 525–34, 2014.

140. **Wei H, Liu L, Chen Q**. Selective removal of mitochondria via mitophagy: distinct pathways for different mitochondrial stresses. *Biochim. Biophys. Acta* (March 31, 2015). doi: 10.1016/j.bbamcr.2015.03.013.

141. **Wong YC, Holzbaur ELF**. Optineurin is an autophagy receptor for damaged mitochondria in parkin-mediated mitophagy that is disrupted by an ALS-linked mutation. *Proc Natl Acad Sci* 111: E4439–E4448, 2014.

142. **Wu H, Rothermel B, Kanatous S, Rosenberg P, Naya FJ, Shelton JM, Hutcheson KA, DiMaio JM, Olson EN, Bassel-Duby R, Williams RS**. Activation of MEF2 by muscle activity is mediated through a calcineurin-dependent pathway. *EMBO J* 20: 6414–23, 2001.

143. **Wu Z, Puigserver P, Andersson U, Zhang C, Adelmant G, Mootha V, Troy A, Cinti S, Lowell B, Scarpulla RC, Spiegelman BM**. Mechanisms Controlling Mitochondrial Biogenesis and Respiration through the Thermogenic Coactivator PGC-1. *Cell* 98: 115–124, 1999.

144. **Wu Z, Puigserver P, Speiglman BM**. Transcriptional activation of adipogenesis [Online]. *Cell Differ.*: 689–694, 1999. http://ac.els-cdn.com/S095506749900037X/1-s2.0-S095506749900037X-main.pdf?_tid=0074044a-0ef2-11e5-a746-00000aab0f02&acdnat=1433887005_ded51fc138a6a47d6a6301207005a7b6 [9 Jun. 2015].

145. **Yakes FM, Van Houten B**. Mitochondrial DNA damage is more extensive and persists longer than nuclear DNA damage in human cells following oxidative stress. *Proc Natl Acad Sci* 94: 514–519, 1997.

146. **Yoon JC, Puigserver P, Chen G, Donovan J, Wu Z, Rhee J, Adelmant G, Stafford J, Kahn CR, Granner DK, Newgard CB, Spiegelman BM**. Control of hepatic gluconeogenesis through the transcriptional coactivator PGC-1. *Nature* 413: 131–8, 2001.

147. **Zhang J, Ney PA**. Role of BNIP3 and NIX in cell death, autophagy, and mitophagy. *Cell Death Differ* 16: 939–46, 2009.

148. **Zhang Y, Uguccioni G, Ljubicic V, Irrcher I, Iqbal S, Singh K, Ding S, Hood DA**. Multiple signaling pathways regulate contractile activity-mediated PGC-1α gene expression and activity in skeletal muscle cells. *Physiol Rep* 2, 2014.

149. **Zhou J, Tan S-H, Nicolas V, Bauvy C, Yang N-D, Zhang J, Xue Y, Codogno P, Shen H-M**. Activation of lysosomal function in the course of autophagy via mTORC1 suppression and autophagosome-lysosome fusion. *Cell Res* 23: 508–23, 2013.

150. **Zoncu R, Bar-Peled L, Efeyan A, Wang S, Sancak Y, Sabatini DM**. mTORC1 senses lysosomal amino acids through an inside-out mechanism that requires the vacuolar H(+)-ATPase. *Science* 334: 678–83, 2011.

The role and expression of TFEB in contracting skeletal muscle myotubes

Diane Brownlee and David A. Hood

Muscle Health Research Centre, School of Kinesiology and Health Science

York University, Toronto, Ontario, M3J 1P3, Canada

Keywords: C2C12, exercise, mitophagy, lysosomal biogenesis, muscle adaptations

Address for correspondence: Dr. David A Hood

School of Kinesiology and Health Science

York University, Toronto, ON

M3J 1P3, Canada

Abstract:

Skeletal muscle adaptations during exercise depend on a functional mitochondrial pool. Optimal mitochondria are regulated by two opposing processes, termed mitochondrial biogenesis and mitochondrial autophagy (mitophagy). A key mechanism in mitophagy is lysosomal biogenesis, and this process is under the control of transcription factor EB (TFEB). TFEB is known to be activated following starvation however, exercise-mediated TFEB activity in skeletal muscle has not been determined. To understand this, we employed both acute and chronic contractile activity of C2C12 myotubes in cell culture. TFEB promoter activity and nuclear localization were upregulated following 2 and 5 hours of acute stimulation. The distal 400 bp region of the 1600 bp promoter was responsible for the contractile activity-mediated increase in transcription. Adenoviral overexpression of TFEB caused marked increases in autophagy markers, LAMP2, LC3 and p62 and mitochondrial biogenesis markers, COXIV and PGC-1α under control conditions. Under the influence of acute contractile activity TFEB mRNA significantly decreased in a stimulation-dependent manner in the overexpressing cells. To analyze the long-term effects of exercise on lysosomal adaptations we utilized chronic contractile activity (CCA; 3 hours/day for 4 days), TFEB, TFE3 and p62 demonstrated no alterations. However, LAMP2 was decreased by 42% and a 160% increase was observed in cathepsin D protein content. Our study indicated that TFEB transcription and localization are regulated by contractile activity, which could contribute to the coordinated biogenesis of both lysosomes and mitochondria.

Acknowledgments:

This work was supported by a Canadian Institutes of Health Research (CIHR) grant to D.A. Hood. D.A. Hood is the holder of a Canada Research Chair in Cell Physiology.

Introduction:

Regular exercise has been well documented to have many beneficial effects on physical health, including adaptations in oxidative capacity, metabolism and cardiovascular health (4). Furthermore, exercise has been demonstrated to protect against diabetes and various metabolic disorders (5). Skeletal muscle has the incredible ability to adapt to the energy demands presented by contractile activity. The alterations that are needed by skeletal muscle cells to respond to the metabolic shift require a remodeling of the mitochondrial network. The quality and quantity of the mitochondrial network is dependent on the intricate balance between two opposing pathways: mitochondrial biogenesis and mitochondrial degradation. Mitochondrial biogenesis is the expansion and synthesis of organelle network, a process that is largely regulated by the co-activator PGC-1α. The opposing pathway, degradation, is not completely understood. The selective degradation of mitochondria is termed mitophagy and this has been documented to increase following cellular stress, increased nutritional and energy demands, and various diseases such as cancer, neurodegenerative disorders and inflammatory disorders (1, 8, 10). The purpose of this pathway is the removal of dysfunctional or damaged mitochondria (15, 18, 39, 44).

During mitophagy, an unhealthy mitochondrion will be separated from the mitochondrial network through fission. Due to the decreased oxidative capacity that the damaged mitochondrion possesses, normally imported proteins such as PINK1 will

accumulate on the outer mitochondrial membrane (17). PINK1 will recruit parkin to the mitochondria where it can ubiquitinate outer membrane proteins such as MFN1 and VDAC which will selectively tag the organelle for removal (14, 43). Targeted mitochondria are engulfed by a double membrane autophagosome, and transported to the lysosome for degradation. Recent publications have highlighted this process of mitophagy being activated following an acute bout of exercise (7, 11, 12). These studies suggest that the beneficial mitochondrial adaptations that are seen with long-term chronic exercise could be due, in part, to the mitophagy pathways activated immediately following a period of exercise (6).

An important player in autophagy is transcription factor EB (TFEB), known for its role as the master regulator of lysosomal biogenesis. TFEB activity is regulated through phosphorylation (23, 27, 35), which retains the protein inactive and sequestered in the cytosol. Two kinases have been identified to date that inhibit TFEB activity, mTORC1 and ERK2, which phosphorylate TFEB on Ser211 and Ser142 respectively (22, 27, 33). However, under conditions such as starvation or cellular stress, TFEB is dephosphorylated into its active form by calcineurin (23). In conditions of stress, calcineurin will be activated by elevations in cytosolic Ca^{2+}. Since it is well known that calcium levels are elevated in muscle during contractile activity, it would be logical to expect the activation of TFEB following exercise. It has recently been shown that, following dephosphorylation, TFEB can translocate to the nucleus (23, 38). Nuclear translocation allows TFEB to upregulate the transcription of essential coordinated

lysosomal expression and regulation (CLEAR) genes such as LC3, SQSTM1 and LAMP1(30, 31, 33)

The purpose of this study was to further document the effect of acute exercise on TFEB expression and activation, as well as to observe the adaptations of TFEB to chronic contractile activity. To facilitate this, an adenoviral overexpression model was utilized for mRNA analysis of the impact of TFEB activation with exercise. Activation of the transcription factor under various conditions was analyzed by promoter activity, as well as by using nuclear and cytosolic fractionations. In addition to this, mitophagy markers were investigated following acute and chronic stimulation to investigate the effect of contractile activity on mitophagy. Mitophagy is an essential process in the health and maintenance of muscle, and it is known to be activated by acute exercise (6, 42). Since TFEB is a major regulator of autophagy, we hypothesized that TFEB activation would play a role in contractile activity- induced mitophagy.

Methods:

Cell culture- C2C12 murine skeletal muscle cells were proliferated on six-well culture dishes (Sarstedt, Montreal, QC, Canada or Biobasic Canada Inc., Markham, ON, Canada) coated with 0.1% gelatin in growth media (GM), Dulbecco's modified Eagle's medium (DMEM) supplemented with 10% fetal bovine serum (FBS) and 1% penicillin-streptomycin (P/S). At 80-95% confluency, differentiation into myotubes was induced by switching the medium to differentiation media (DM), DMEM supplemented with 5% heat-inactivated horse serum (HS) and 1% P/S.

Stimulation of muscle cells- Lids from plastic six-well dishes (3.5-mm wells) were fitted with two platinum wire electrodes such that 2-cm lengths ran parallel to each other at opposite ends of the dish 2 cm apart. This protocol has previously been described in detail (3). Myotubes were subjected to electrical stimulation-induced contractile activity in a parallel circuit at a frequency of 5 Hz and an intensity of 11 V acutely for one bout of 2 or 5 hours of stimulation, with or without two hours of recovery. Differentiation medium (2 ml) was replenished 1 h prior to stimulation. Following this time, custom-made lids with implanted electrodes replaced typical lids, and dishes were attached to the electrical stimulator unit. Each well was carefully inspected to ensure that the electrodes were submerged in the medium prior to the stimulation. Cells were collected for enzyme, protein, or RNA extractions immediately after the stimulation or recovery period. Chronic contractile activity (CCA) was achieved using the same preparation but with an

intensity of 9 V chronically for 3 h/day over 4 successive days, cells were harvested 21 hours after last stimulation. Stimulation was performed at 37°C and 5% CO_2 for all conditions.

Cyclosporin A (CsA) treatment- Myotubes were differentiated in 6-well plates as supplemented with CsA (Sigma-C3662). Media was changed 30 minutes prior to stimulation, and the final concentration of CsA per well was 10nM. Myotubes were acutely stimulated for 5 hours and immediately following stimulation whole cell extracts were collected for nuclear and cytosolic fractionation and western blotting.

Transfection experiments- Where indicated, the TFEB promoter containing either 1200 or 1600 bp upstream of the transcription start site, or the 2190 bp PGC-1α promoter and PRL-CMV vector as a normalization control were transfected into C2C12 cells cultured in 6-well plates. For transfection of the promoter sequence, C2C12 cells were grown as described previously, and the medium was switched to pre-transfection medium (DMEM and 10% FBS) when the cells were at 30% confluence. The following day, myoblasts were incubated with 2μg/well of TFEB or PGC-1α promoter DNA and 10 μl of Lipofectamine 2000 for 6 h in 2 ml of DMEM. The medium was then changed back to DMEM supplemented with 5% HS and 1% P/S, and the cells were then differentiated, as described above. The differentiated cells were then subjected to stimulation, or kept as a control.

Luciferase Reporter Assays- Following treatments, cell extracts containing

expressed luciferase enzyme were prepared using 1X passive lysis buffer supplemented with protease (Complete, Roche, 1169749801; Roche diagnostics, Basel, Switzerland) and phosphatase inhibitors (Cocktails 2 and 3 Sigma, P5726 and P0044). Luciferase activity was measured as an indicator of transcription using an EG&G Berthold (Lumat LB9507) luminometer, according to the manufacturers instructions.

Nuclear and Cytosolic Fractionation- NE-PER extraction reagents (Pierce, Thermo Scientific #38835) were used to obtain cytoplasmic and nuclear fractions using modifications of the manufacturer's recommendations and differential centrifugation.

Western Blotting- Total protein was isolated from C2C12 cells as described previously(9). Total protein extracts (30-80 μg) were separated on an SDS-polyacrylamide gel and transferred onto nitrocellulose membranes. Following the transfer, the membranes were blocked for 1 hour in 1X TBST containing 5% skim milk. The membranes were subsequently probed overnight at 4°C with antibodies that detected COXIV (1:750; Abcam, ab14744), LAMP2 (1:1000; Abcam ab13524), VDAC/porin (1:3000; Abcam), p-ERK1/2 (1:2500; Cell Signaling #9106S), Total-ERK1/2 (1:1000; Cell Signalling #9102), p-AMPK(1:3000; Cell Signalling #2535S), Total-AMPK(1:500; Cell Signalling #2532S), p-CamK-II(1:1000; Cell Signalling #3361S), p-p38(1:500; Cell Signalling #9211S), Total-p38(1:000; Cell Signalling #9212S), GAPDH(1:10000, Abcam), Aciculin(1:200, in house), COXI (1:500; Invitrogen ab14705), TFEB (1:500, MBS), YY1(1:500; Santa Cruz, sc7341), H2B(1:1000; Cell Signalling, #2934S), α-

tubulin (1:10000; Calbiochem), Cathepsin D (1:1000; Santa Cruz, SC6486), TFE3 (1:2000; Sigma, PA023881), parkin (1:500; Santa Cruz, sc32282), LC3A/B (1:1000; Cell Signaling #2775) or p62/SQSTM1 (1:5000; Sigma-Aldrich P0067). The membranes were washed 3X5 minutes with 1X TBST and incubated for 1 hour at room temperature with the appropriate secondary antibodies conjugated to horseradish peroxidase (Santa-Cruz Biotechnologies). Blots were visualized with enhanced chemilluminesence and were quantified using ImageJ software.

Fluorescence microscopy- C2C12 cells were plated on glass cover slips on 6 well dishes (3.5 mm wells) coated with 0.1% gelatin. Cells were differentiated on the cover slips and electrically stimulated for 5 hours. Following treatment, cells were fixed to the coverslips with 4% paraformaldehyde in PBS and permeabilized with 0.3% Trition. Non-specific binding was blocked with 5% normal goat serum in PBS. Slides were probed for 1 hour at room temperature with primary antibodies specific for LAMP2 (1:500), VDAC/Porin (1:500), p62/ SQSTM1 (1:500) or TFEB(1:500). Subsequently, slides were treated with the appropriate Alexafluor secondary antibody (Life Technologies) for 1 hour at room temperature. Lastly, slides were washed with DAPI nuclei staining (1:500) for 15 minutes. Mounted slides were visualized with an inverted Nikon Eclipse TE2000-U fluorescent microscope equipped with 20X objective lens. All representative images were taken at the same exposure per condition.

RNA extraction and mRNA analysis- Total RNA was isolated from cultured C2C12 myotubes using TRIzol reagent (Invitrogen) according to manufacturer's

instructions. RNA concentration and quality were assessed using spectrophotometry (NanoDrop 2000; Thermo Scientific). The mRNA expression of COXI, COXIV, TFAM, PGC-1α, TFEB, LAMP-2, Cathepsin D, LC3B, p62 and Beclin-1 was quantified using StepONE Plus PCR System (Applied Biosystems, California, USA) and SYBR® Green Supermix (Quanta Biociences, MD, USA). First-strand cDNA synthesis from 2 μg of total RNA was performed with primers using Superscript III transcriptase and $Oligo(dt)_{20}$ (Invitrogen) according to manufacturer's instructions. Forward and reverse primers (Table 1) were optimized to verify primer efficiency and dissociation melt curves were analyzed for primer specificity. All samples were run in duplicate. Transcript levels were normalized to two housekeeping genes, GAPDH and β-Actin, and analyzed using the $\Delta\Delta^{Ct}$ method. Statistical significance was calculated on 2^-ΔΔct values using two-way ANOVA and Tukey post hoc tests.

Mitochondrial isolation- Mitochondria were isolated from myotubes in tissue culture using an adapted protocol (21) via differential centrifugation. Briefly, myotubes were washed 2x in ice-cold PBS and scraped on ice using rubber policemen in mitochondrial isolation buffer (MIB; 10% 0.1 M Tris-MOPS, 1% EGTA-Tris, and 20% 1 M sucrose, pH 7.4). Cells were pelleted at a centrifugation speed of 600 g (Beckman JA25.5) for 10 minutes at 4°C and pellets were resuspended in 3 ml of MIB on ice. Suspensions were transferred to chilled 7ml glass potters and subjected to homogenization with an Elvehjem PTFE Tissue Grinder (Wheaton, NJ, USA) at 800 rpm for 30 strokes. Homogenates were transferred to fresh 1.5 ml eppendorf tubes and respun

at 10000 g. The supernatant fractions were collected, the resulting mitochondrial fractions were resuspended in 100 µl of PBS supplemented with protease (Complete, Roche, 1169749801; Roche diagnostics, Basel, Switzerland) and phosphatase inhibitors (Cocktails 2 and 3 Sigma, P5726 and P0044) and transferred to 1.5 ml eppendorf tubes. Crude mitochondrial samples were used for protein analysis and western blotting.

Infection of target cells- C2C12 mytoubes were differentiated in six well plates as described previously. On day 5 of differentiation, pre-made pAdEasy-TFEB virus and pAdEasy-GFP control virus were thawed at 37°C. Viral containers were spun down at 1400rpm for 3 minutes to ensure all viral contents were off the lid. In a 50ml falcon tube, 1ml of media was added per well for infection, as well as 10 MOI of viral stock. The viral mixture was made for the GFP control. For each 6-well plate, 3 wells were used as TFEB infected cells, and 3 wells were used as GFP control cells. Media was removed from the target cells and replaced with 1ml of viral mixture. Cells were incubated with the virus at 37°C for 24 hours. Immediately following, the virus DM was removed from the target cells, myotubes were washed twice with DM, then media was replenished. Media was replenished each day for desired days of infection.

Statistical Analysis- The means and standard errors were calculated for all measured values, and statistical significance between groups was determined by ANOVA or t-test where applicable with Tukey *post-hoc* tests (Graphpad, La Jolla, CA). Results were considered statistically significant when $p<0.05$.

TABLE 1:

	Primer (5'→3')	
Gene	Forward	Reverse
Maplc3b	GCTTGCAGCTCAATGCTAAC	CCTGCGAGGCATAAACCATGT
LAMP2	GCTGAACAGCCAAATTA	CTGAGCCATTAGCCAAATACA
CatsD	TTTGCAATGCTGTCGTACT	AGCGACTGTGACTATGTGTGAG
PGC-1α	TTCCACCAAGAGCAAGTAT	CGCTGTCCCATGAGGTATT
TFEB	AGCTCCAACCCGAGAAAGAGTTTG	CGTTCAGGTGGCTGCTAGAC
GAPDH	AACACTGAGCATCTCCCTCA	GTGGGTGCAGCGAACTTTAT
Actb	TGTGACGTTGACATCCGTAA	GCTAGGAGCCAGAGCAGTAA
Coxiv	CTCCAACGAATGGAAGACAG	TGACAACCTTCTTAGGGAAC
Coxi	CTAGCCGCAGGCATTACTAT	TGCCCAAAGAATCAGAACAG
TFAM	GAAGGGAATGGGAAAGGTAGA	AACAGGACATGGAAAGCAGAT
Sqstm1	TGTGGTGGGAACTCGCTATAA	CAGCGGCTATGAGAAGCTAT

Results:

Kinase activation with acute contractile activity

Acute contractile activity of myotubes was sufficient to activate kinases known to significantly increase following exercise. Phosphorylation of p44 (ERK1) and CamK increased 4.4- and 1.8-fold compared to control cells, respectively, immediately after 2 hours of stimulation. Phosphorylation levels returned to control levels following 2 hours of recovery (Fig. 1A, 1D). AMPK and p38 also demonstrated trends to increase after 2 hours of stimulation and 2 hours of recovery (Fig. 1C, 1E), but this was not observed for p42 (ERK2) (Fig. 1B). Similar trends were observed with 5 hours of stimulation. The phosphorylation of kinases Camk, p44 and p38 were increased ($p<0.05$) as a result of contractile activity (Figs. 2A, 2D, 2E), while two kinases, p42 and AMPK were not significantly altered with stimulation (Figs. 2B, 2C).

TFEB promoter activity

Similar to the documented literature, serum starvation for 4 or 6 hours tended to increase the luciferase activity of the TFEB 1600 bp pair promoter by 1.8-fold compared to control myotubes (Fig. 3A) ($p=0.07$). This tendency was not observed in cells transfected with TFEB 1200 bp promoter (Fig. 3A). In response to acute contractile activity, we first tested the response of the PGC-1α promoter, which we have shown to increase previously (47). Our data demonstrate that the acute stimulation protocol was effective, since PGC-1α promoter activity was upregulated by 1.6-fold ($p<0.05$) (Fig. 3B).

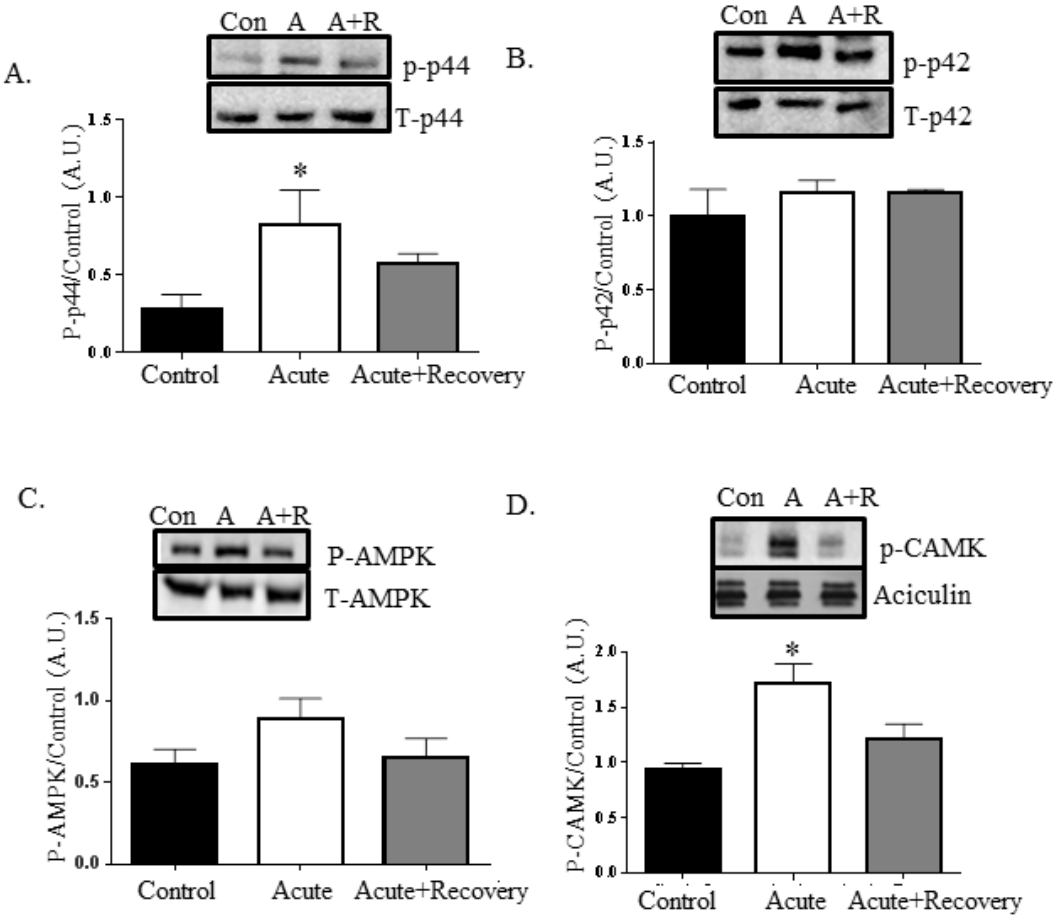

Figure 1: Acute contractile activity induces the phosphorylation of kinases. C2C12 myotubes were subjected to 2 hours of acute stimulation followed by a 2 hour recovery period. A) p44; B) p42; C) AMPK; D) CamK; E) p38 (n=3-7). Data are expressed in arbitrary units of phosphorylated protein content over control, loading control or total kinase content (A.U ± SEM).
*, $p<0.05$ Control vs. Acute.

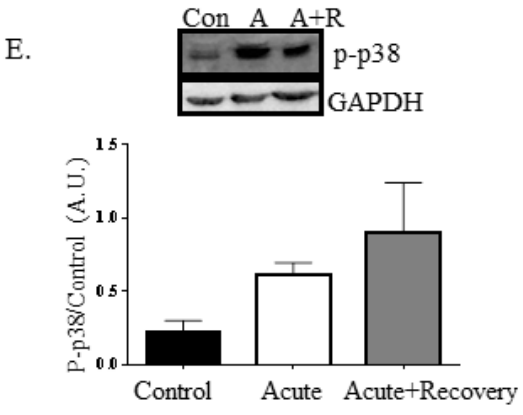

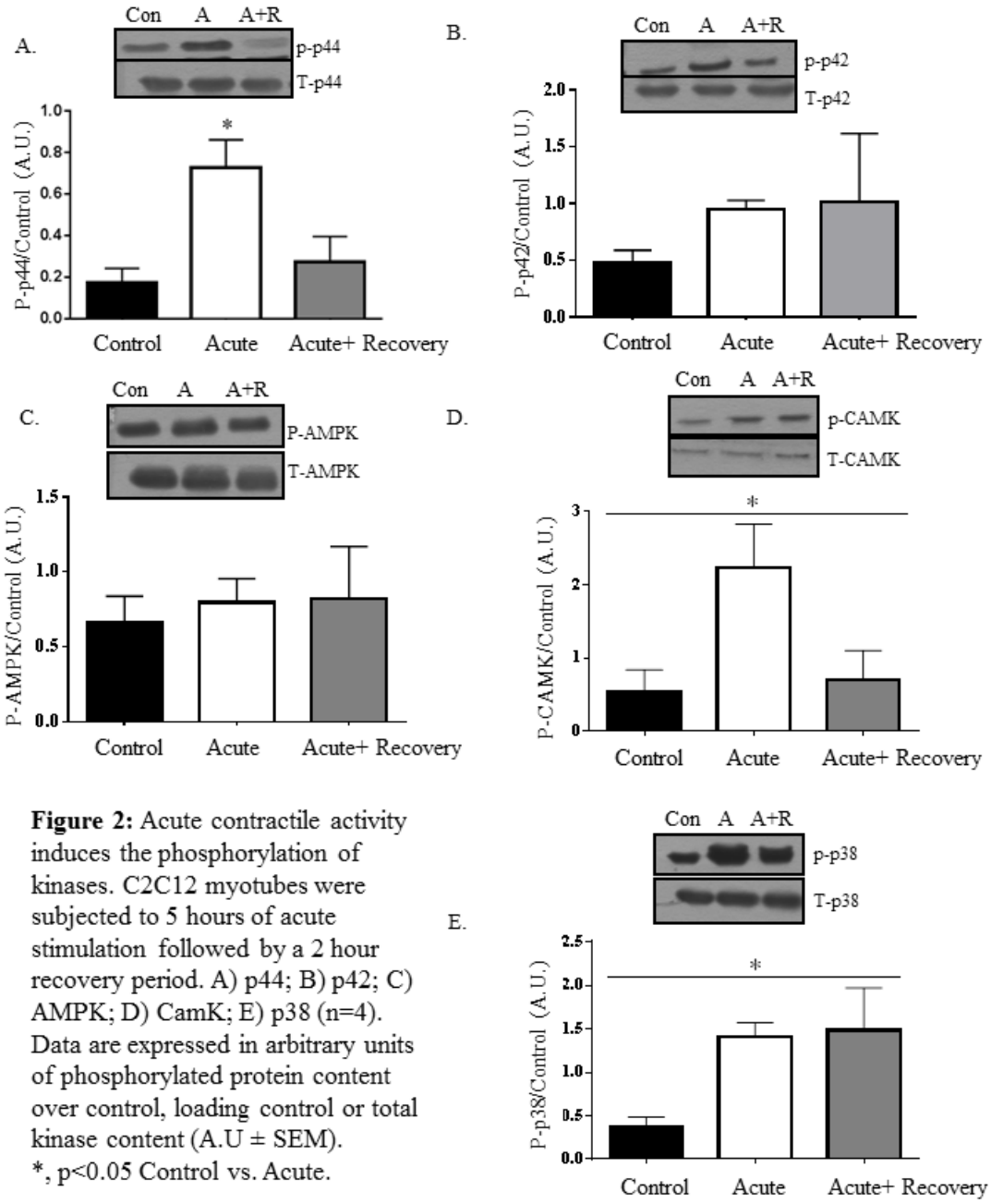

Figure 2: Acute contractile activity induces the phosphorylation of kinases. C2C12 myotubes were subjected to 5 hours of acute stimulation followed by a 2 hour recovery period. A) p44; B) p42; C) AMPK; D) CamK; E) p38 (n=4). Data are expressed in arbitrary units of phosphorylated protein content over control, loading control or total kinase content (A.U ± SEM). *, $p<0.05$ Control vs. Acute.

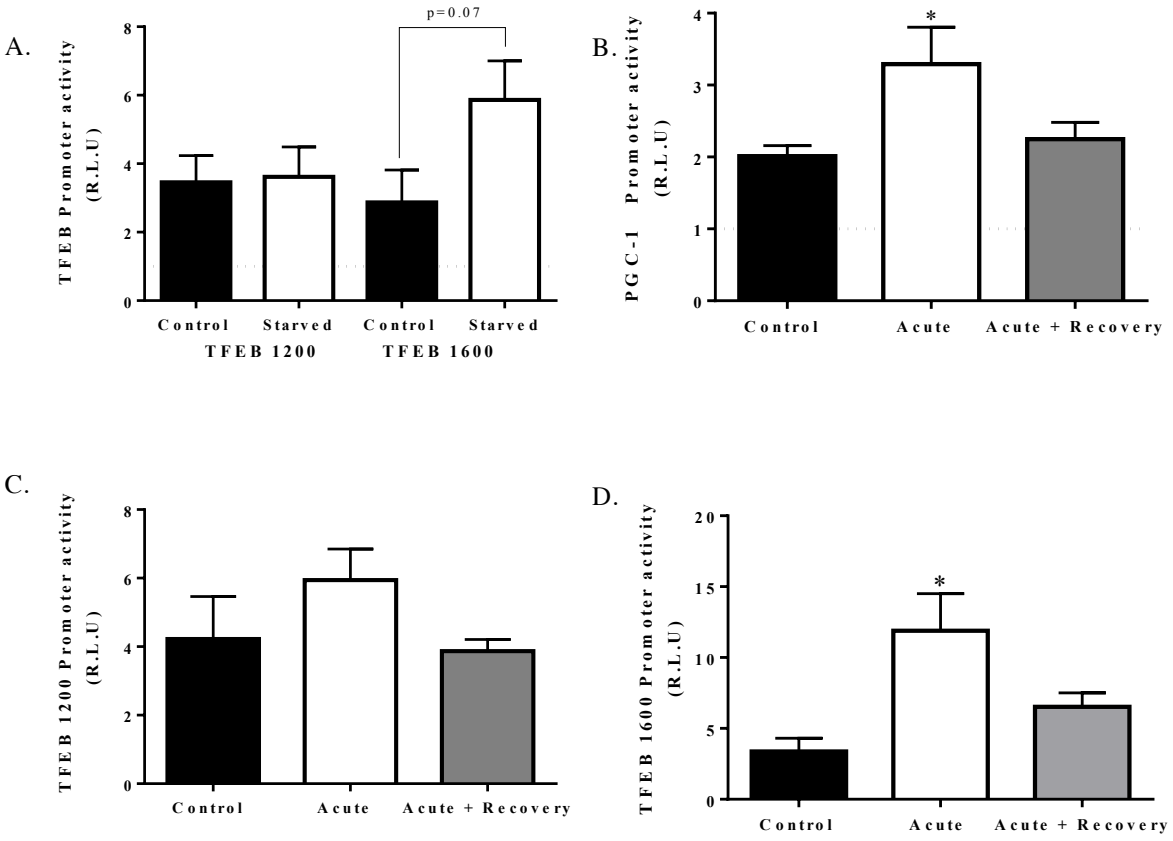

Figure 3: A) Cells transfected with TFEB 1200bp or 1600bp promoter construct were subjected to 4 hours of serum starvation. Cells transfected with B) PGC-1α promoter, C) TFEB 1200 bp promoter or D) the TFEB 1600 bp promoter were subjected to 2 hours of acute stimulation or 2 hours of stimulation and 2 hours of recovery. Graphs represent luciferase activity, fold over PGL3-Basic empty vector (n=4-9, data are X ± SEM) *, $p<0.05$, Control vs. Acute.

Interestingly, myotubes transfected with the 1600 bp, but not 1200 bp TFEB promoter, demonstrated increased activity following 2 hours of contractile activity (Fig. 3C, 3D).

TFEB Localization

Using serum starvation as a positive control, we observed TFEB translocation to the nucleus following 6 hours of treatment (Fig. 4A). In response to contractile activity, 2 hours of stimulation and recovery induced TFEB translocation to the nucleus (Fig. 4B). This trend was further amplified with 5 hours of stimulation (Fig. 4C). To examine whether this translocation was due to calcineurin dephosphorylation of TFEB, we used cyclosporin A, a well-established inhibitor of calcineurin. Cells treated with the DMSO vehicle exhibited a 2-fold increase in nuclear TFEB content following acute stimulation, however cyclosporin A treated cells demonstrated no contractile activity-induced TFEB translocation (Fig. 4D). Immunofluorescent staining of myotubes following 5 hours of acute stimulation supported the protein translocation data by demonstrating a potential increase in the co-localization of DAPI nuclear staining and TFEB (Fig. 5).

TFEB overexpression

To further examine the role of TFEB in muscle cells, adenoviral infection for 4 or 7 days was utilized to overexpress the protein. Seven days of viral infection revealed a marked escalation of TFEB protein content, as expected, compared to GFP-infected cells (Fig. 6A). When these cells were stimulated to contract, an approximate 2-fold increase

in TFEB nuclear translocation was observed following 5 hours of acute stimulation and recovery (Fig. 6B, 6C).

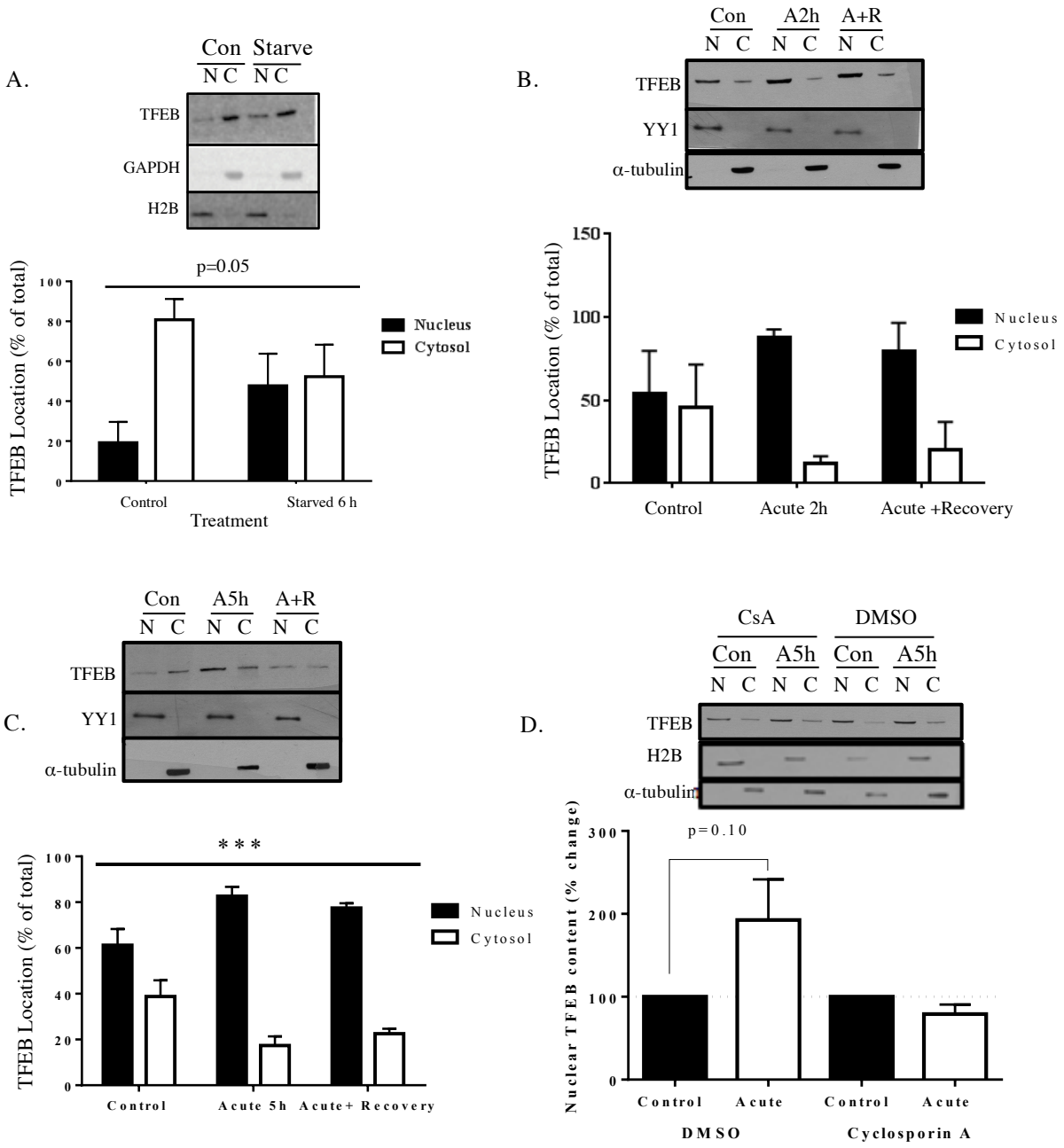

Figure 4: The location of TFEB protein following A) 6 hours of serum starvation, B) 2 hours of stimulation and recovery or C) 5 hours of stimulation and recovery. D) Nuclear TFEB content change following 5 hours of stimulation with either Cyclosporin A (CsA) (10nM per well) or DMSO as a control. (A-C) Black bars represent nuclear TFEB content and white bars represent cytosolic TFEB content. D) Black bars are representative of control levels, white bars represent 5 hours of acute stimulation. Above graphs are representative western blots. YY1 or H2B and α-tubulin or GAPDH are used as nuclear and cytosolic loading controls, respectively (n=4-5, data are X ± SEM, ***, $p<0.0005$, interaction effect of fraction and stimulation).

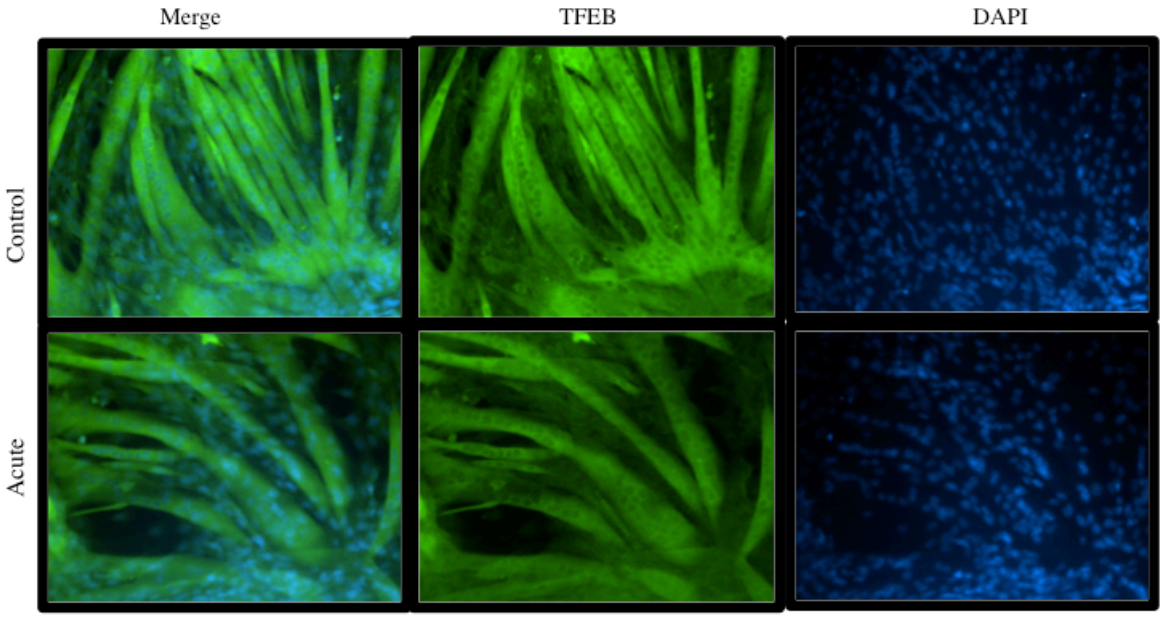

Figure 5: Fixed cell immunofluorescent microscopy of C2C12 myotubes co-stained for DAPI and TFEB (20x magnification). Fully differentiated myotubes were acutely stimulated for 5 hours or left as control cells and then used immediately for staining. Merge is an overlay of TFEB and DAPI staining.

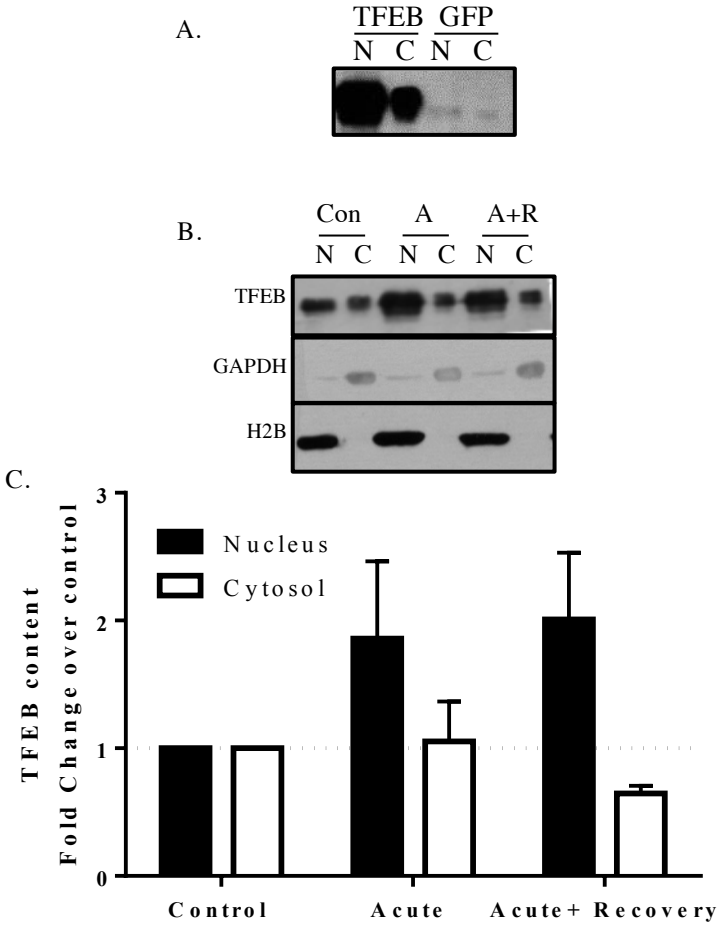

Figure 6: A) Representative TFEB blot of cells infected with either TFEB or GFP adenovirus, B, C) Representative blot and graphical representations of nuclear and cytosolic cellular fractions of TFEB overexpressing cells following 5 hours of acute stimulation and recovery normalized to nuclear and cytosolic loading controls, H2B and GAPDH, respectively. (n=4, data are X ± SEM).

To document the impact of TFEB on its potential downstream targets, as well as the effect of contractile activity, a shorter infection time (4 days) using either TFEB or GFP (control), was employed. Using GFP-infected control cells as a standard, mRNA levels of the mitochondrial biogenesis markers COXIV and COXI indicated trends to increase following 5 hours of acute contractile activity (Fig. 7A), however no change was observed in PGC-1α or TFAM mRNA levels. Furthermore, we observed no alterations following stimulation or recovery on the autophagy markers TFEB, LC3 LAMP2, Cathepsin D or Belcin 1 (Fig. 7B). However, p62 was significantly increased with acute stimulation and recovery (Fig. 7B).

In TFEB overexpressing cells, the mRNA levels of mitochondrial biogenesis markers PGC-1α and COXIV were significantly increase by 5-6-fold in control, non-stimulated cells (Fig. 7C). TFEB overexpression also produced significant increases in TFEB mRNA, as well as in the autophagy markers, LC3, LAMP2 and p62 (Fig. 7D). Contractile activity induced some intriguing trends. TFEB mRNA, though increased in control conditions, was significantly reduced following stimulation, and further decreased with 2 hours of recovery (Fig. 7D). LC3 and LAMP2 mRNAs displayed a similar pattern. PGC-1α and COXIV mRNAs, elevated under TFEB overexpression conditions, were not further changed by contractile activity and/or recovery (Fig. 7D).

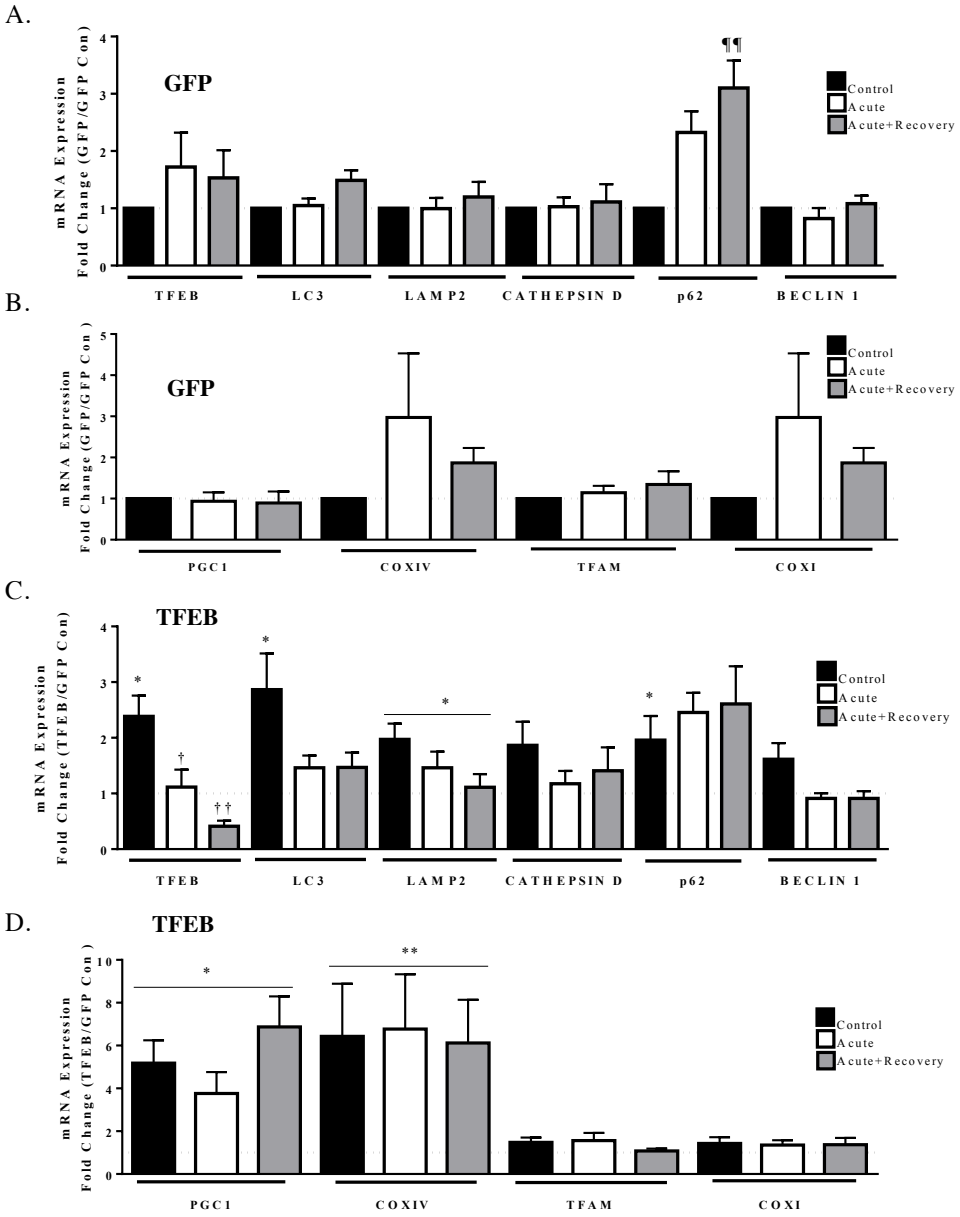

Figure 7: Real Time PCR analysis of mRNA in cells overexpressing adenoviral (A, B) GFP or (C, D) TFEB under control settings, following 5 hours of acute stimulation with or without 2 hours of recovery. A, B) Effect of stimulation and recovery on GFP infected cells A) autophagy mRNAs and B) mitochondrial biogenesis mRNAs. C, D) Effect of stimulation and recovery on TFEB overexpressing cells C) autophagy mRNAs and D) mitochondrial biogenesis mRNAs. Transcript levels are normalized to both β-Actin and GAPDH. (*,$P < 0.05$, **,$P < 0.05$,vs. Control levels of GFP cells of the transcript. †, $P < 0.05$, ††, $P < 0.005$ vs. Control levels of TFEB cells of the transcript. ¶ , $p<0.05$, ¶ ¶ , $p<0.005$ effect of stimulation).

Mitophagy activation with acute contractile activity

Isolated mitochondria obtained from myotubes subjected to control conditions, or acute stimulation for 5 hours with or without 2 hours of recovery, were collected and probed for mitophagy markers. Mitochondrially-localized LC3-II increased significantly following stimulation and recovery (Fig. 8A, 8B). No alterations in mitochondrially-localized parkin was observed (Fig. 8A, 8C). Western blotting for p62 localization on mitochondria revealed a tendency to increase with stimulation and recovery (Fig. 8A, 8D). This corresponded with an increase in the co-localization of the mitochondrial target VDAC with p62 revealed by an increase in puncta using immunofluorescent staining immediately following 5 hours of stimulation compared to control cells (Fig. 9A). This trend was not observed when investigating the co-localization of VDAC and LAMP2 through immunofluorescent staining (Fig. 9B).

Effect of chronic contractile activity (CCA)

CCA successfully induced mitochondrial biogenesis, resulting in 2.3- and 2.2-fold increases ($p<0.05$) of cytochrome c oxidase subunits I and IV (COXI and COXIV) protein levels, respectively (Fig. 10A, 10B). To examine TFEB expression, cells were transfected with the 1200bp or 1600 bp TFEB promoter sequence and subjected to CCA. No effect of CCA was observed on the TFEB promoter activity (Fig. 11A, 11B). TFEB, TFE3 and p62 protein also exhibited no changes following 4 days of stimulation (Fig. 12A, 12B). However, the lysosomal marker cathepsin D was increased by 1.5-fold

($p<0.05$) with CCA, while LAMP2 was significantly reduced by 42% with CCA (Fig. 12A, 12B).

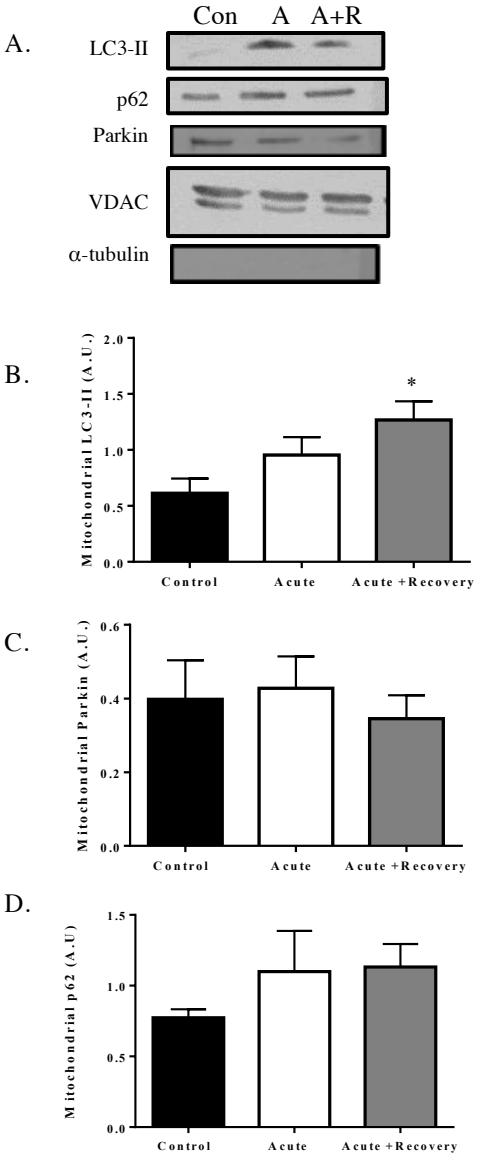

Figure 8: A) Representative western blots performed on isolated mitochondria from myotubes following 5 hours of stimulation with or without recovery and the corresponding graphical representation of mitochondrially localized B) LC3 C) Parkin and D) p62. (n=8-9, Data are expressed in arbitrary units X ± SEM *, $p<0.05$ compared to control samples.)

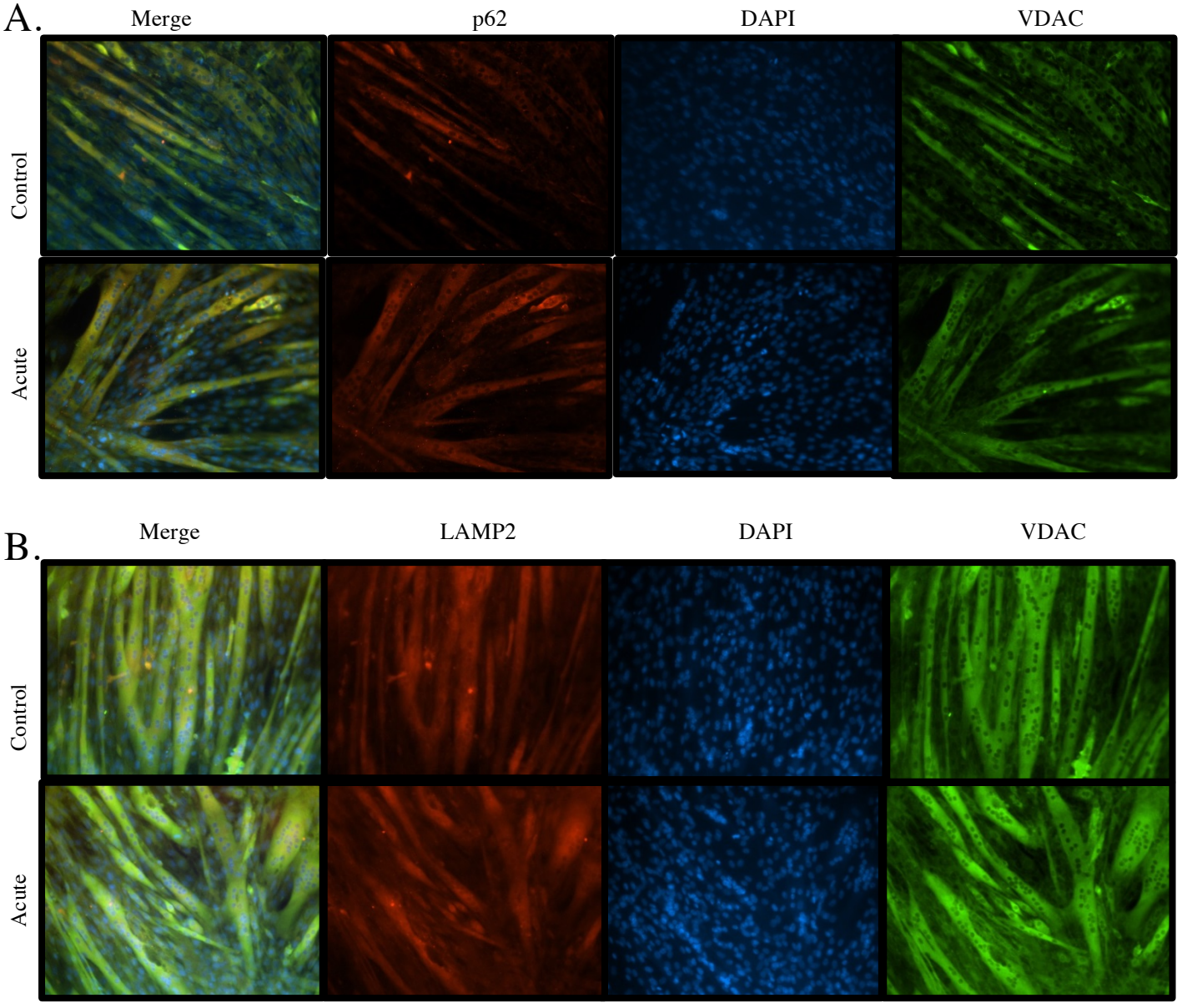

Figure 9: Fixed cell immunofluorescent microscopy of C2C12 myotubes co-stained for DAPI, VDAC and A) p62 or B) LAMP2 (20x magnification). Fully differentiated myotubes were acutely stimulated for 5 hours or left as control cells and then used immediately for staining. Merge is an overlay of A) p62, VDAC and DAPI stains, or B) LAMP2, VDAC and DAPI.

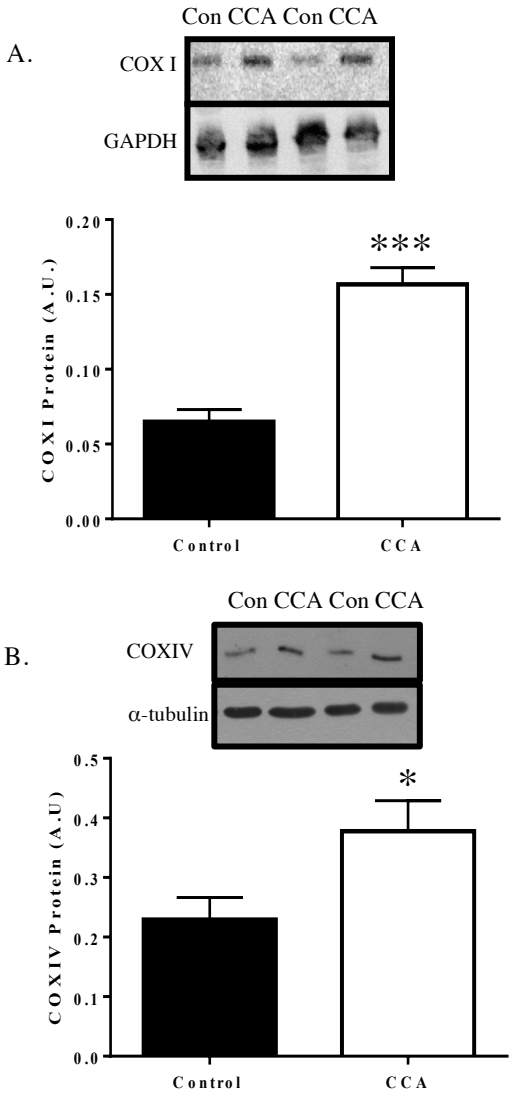

Figure 10: Western Blot demonstrating the effect of chronic contractile activity (CCA, 4 days of 3h/day followed by 21 hours of recovery) on A) COXI protein, and B) COXIV protein levels. Lanes represent control conditions and CCA. Graphical representation of the western blot (mean of n=4-11 experiments). Data are expressed in arbitrary units (A.U.). *, $p<0.05$, CCA vs. Control, ***, $p<0.0005$, CCA vs. Control

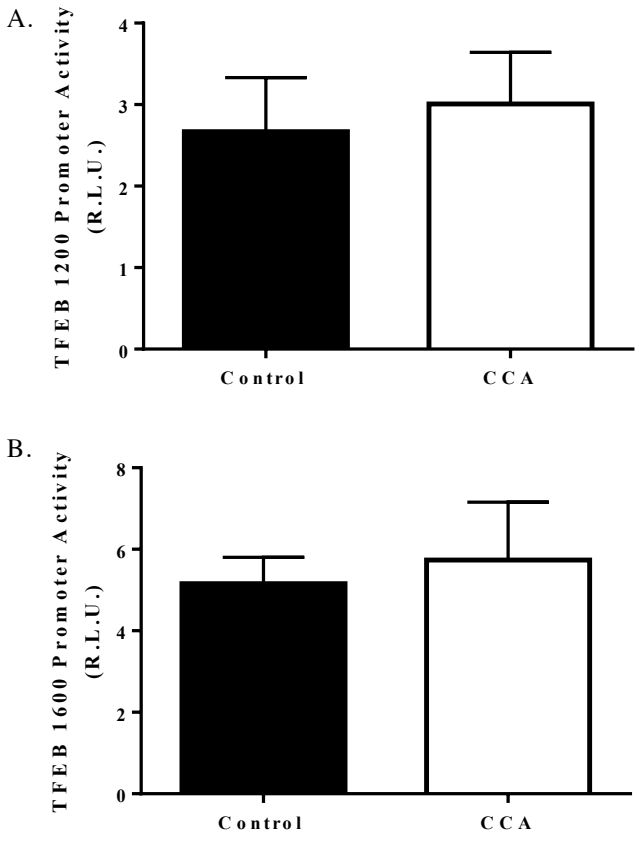

Figure 11: Cells transfected with A) the TFEB 1200 bp promoter, B) the TFEB 1600 bp promoter where subjected to 4 days of 3h/day chronic contractile activity (CCA) followed by 21 hours of recovery prior to collection. Graphs represent luciferase activity, fold over PGL3-Basic empty vector. There was no difference observed between treatments, (n=5-6, data are X ± SEM)

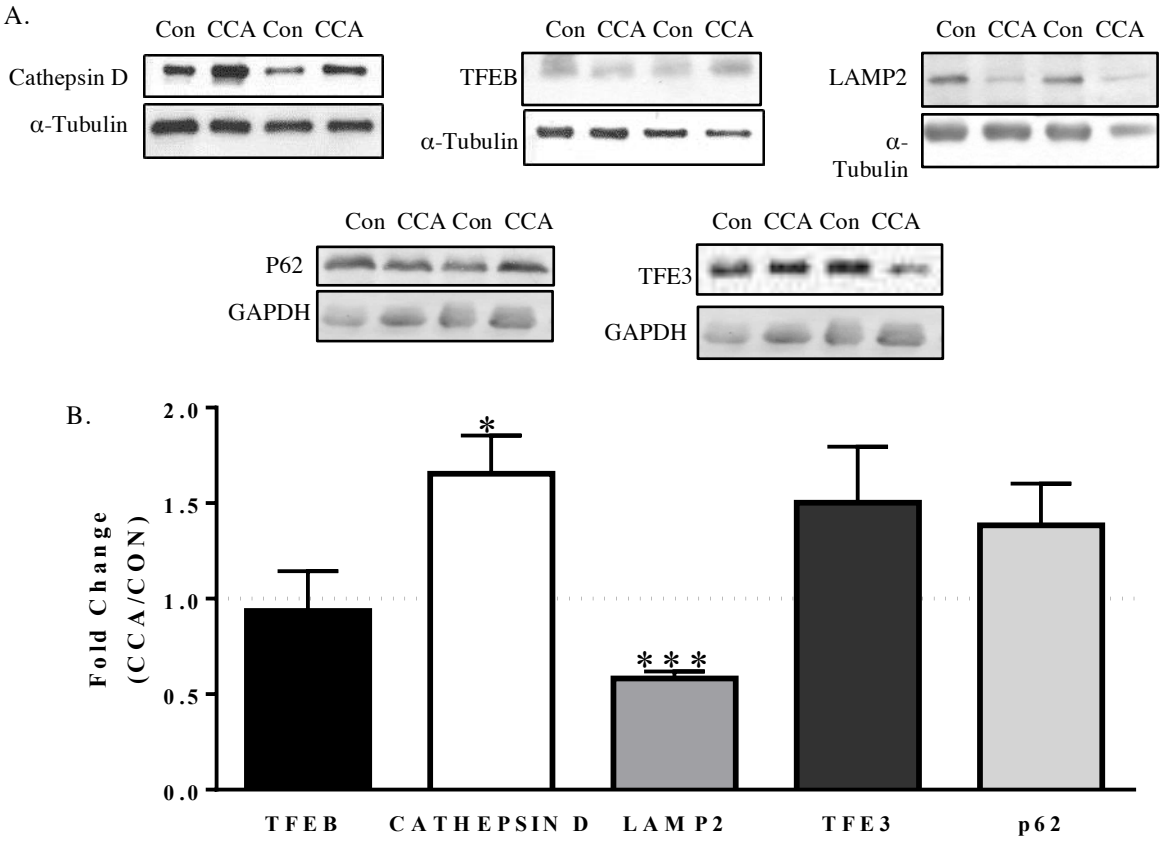

Figure 12: The effect of chronic contractile activity (CCA) on lysosomal markers. C2C12 myotubes were subjected to 3 hours/day for four days of chronic stimulation followed by a 21 hour recovery prior to collection. A) blots representing mature Cathepsin D, TFEB, LAMP2, p62 and TFE3 B) representative graphs (n=6-12) . Data are expressed in arbitrary units (X ± SEM). *, $p<0.05$, ***, $p<0.0005$ Control vs. Treatment.

Discussion:

Autophagy is an important and protective cellular maintenance pathway that is essential for muscle health. The value of this pathway is emphasized when the cellular stress is increased, as in exercising muscle. TFEB, as the documented master regulator of lysosomal biogenesis, controls the expression of multiple genes within the autophagy-lysosomal pathway. The overall objective of this study was to examine the activation and expression of TFEB and its downstream targets following acute or chronic exercise. Several studies have now documented that mitophagy is activated following a bout of exercise (12, 19, 42). However, only one study has demonstrated that TFEB is activated with exercise (24). Therefore, through the utilization of various cell culture investigations, we sought to elucidate the effect of contractile activity on TFEB expression, and on mitophagy. We hypothesized that TFEB would be activated following contractile activity and that it would upregulate the transcription of its downstream targets. Furthermore, we also surmised that following chronic contractile activity, there would be adaptations in TFEB and its downstream genes.

TFEB activation has been thoroughly investigated following serum starvation in cell culture (32, 33, 35). Thus, we used this treatment as a positive control for our findings, and we demonstrated that TFEB translocates to the nucleus with 6 hours of starvation. In addition, similar to the results of others (31, 48), we found that starvation increased TFEB transcription, as revealed by the transfection of myotubes with the TFEB

1600 bp promoter. The 1200 bp promoter did not respond to serum starvation. Similarly, contractile activity impacted only the 1600 bp promoter activity, while the 1200 bp promoter remained unaffected. Thus, these data suggest that the 400 bp segment which distinguishes these two promoter constructs is responsible for the differences in response to both starvation, as well as contractile activity. Investigation the promoter sequence unveiled a high concentration of putative transcription binding sites in the 400 bp region differentiating these two sequences. Putative sites included those that bind PPARα, GATA-1, Sp1, p53, myogenin and NF-κB. Confirmation of the functionality of these transcription factor binding sites on specific regions of the promoter will require a series of DNA binding ChIP assays. Interestingly, increased promoter activity coincided with trends seen in TFEB mRNA following acute contractile activity and recovery, as indicated with our mock GFP-infected cells. This tendency for an increase in TFEB mRNA coincided with contractile activity-induced increases in mitochondrial biogenesis marker mRNAs, such as, COXI and COXIV, as we have shown previously (28, 42), indicative that the stimulation paradigm was successful.

We then analyzed the impact of acute contractile activity on TFEB activation, measured by TFEB localization. TFEB translocation from the cytosol to the nucleus was increased with both 2 and 5 hours of acute contractile activity. TFEB translocation could be indicative of a decrease in TFEB inhibitor activity, or by increases in TFEB activator influences. TFEB is inhibited via phosphorylation by mTORC1 or ERK2 (13, 26, 27, 34, 35), and activated by the calcium-sensitive phosphatase calcineurin (23). To confirm the

activation of TFEB by calcineurin, we inhibited calcineurin activity with cyclosporin A. This drug completely inhibited TFEB translocation to the nucleus during contractile activity, suggesting an important role for calcineurin in the activity of TFEB during muscle contractions.

To further examine the role that TFEB plays in regulating its downstream target genes during and after an acute bout of exercise, we utilized an adenoviral overexpression model. Adenoviral infection resulted in large increases in TFEB protein in both the cytosolic and nuclear components. As predicted, TFEB overexpression alone resulted in the upregulation of mRNAs encoding the autophagy markers, LC3, LAMP2 and p62 (33, 34), but had no effect on cathepsin D. However, there was a substantial increase observed in the mRNA encoding the master regulator of mitochondrial biogenesis, PGC-1α, in addition to its downstream target COXIV. This suggests that the influence of TFEB as a regulator of lysosomal synthesis may be extended to mitochondrial biogenesis as well. Interestingly, in the TFEB overexpressing cells, an acute bout of contractile activity resulted in a significant decrease in TFEB mRNA, with a further decrease following a two-hour recovery period. This decrease was not observed in mock-infected cells. Thus, the TFEB overexpression model allows us the interpretation that contractile activity, in combination with excessive TFEB levels induces a decrease in TFEB mRNA levels, potentially via a decrease in transcription, or an increase in mRNA degradation. This result requires further investigation, suggesting that TFEB plays a role in controlling its own mRNA expression. A similar pattern was observed for LC3 and LAMP2. These

mRNAs were significantly increased following TFEB overexpression, however the levels were decreased with contractile activity. In contrast, p62 mRNA levels were increased with TFEB overexpression, and were further upregulated with contractile activity, indicative of a greater transcriptional drive for autophagy (11, 12, 19, 42). These divergent mRNA response suggest that these patterns are specific to the transcript, and not a result of non-specific mRNA degradation brought about by contractile activity.

Our data also provide further support for the mounting evidence which support the activation of mitophagy following a bout of exercise (6, 42). Our findings demonstrate that immediately following an acute bout of contractile activity, LC3-II is recruited to the mitochondria. Furthermore, a recovery period significantly increased the amount of LC3-II localized to the mitochondria, suggestive of continued mitophagy induction. We also noted that there was a trend for p62 to increase its localization to the mitochondria, in addition to LC3-II. These data suggest that signals generated during contractile activity (Fig. 1) are likely to serve to activate the autophagy pathway to flag specific mitochondrial segments for degradation and removal (41, 45).

Induction of the autophagic process has been documented to be essential for the benefits achieved from long-term chronic exercise (19). To examine the impact of chronic exercise on autophagy markers and TFEB expression, we chronically stimulated myotubes for four days to induce mitochondrial adaptations which are typical of regularly exercised muscle (20, 40). Following the 4 days stimulation and 21 hours recovery CCA

protocol, both TFEB promoter, as well as TFEB protein levels were found to be similar to control levels, while mitochondrial markers and cathepsin D were markedly elevated. It has been previously documented that various cathepsins increase in quantity and activity following exercise (2, 25, 29). Our results on p62 are also consistent with other studies analyzing exercise adaptations on autophagy which have observed no alterations in p62 protein content (19, 36, 37). The lack of change in p62 protein after 4 days of chronic stimulation demonstrates that autophagy is functioning, since an increase in p62 protein would be symptomatic of a dysfunctional pathway, or of autophagic build-up. Interestingly, LAMP2 protein content was severely decreased as a result of CCA. This has been demonstrated previously following a recovery period after a moderate bout of exercise (16). However, this essential lysosomal protein has scarcely been examined in context of exercise adaptations. Wohlgemuth et al. (2010) examined the alterations in LAMP2 mRNA with ageing, caloric restriction and life long exercise. These authors found that, although LAMP2 mRNA declined as a result of ageing compared to young animals, it was significantly increased with caloric restriction, and further increased in combination with exercise (46). However, there is much more examination that needs to be done as the pathways of autophagy remains generally unknown.

In summary, the present study has demonstrated that exercise, in the form of acute contractile activity, can activate TFEB transcription as well as its localization to the nucleus. The role of TFEB is important for long-term adaptation of lysosomes and lysosomal function, and it may also be important for mitochondrial biogenesis. Our

results also indicate that TFEB overexpression could act on its own transcript levels to decrease the over-abundance of TFEB mRNA present following contractile activity. Though further work needs to be done to elaborate on the many roles that TFEB plays, this study has shed some light on the part that TFEB plays in response to exercise

FUTURE WORK

In this study we show that TFEB responds to contractile activity by activating and translocating to the nucleus. It would be interesting to examine the activation of mitophagy that is dependent on TFEB. To answer this, TFEB could be silenced with the use of shRNA. Additionally, halting the autophagosome and lysosomal fusion with baflomycin A would allow for a measure of autophagy flux. Following this inhibition of autophagy and silencing of TFEB, we would chronically stimulate the cells to observe how much of the mitophagy pathways is dependent on TFEB activation and upregulation of it downstream targets. Furthermore, using this method, it would be interesting to analyze downstream target genes to examine if there are any compensatory mechanisms that have overlapping roles with the master regulator of lysosomal biogenesis.

We obtained interesting results concerning overexpressed TFEB mRNA levels in response to contractile activity. Some future work in regard to this would be to examine if the endogenous or exogenous TFEB, or both, are decreasing in response to exercise. If TFEB levels are demonstrating a decrease as a reaction to acute contractile activity, then it could provide novel insight into the autoregulatory pathway of TFEB. Adenoviral TFEB is GFP tagged and therefore through western blotting we could assess the levels of exogenous TFEB following contractile activity and recovery.

Further investigations remain to be done on lysosomal adaptations following chronic contractile activity. Many papers in the literature examining adaptations

following exercise are concerned with the autophagosomal pathway, and not the adaptations of lysosomal machinery (36, 37, 46). In our study we note that Cathepsin D levels are raised, accompanied with a decrease in LAMP2 protein following CCA. If this were a result of adaptations in the lysosome, we could utilize a tandem fluorescent-tagged LC3 to observe the functionality of lysosomes following chronic exercise and potential adaptations

Works Cited:

1. **Antunes D, Padrão AI, Maciel E, Santinha D, Oliveira P, Vitorino R, Moreira-Gonçalves D, Colaço B, Pires MJ, Nunes C, Santos LL, Amado F, Duarte JA, Domingues MR, Ferreira R**. Molecular insights into mitochondrial dysfunction in cancer-related muscle wasting. *Biochim Biophys Acta* 1841: 896–905, 2014.

2. **Carmeli E, Haimovitz T, Nemcovsky EC**. Cathepsin D and MMP-9 activity increase following a high intensity exercise in hind limb muscles of young rats. [Online]. *J Basic Clin Physiol Pharmacol* 18: 79–86, 2007. http://www.ncbi.nlm.nih.gov/pubmed/17569248 [18 Aug. 2015].

3. **Connor MK, Irrcher I, Hood DA**. Contractile activity-induced transcriptional activation of cytochrome C involves Sp1 and is proportional to mitochondrial ATP synthesis in C2C12 muscle cells. *J Biol Chem* 276: 15898–904, 2001.

4. **Ferraro E, Giammarioli AM, Chiandotto S, Spoletini I, Rosano G**. Exercise-induced skeletal muscle remodeling and metabolic adaptation: redox signaling and role of autophagy. *Antioxid Redox Signal* 21: 154–76, 2014.

5. **Handschin C, Spiegelman BM**. The role of exercise and PGC1alpha in inflammation and chronic disease. *Nature* 454: 463–9, 2008.

6. **He C, Bassik MC, Moresi V, Sun K, Wei Y, Zou Z, An Z, Loh J, Fisher J, Sun Q, Korsmeyer S, Packer M, May HI, Hill JA, Virgin HW, Gilpin C, Xiao G, Bassel-Duby R, Scherer PE, Levine B**. Exercise-induced BCL2-regulated autophagy is required for muscle glucose homeostasis. *Nature* 481: 511–5, 2012.

7. **Hood DA, Uguccioni G, Vainshtein A, D'souza D**. Mechanisms of exercise-induced mitochondrial biogenesis in skeletal muscle: implications for health and disease. *Compr Physiol* 1: 1119–34, 2011.

8. **Huang JH, Hood DA**. Age-associated mitochondrial dysfunction in skeletal muscle: Contributing factors and suggestions for long-term interventions. *IUBMB Life* 61: 201–14, 2009.

9. **Irrcher I, Adhihetty PJ, Sheehan T, Joseph A-M, Hood DA**. PPARgamma coactivator-1alpha expression during thyroid hormone- and contractile activity-induced mitochondrial adaptations. *Am J Physiol Cell Physiol* 284: C1669–77, 2003.

10. **Irwin WA, Bergamin N, Sabatelli P, Reggiani C, Megighian A, Merlini L, Braghetta P, Columbaro M, Volpin D, Bressan GM, Bernardi P, Bonaldo P**. Mitochondrial dysfunction and apoptosis in myopathic mice with collagen VI deficiency. *Nat Genet* 35: 367–71, 2003.

11. **Jamart C, Benoit N, Raymackers J-M, Kim HJ, Kim CK, Francaux M**. Autophagy-related and autophagy-regulatory genes are induced in human muscle after ultraendurance exercise. *Eur J Appl Physiol* 112: 3173–7, 2012.

12. **Jamart C, Naslain D, Gilson H, Francaux M**. Higher activation of autophagy in skeletal muscle of mice during endurance exercise in the fasted state. *Am J Physiol Endocrinol Metab* 305: E964–74, 2013.

13. **Joassard OR, Amirouche A, Gallot YS, Desgeorges MM, Castells J, Durieux A-C, Berthon P, Freyssenet DG**. Regulation of Akt-mTOR, ubiquitin-proteasome and autophagy-lysosome pathways in response to formoterol administration in rat skeletal muscle. *Int J Biochem Cell Biol* 45: 2444–55, 2013.

14. **Kane LA, Lazarou M, Fogel AI, Li Y, Yamano K, Sarraf SA, Banerjee S, Youle RJ**. PINK1 phosphorylates ubiquitin to activate Parkin E3 ubiquitin ligase activity. *J Cell Biol* 205: 143–53, 2014.

15. **Kim I, Rodriguez-Enriquez S, Lemasters JJ**. Selective degradation of mitochondria by mitophagy. *Arch Biochem Biophys* 462: 245–53, 2007.

16. **Kim YA, Kim YS, Song W**. Autophagic response to a single bout of moderate exercise in murine skeletal muscle. *J Physiol Biochem* 68: 229–35, 2012.

17. **Kondapalli C, Kazlauskaite A, Zhang N, Woodroof HI, Campbell DG, Gourlay R, Burchell L, Walden H, Macartney TJ, Deak M, Knebel A, Alessi DR, Muqit MMK**. PINK1 is activated by mitochondrial membrane potential depolarization and stimulates Parkin E3 ligase activity by phosphorylating Serine 65. *Open Biol* 2: 120080, 2012.

18. **Lemasters JJ**. Selective Mitochondrial Autophagy, or Mitophagy, as a Targeted Defense Against Oxidative Stress, Mitochondrial Dysfunction, and Aging. *Rejuvenation Res* 8: 3–5, 2005.

19. **Lira VA, Okutsu M, Zhang M, Greene NP, Laker RC, Breen DS, Hoehn KL, Yan Z**. Autophagy is required for exercise training-induced skeletal muscle adaptation and improvement of physical performance. *FASEB J* 27: 4184–93, 2013.

20. **Little JP, Safdar A, Wilkin GP, Tarnopolsky MA, Gibala MJ**. A practical model of low-volume high-intensity interval training induces mitochondrial biogenesis in human skeletal muscle: potential mechanisms. *J Physiol* 588: 1011–22, 2010.

21. **Maitra PK, Estabrook RW**. Studies of baker's yeast metabolism. II. The role of adenine nucleotides and inorganic phosphate in the control of respiration during alcohol oxidation. *Arch Biochem Biophys* 121: 129–39, 1967.

22. **Martina JA, Chen Y, Gucek M, Puertollano R**. MTORC1 functions as a transcriptional regulator of autophagy by preventing nuclear transport of TFEB. *Autophagy* 8: 903–14, 2012.

23. **Medina DL, Di Paola S, Peluso I, Armani A, De Stefani D, Venditti R, Montefusco S, Scotto-Rosato A, Prezioso C, Forrester A, Settembre C, Wang W, Gao Q, Xu H, Sandri M, Rizzuto R, De Matteis MA, Ballabio A**. Lysosomal calcium signalling regulates autophagy through calcineurin and TFEB. *Nat Cell Biol* 17: 288–299, 2015.

24. **Medina DL, Di Paola S, Peluso I, Armani A, De Stefani D, Venditti R, Montefusco S, Scotto-Rosato A, Prezioso C, Forrester A, Settembre C, Wang W, Gao Q, Xu H, Sandri M, Rizzuto R, De Matteis MA, Ballabio A**. Lysosomal calcium signalling regulates autophagy through calcineurin and TFEB. *Nat Cell Biol* 17: 288–299, 2015.

25. **Ohno H, Kizaki T, Ohishi S, Yamashita H, Tanaka J, Gasa S**. Effects of swimming training on the lysosomal enzyme system in brown adipose tissue of rats: an analogy between swimming exercise and cold acclimation. *Acta Physiol Scand* 155: 333–4, 1995.

26. **Peña-Llopis S, Vega-Rubin-de-Celis S, Schwartz JC, Wolff NC, Tran TAT, Zou L, Xie X-J, Corey DR, Brugarolas J**. Regulation of TFEB and V-ATPases by mTORC1. *EMBO J* 30: 3242–58, 2011.

27. **Roczniak-Ferguson A, Petit CS, Froehlich F, Qian S, Ky J, Angarola B, Walther TC, Ferguson SM**. The transcription factor TFEB links mTORC1 signaling to transcriptional control of lysosome homeostasis. *Sci Signal* 5: ra42, 2012.

28. **Saleem A, Carter HN, Hood DA**. p53 is necessary for the adaptive changes in cellular milieu subsequent to an acute bout of endurance exercise. *Am J Physiol Cell Physiol* 306: C241–9, 2014.

29. **Salminen A**. Lysosomal changes in skeletal muscles during the repair of exercise injuries in muscle fibers. [Online]. *Acta Physiol Scand Suppl* 539: 1–31, 1985. http://www.ncbi.nlm.nih.gov/pubmed/2988270 [18 Aug. 2015].

30. **Sardiello M, Palmieri M, di Ronza A, Medina DL, Valenza M, Gennarino VA, Di Malta C, Donaudy F, Embrione V, Polishchuk RS, Banfi S, Parenti G, Cattaneo E, Ballabio A**. A gene network regulating lysosomal biogenesis and function. *Science* 325: 473–7, 2009.

31. **Settembre C, De Cegli R, Mansueto G, Saha PK, Vetrini F, Visvikis O, Huynh T, Carissimo A, Palmer D, Klisch TJ, Wollenberg AC, Di Bernardo D, Chan L, Irazoqui JE, Ballabio A**. TFEB controls cellular lipid metabolism through a starvation-induced autoregulatory loop. *Nat Cell Biol* 15: 647–58, 2013.

32. **Settembre C, De Cegli R, Mansueto G, Saha PK, Vetrini F, Visvikis O, Huynh T, Carissimo A, Palmer D, Klisch TJ, Wollenberg AC, Di Bernardo D, Chan L, Irazoqui JE, Ballabio A**. TFEB controls cellular lipid metabolism through a starvation-induced autoregulatory loop. *Nat Cell Biol* 15: 647–58, 2013.

33. **Settembre C, Di Malta C, Polito VA, Garcia Arencibia M, Vetrini F, Erdin S, Erdin SU, Huynh T, Medina D, Colella P, Sardiello M, Rubinsztein DC, Ballabio A**. TFEB links autophagy to lysosomal biogenesis. *Science* 332: 1429–33, 2011.

34. **Settembre C, Medina DL**. TFEB and the CLEAR network. *Methods Cell Biol* 126: 45–62, 2015.

35. **Settembre C, Zoncu R, Medina DL, Vetrini F, Erdin S, Erdin S, Huynh T, Ferron M, Karsenty G, Vellard MC, Facchinetti V, Sabatini DM, Ballabio A**. A lysosome-to-nucleus signalling mechanism senses and regulates the lysosome via mTOR and TFEB. *EMBO J* 31: 1095–108, 2012.

36. **Tam BT, Pei XM, Yu AP, Sin TK, Leung KK, Au KK, Chong JT, Yung BY, Yip SP, Chan LW, Wong CS, Siu PM**. Autophagic adaptation is associated with exercise-induced fibre-type shifting in skeletal muscle. *Acta Physiol (Oxf)* 214: 221–36, 2015.

37. **Tam BT, Pei XM, Yung BY, Yip SP, Chan LW, Wong CS, Siu PM**. Autophagic Adaptations to Long-term Habitual Exercise in Cardiac Muscle. *Int J Sports Med* 36: 526–34, 2015.

38. **Tong Y, Song F**. Intracellular calcium signaling regulates autophagy via calcineurin-mediated TFEB dephosphorylation. *Autophagy* (June 4, 2015). doi: 10.1080/15548627.2015.1054594.

39. **Twig G, Elorza A, Molina AJA, Mohamed H, Wikstrom JD, Walzer G, Stiles L, Haigh SE, Katz S, Las G, Alroy J, Wu M, Py BF, Yuan J, Deeney JT, Corkey BE, Shirihai OS**. Fission and selective fusion govern mitochondrial segregation and elimination by autophagy. *EMBO J* 27: 433–46, 2008.

40. **Uguccioni G, Hood DA**. The importance of PGC-1α in contractile activity-induced mitochondrial adaptations. *Am J Physiol Endocrinol Metab* 300: E361–71, 2011.

41. **Vainshtein A, Desjardins EM, Armani A, Sandri M, Hood DA**. PGC-1α modulates denervation-induced mitophagy in skeletal muscle. *Skelet Muscle* 5: 9, 2015.

42. **Vainshtein A, Tryon LD, Pauly M, Hood DA**. Role of PGC-1α during acute exercise-induced autophagy and mitophagy in skeletal muscle. *Am J Physiol Cell Physiol* 308: C710–9, 2015.

43. **Vincow ES, Merrihew G, Thomas RE, Shulman NJ, Beyer RP, MacCoss MJ, Pallanck LJ**. The PINK1-Parkin pathway promotes both mitophagy and selective respiratory chain turnover in vivo. *Proc Natl Acad Sci U S A* 110: 6400–5, 2013.

44. **Wei H, Liu L, Chen Q**. Selective removal of mitochondria via mitophagy: distinct pathways for different mitochondrial stresses. *Biochim. Biophys. Acta* (March 31, 2015). doi: 10.1016/j.bbamcr.2015.03.013.

45. **Wei H, Liu L, Chen Q**. Selective removal of mitochondria via mitophagy: distinct pathways for different mitochondrial stresses. *Biochim. Biophys. Acta* (March 31, 2015). doi: 10.1016/j.bbamcr.2015.03.013.

46. **Wohlgemuth SE, Seo AY, Marzetti E, Lees HA, Leeuwenburgh C**. Skeletal muscle autophagy and apoptosis during aging: effects of calorie restriction and life-long exercise. *Exp Gerontol* 45: 138–48, 2010.

47. **Zhang Y, Uguccioni G, Ljubicic V, Irrcher I, Iqbal S, Singh K, Ding S, Hood DA**. Multiple signaling pathways regulate contractile activity-mediated PGC-1α gene expression and activity in skeletal muscle cells. *Physiol Rep* 2, 2014.

48. **Zhou J, Tan S-H, Nicolas V, Bauvy C, Yang N-D, Zhang J, Xue Y, Codogno P, Shen H-M**. Activation of lysosomal function in the course of autophagy via mTORC1 suppression and autophagosome-lysosome fusion. *Cell Res* 23: 508–23, 2013.

APPENDIX A:

DATA AND STATISTICAL ANALYSIS

Table 1A Individual values and Statistical analysis p-44 kinase western quantification

N	Control	Acute	Acute +Recovery
1	0.593762	0.704117	0.395528
2	0.168865	0.521097	0.398746
3	0.278891	1.972107	0.795919
4	0.06718	0.397177	0.41175
5	0.075221	0.189769	0.615285
6	0.108223	1.075855	0.514859
7	0.656131	0.913855	0.833479
Average	**0.278324714**	**0.824853857**	**0.566509429**
Std. Dev	**0.247987843**	**0.588812143**	**0.18720667**
Std. Error	**0.470061309**	**0.648318259**	**0.248724031**

One-way ANOVA summary	
F	3.541
P value	0.05
P value summary	ns
Are differences among means statistically significant? (P < 0.05)	no

Tukey's multiple comparisons test	Mean Diff.	95% CI of diff.	Significant?	Summary
Control vs. Acute	-0.5465	-1.071 to -0.02216	Yes	*
Control vs. Acute+ Recovery	-0.2882	-0.8126 to 0.2362	No	ns
Acute vs. Acute+ Recovery	0.2583	-0.2660 to 0.7827	No	ns

Table 1B Individual values and Statistical analysis p-38 kinase western quantification

N	Control	Acute	Acute +Recovery
1	0.071377	0.587715	0.425587
2	0.518297	0.545101	0.586465
3	0.22114	0.419732	0.315909
4	0.130479	0.93369	1.00915
5	0.188374	0.575888	2.177332
Average	**0.2259334**	**0.6124252**	**0.9028886**
Std. Dev	**0.173139671**	**0.191585392**	**0.759602401**
Std. Error	**0.364255711**	**0.244813784**	**0.799409387**

One-way ANOVA summary	
F	2.688
P value	0.1085
P value summary	ns
Are differences among means statistically significant? (P < 0.05)	No

Table 1C Individual values and Statistical analysis CamK kinase western quantification

N	Control	Acute	Acute +Recovery
1	0.894713	2.070499	1.4594
2	1.052291	1.594078	1.180135
3	0.857188	1.458613	0.981092
Average	**0.934730667**	**1.70773**	**1.206875667**
Std. Dev	**0.103524661**	**0.321385597**	**0.240272623**
Std. Error	**0.107078079**	**0.245932999**	**0.218712207**

One-way ANOVA summary	
F	8.057
P value	0.02
P value summary	*
Are differences among means statistically significant? (P < 0.05)	Yes

Tukey's multiple comparisons test	Mean Diff.	95% CI of diff.	Significant?	Summary
Control vs. Acute	-0.773	-1.372 to -0.1736	Yes	*
Control vs. Acute+Recovery	-0.2721	-0.8715 to 0.3273	No	ns
Acute vs. Acute+Recovery	0.5009	-0.09855 to 1.100	No	ns

Table 1D Individual values and Statistical analysis AMPK kinase western quantification

N	Control	Acute	Acute +Recovery
1	0.445202	0.663757	0.842799
2	0.562307	0.85757	0.568272
3	0.790585	1.321425	0.644742
4	0.521326	0.684622	1.005104
5	0.612414	0.914311	0.961524
6	1.056866	1.32801	0.29069
7	0.261742	0.429396	0.264636
Average	**0.607206**	**0.885584429**	**0.653966714**
Std. Dev	**0.255222472**	**0.337887704**	**0.301253925**
Std. Error	**0.327529848**	**0.359052043**	**0.372524545**

One-way ANOVA summary	
F	1.728
P value	0.2058
P value summary	ns
Are differences among means statistically significant? (P < 0.05)	No

Table 1E Individual values and Statistical analysis p-42 kinase western quantification

N	Control	Acute	Acute +Recovery
1	1.316398	1.12081	1.138547
2	0.693588	1.045773	1.203962
3	0.997958	1.318885	1.121405
Average	**1.002648**	**1.161822667**	**1.154638**
Std. Dev	**0.311431487**	**0.141099505**	**0.043567244**
Std. Error	**0.311019969**	**0.130904799**	**0.040544987**

One-way ANOVA summary	
F	0.6123
P value	0.5728
P value summary	ns
Are differences among means statistically significant? (P < 0.05)	No

Table 2A. Individual values and Statistical analysis 5 hours stimulation western blot for p-44

	Control	Acute	Acute+Recovery
1	0.194074	0.623001	0
2	0.329702	0.645426	0.206111
3	0.171314	0.521897	0.594043
4	0	1.120794	0.288464
Average	**0.1737725**	**0.72778**	**0.272155**
Std. Dev.	**0.117184775**	**0.231629356**	**0.213487717**
Std. Error	**0.281112829**	**0.271514914**	**0.409227805**

ANOVA summary	
F	6.961
P value	0.0149
P value summary	*
Are differences among means statistically significant? (P < 0.05)	Yes

Tukey's multiple comparisons test	Mean Diff.	95% CI of diff.	Significant?	Summary
Control vs. Acute	-0.5540	-0.9964 to -0.1116	Yes	*
Control vs. Acute +Recovery	-0.09838	-0.5407 to 0.3440	No	ns
Acute vs. Acute +Recovery	0.4556	0.01327 to 0.8980	Yes	*

Table 2B. Individual values and Statistical analysis 5 hours stimulation western blot for p-p42

	Control	Acute	Acute+Recovery
1	0.394121	0.716859	0.12947
2	0.707449	0.95876	0.509263
3	0.602481	1.007309	0.590488
4	0.202331	1.105908	2.812534
Average	**0.4765955**	**0.947209**	**1.010439**
Std. Dev.	**0.194398789**	**0.143171166**	**1.054892055**
Std. Error	**0.281590881**	**0.147106768**	**1.049428912**

ANOVA summary	
F	0.6538
P value	0.5431
P value summary	ns
Are differences among means statistically significant? (P < 0.05)	No

Table 2C. Individual values and Statistical analysis 5 hours stimulation western blot for p-AMPK

	Control	Acute	Acute+Recovery
1	0.385131	0.656583	0.643913
2	0.394078	0.417549	0
3	1.096307	1.047269	0.988801
4	0.791351	1.067405	1.657514
Average	**0.66671675**	**0.797202**	**0.822557**
Std. Dev.	**0.297365054**	**0.273611618**	**0.598603365**
Std. Error	**0.364182646**	**0.306443547**	**0.660018567**

ANOVA summary	
F	0.1207
P value	0.8878
P value summary	ns
Are differences among means statistically significant? (P < 0.05)	No

Table 2D. Individual values and Statistical analysis 5 hours stimulation western blot for p-CAMK

	Control	Acute	Acute+Recovery
1	0	3.889847	0
2	0	2.29934	0
3	0.955187	1.342403	1.508649
4	0	1.405455	1.27841
Average	**0.23879675**	**2.234261**	**0.696765**
Std. Dev.	**0.413608104**	**1.028047951**	**0.701503647**
Std. Error	**0.846398399**	**0.687775015**	**0.840401555**

ANOVA summary	
F	4.343
P value	0.0478
P value summary	*
Are differences among means statistically significant? (P < 0.05)	Yes

Tukey's multiple comparisons test	Mean Diff.	95% CI of diff.	Significant?	Summary
Control vs. Acute	-1.707	-3.488 to 0.07506	No	ns
Control vs. Acute +Recovery	-0.1691	-1.951 to 1.613	No	ns
Acute vs. Acute +Recovery	1.537	-0.2442 to 3.319	No	ns

Table 2E. Individual values and Statistical analysis 5 hours stimulation western blot for p-P38

	Control	Acute	Acute+Recovery
1	0.641502	1.598721	1.150089
2	0.389759	1.179306	1.857017
3	0.372638	1.755433	2.601992
4	0.065344	1.117883	0.325631
Average	**0.36731075**	**1.412836**	**1.483682**
Std. Dev.	**0.204265185**	**0.270859498**	**0.842965404**
Std. Error	**0.337036963**	**0.227875813**	**0.692052912**

ANOVA summary	
F	4.259
P value	0.0499
P value summary	*
Are differences among means statistically significant? (P < 0.05)	Yes

Tukey's multiple comparisons test	Mean Diff.	95% CI of diff.	Significant?	Summary
Control vs. Acute	-1.046	-2.241 to 0.1504	No	ns
Control vs. Acute +Recovery	-1.116	-2.312 to 0.07959	No	ns
Acute vs. Acute +Recovery	-0.07085	-1.267 to 1.125	No	ns

Table 3A: Individual values and Statistical analysis TFEB 1200 and TFEB 1600 Luciferase activity following 4 hours starvation.

	Control		Starved	
n	TFEB 1200	TFEB 1600	TFEB 1200	TFEB 1600
1	2.549756	2.066257	1.162701	1.888261
2	1.46021	5.099775	6.318415	5.414047
3	5.421218	6.294776	2.79602	8.015032
4	2.711568	2.153658	2.944525	8.230788
5	5.144786	2.456094	1.144682	5.752306
Average	**3.457507437**	**3.614111986**	**2.873268526**	**5.860086801**
Std. Dev	**1.553879172**	**1.747165705**	**1.886485019**	**2.291287189**
Std. Error	**0.835671679**	**0.91903763**	**1.112923347**	**0.946515003**

Unpaired t test	**TFEB 1200**
P value	0.8967
P value summary	ns
Significantly different? (P < 0.05)	No
One- or two-tailed P value?	Two-tailed
t, df	t=0.1340 df=8

Unpaired t test	**TFEB 1600**
P value	0.0789
P value summary	ns
Significantly different? (P < 0.05)	No
One- or two-tailed P value?	Two-tailed
t, df	t=2.013 df=8

Table 3B. Individual values and Statistical analysis for PGC-1α acute luciferase activity

N	Control	Acute	Acute +Recovery
1	2.291693	3.98788	3.51478
2	2.274057	3.10659	3.080477
3	2.4744	6.114063	2.263047
4	2.609477	3.87165	2.341885
5	2.12922	4.747927	2.226393
6	1.669398	1.58822	2.215397
7	1.461197	1.855363	1.750037
8	1.725403	1.58822	1.468689
9	1.484488	2.759499	1.386157
Average	**2.013259**	**3.291046**	**2.249651**
Std. Dev	**0.38892**	**1.381723**	**0.625009**
Std. Error	**0.274101**	**0.761648**	**0.416705**

One-way ANOVA summary	
F	4.073
P value	0.0300
P value summary	*
Are differences among means statistically significant? (P < 0.05)	Yes

Tukey's multiple comparisons test	Mean Diff.	95% CI of diff.	Significant?	Summary
Control vs. Acute	-1.278	-2.467 to -0.08810	Yes	*
Control vs. Acute+ Recovery	-0.2364	-1.426 to 0.9533	No	ns
Acute vs. Acute+ Recovery	1.041	-0.1483 to 2.231	No	ns

Table 3C. Individual values and Statistical analysis for TFEB 1200 acute luciferase activity

N	Control	Acute	Acute +Recovery
1	1.3789	4.47459	3.31075
2	9.467917	6.91045	3.49795
3	5.337527	4.37872	3.34581
4	1.378899897	9.467916	5.337529
5	4.474587363	6.910456	4.378714
6	3.310753327	3.497946	3.345809
Average	**4.2247641**	**5.94001**	**3.86943**
Std. Dev	**2.76359086**	**2.03627**	**0.75423**
Std. Error	**1.34453625**	**0.83549**	**0.38342**

One-way ANOVA summary	
F	1.489
P value	0.2572
P value summary	ns
Are differences among means statistically significant? (P < 0.05)	No

Table 3D. Individual values and Statistical analysis for TFEB 1600 acute luciferase activity

N	Control	Acute	Acute+Recovery
1	0.925943	12.85239	7.435615
2	4.84641	17.1473	5.711336
3	4.749111	4.67643	4.265276
4	3.000315	12.91322	8.705215
Average	**3.380445**	**11.89734**	**6.529361**
Std. Dev	**1.596197**	**4.517957**	**1.684554**
Std. Error	**0.86816**	**1.309837**	**0.659249**

One-way ANOVA summary	
F	0.0181
P value	*
P value summary	Yes
Are differences among means statistically significant? (P < 0.05)	0.5898

Tukey's multiple comparisons test	Mean Diff.	95% CI of diff.	Significant?	Summary
Control vs. Acute	-8.517	-15.20 to -1.832	Yes	*
Control vs. Acute +Recovery	-3.149	-9.834 to 3.536	No	ns
Acute vs. Acute +Recovery	5.368	-1.317 to 12.05	No	ns

Table 4A.i Individual values and Statistical analysis for 6 hour starvation nuclear and cytosolic western protein

A.U.	Control		Starved	
n	Nuclear	Cytosolic	Nuclear	Cytosolic
1	0.109404	2.032143	0.242523	2.15952
2	0.001921	0.475147	3.182567	0.495454
3	0.767936	0.902534	1.109008	0.868081
4	0.834045	0.206141	0.460372	0.169094
Average	**0.428326**	**0.903991**	**1.248618**	**0.923037**
Std. Dev	**0.375325**	**0.697071**	**1.161164**	**0.755508**
Std. Error	**0.573483**	**0.733153**	**1.039151**	**0.786374**

%	Control		Starved	
n	Nuclear	Cytosolic	Nuclear	Cytosolic
1	5.108624	94.89138	10.09654	89.90346
2	0.402619	99.59738	86.52932	13.47068
3	45.97125	54.02875	56.09298	43.90702
4	80.18232	19.81768	73.13693	26.86307
Average	**32.9162**	**67.0838**	**56.46394**	**43.53606**
Std. Dev	**32.53811**	**32.53811**	**28.86169**	**28.86169**
Std. Error	**5.671363**	**3.97268**	**3.840928**	**4.374186**

Table 4A. ii Individual values and Statistical analysis for 6 hour starvation nuclear and cytosolic western protein

Summary of Two- way ANOVA			
Source of Variation	P value	P value summary	Significant?
Interaction	0.0565	ns	No
Stimulation	> 0.9999	ns	No
Fractionation	0.0308	*	Yes

Tukey's multiple comparisons test	Significant?	Summary
Control :Nuclear vs. Control :Cytosol	Yes	*
Control :Nuclear vs. Starved 6:Nuclear	No	ns
Control :Nuclear vs. Starved 6:Cytosol	No	ns
Control :Cytosol vs. Starved 6:Nuclear	No	ns
Control :Cytosol vs. Starved 6:Cytosol	No	ns
Starved 6:Nuclear vs. Starved 6:Cytosol	No	ns

Table 4B.i Individual values and Statistical analysis for 2 hour stimulation nuclear and cytosolic western protein

2 HOUR A.U.	Control		Acute		Acute+ Recovery	
n	Nuclear	Cytosolic	Nuclear	Cytosolic	Nuclear	Cytosolic
1	0.195	0.093	1.506	0.163	0.980	0.035
2	0.0124	0.252	1.306	0.340	0.259	0.300
3	1.074	0.096	1.888	0.100	0.997	0.118
4	0.963	0.070	1.541	0.154	2.036	0.038
5	0.676	0.327	1.789	0.718	1.046	0.492
Average	**0.584**	**0.167**	**1.606**	**0.295**	**1.064**	**0.197**
Std. Dev	**0.466**	**0.114**	**0.233**	**0.253**	**0.633**	**0.197**
Std. Error	**0.610**	**0.279**	**0.184**	**0.466**	**0.614**	**0.444**

2 HOUR (%)	Control		Acute		Acute + Recovery	
n	Nuclear	Cytocolic	Nuclear	Cytocolic	Nuclear	Cytocolic
1	67.588	32.411	90.216	9.783795	96.480	3.519
2	4.691	95.308	79.340	20.65918	46.317	53.682
3	91.788	8.211	94.964	5.035862	89.415	10.584
4	93.176	6.823	90.896	9.103112	98.146	1.853
5	67.412	32.587	71.346	28.65302	67.997	32.002
Average	**64.931**	**35.068**	**85.353**	**14.6469938**	**79.671**	**20.328**
Std. Dev	**35.920**	**35.920**	**9.734**	**9.73491570**	**22.178**	**22.178**
Std. Error	**4.457**	**6.065**	**1.053**	**2.54365347**	**2.484**	**4.919**

Table 4B.ii Individual values and Statistical analysis for 5 hour stimulation nuclear and cytosolic western protein

Summary of Two- way ANOVA			
Source of Variation	P value	P value summary	Significant?
Interaction	0.1909	ns	No
Stimulation	> 0.9999	ns	No
Fractionation	< 0.0001	****	Yes

Tukey's multiple comparisons test	Significant?	Summary
Control :Nucleus vs. Control :Cytosol	No	ns
Control :Nucleus vs. Acute 5h:Nucleus	No	ns
Control :Nucleus vs. Acute 5h:Cytosol	No	ns
Control :Nucleus vs. Acute+ Recovery:Nucleus	No	ns
Control :Nucleus vs. Acute+ Recovery:Cytosol	No	ns
Control :Cytosol vs. Acute 5h:Nucleus	No	ns
Control :Cytosol vs. Acute 5h:Cytosol	No	ns
Control :Cytosol vs. Acute+ Recovery:Nucleus	No	ns
Control :Cytosol vs. Acute+ Recovery:Cytosol	No	ns
Acute 5h:Nucleus vs. Acute 5h:Cytosol	Yes	**
Acute 5h:Nucleus vs. Acute+ Recovery:Nucleus	No	ns
Acute 5h:Nucleus vs. Acute+ Recovery:Cytosol	Yes	**
Acute 5h:Cytosol vs. Acute+ Recovery:Nucleus	Yes	**
Acute 5h:Cytosol vs. Acute+ Recovery:Cytosol	No	ns
Acute+ Recovery:Nucleus vs. Acute+ Recovery:Cytosol	Yes	*

Table 4C. i Individual values and Statistical analysis for 5 hour stimulation nuclear and cytosolic western protein

5 HOUR A.U.	Control		Acute		Acute+ Recovery	
n	Nuclear	Cytosolic	Nuclear	Cytosolic	Nuclear	Cytosolic
1	0.107	0.145	0.830	0.115	0.144	0.047
2	1.010	0.573	4.204	1.325	5.548	1.945
3	4.610	1.369	7.963	0.752	1.186	0.3504
4	1.561	0.431	1.189	0.318	0.734	3.621
5	0.762	0.482	1.433	0.466	1.281	0.254
Average	**1.610**	**0.600**	**3.124**	**0.595**	**1.779**	**1.244**
Std. Dev	**1.756**	**0.458**	**3.018**	**0.4694**	**2.154**	**1.529**
Std. Error	**1.383**	**0.592**	**1.707**	**0.6081**	**1.615**	**1.370**

5 HOUR (%)	Control		Acute		Acute +Recovery	
n	Nuclear	Cytosolic	Nuclear	Cytosolic	Nuclear	Cytosolic
1	42.660	57.339	87.775	12.224	75.051	24.948
2	63.813	36.186	76.031	23.968	74.038	25.961
3	77.097	22.902	91.361	8.638	77.196	22.803
4	78.347	21.652	78.889	21.110	16.863	83.136
5	61.251	38.748	75.448	24.551	83.409	16.590
Average	**64.634**	**35.365**	**81.901**	**18.098**	**65.311**	**34.688**
Std. Dev	**14.477**	**14.477**	**7.231**	**7.231**	**27.326**	**27.326**
Std. Error	**1.800**	**2.434**	**0.799**	**1.699**	**3.381**	**4.639**

Table 4C. ii Individual values and Statistical analysis for 5 hour stimulation nuclear and cytosolic western protein

Summary of Two- way ANOVA			
Source of Variation	P value	P value summary	Significant?
Interaction	0.0009	***	Yes
Stimulation	> 0.9999	ns	No
Fractionation	< 0.0001	****	Yes

Tukey's multiple comparisons test	Significant?	Summary
Control :Nucleus vs. Control :Cytosol	No	ns
Control :Nucleus vs. Acute 5h:Nucleus	No	ns
Control :Nucleus vs. Acute 5h:Cytosol	Yes	**
Control :Nucleus vs. Acute+ Recovery:Nucleus	No	ns
Control :Nucleus vs. Acute+ Recovery:Cytosol	No	ns
Control :Cytosol vs. Acute 5h:Nucleus	Yes	**
Control :Cytosol vs. Acute 5h:Cytosol	No	ns
Control :Cytosol vs. Acute+ Recovery:Nucleus	No	ns
Control :Cytosol vs. Acute+ Recovery:Cytosol	No	ns
Acute 5h:Nucleus vs. Acute 5h:Cytosol	Yes	***
Acute 5h:Nucleus vs. Acute+ Recovery:Nucleus	No	ns
Acute 5h:Nucleus vs. Acute+ Recovery:Cytosol	Yes	**
Acute 5h:Cytosol vs. Acute+ Recovery:Nucleus	Yes	**
Acute 5h:Cytosol vs. Acute+ Recovery:Cytosol	No	ns
Acute+ Recovery:Nucleus vs. Acute+ Recovery:Cytosol	No	ns

Table 4D: Individual values and Statistical analysis for myotubes treated with Cyclosporin A or DMSO

	Cyclosporin A				DMSO			
A.U.	Control		Acute		Control		Acute	
n	Nuclear	Cytosolic	Nuclear	Cytosolic	Nuclear	Cytosolic	Nuclear	Cytosolic
1	1.521	0.347	2.072	0.471	0.182	0.261	2.352	0.478
2	0.310	0.241	0.190	0.279	0.216	0.416	0.241	0.490
3	0.113	0.394	0.206	0.773	0.193	0.440	1.025	1.586
4	0.209	0.282	0.153	1.240	0.143	0.550	1.862	0.890
Average	**0.538**	**0.316**	**0.655**	**0.691**	**0.183**	**0.417**	**1.370**	**0.861**
Std. Dev	**0.571**	**0.058**	**0.818**	**0.362**	**0.026**	**0.103**	**0.806**	**0.450**
Std. Error	**0.778**	**0.104**	**1.010**	**0.436**	**0.061**	**0.159**	**0.688**	**0.485**

	Cyclosporin A		DMSO	
Δ% Change	Control	Acute	Control	Acute
n	Nuclear	Nuclear	Nuclear	Nuclear
1	100	100.0611	100	202.106
2	100	49.49043	100	112.7844
3	100	93.98918	100	128.6953
4	100	73.16716	100	327.3711
Average	**100**	**79.177**	**100**	**192.739**
Std. Dev	**0**	**19.8303**	**0**	**84.717**
Std. Error	**0**	**2.22858**	**0**	**6.10219**

One-way ANOVA summary	
F	0.9363
P value	0.4534
P value summary	ns
Are differences among means statistically significant? (P < 0.05)	No

Table 6A.i Individual values and Statistical analysis for TFEB overexpressing cells stimulated for 5 hours.

A.U	Control		Acute		Acute+ Recovery	
n	Nuclear	Cytosolic	Nuclear	Cytosolic	Nuclear	Cytosolic
1	0.373	5.836	1.253	7.523	1.114	3.970
2	0.741	4.12	0.853	3.905	1.181	3.090
3	0.868	0.348	1.989	0.602	2.375	0.164
4	2.790	1.443	1.802	0.351	2.041	0.982
Average	**1.193**	**2.938**	**1.474**	**3.095**	**1.678**	**2.051**
Std. Dev	**0.939**	**2.16**	**0.449**	**2.915**	**0.543**	**1.538**
Std. Error	**0.860**	**1.263**	**0.369**	**1.657**	**0.419**	**1.073**

%	Control		Acute		Acute+ Recovery	
n	Nuclear	Cytocolic	Nuclear	Cytocolic	Nuclear	Cytocolic
1	6.018	93.981	14.285	85.714	21.917	78.082
2	15.23	84.763	17.92576	82.074	27.659	72.340
3	71.40	28.599	76.74535	23.254	93.518	6.481
4	65.913	34.086	83.67853	16.321	67.512	32.487
Average	**39.64**	**60.357**	**48.15877**	**51.841**	**52.651**	**47.348**
Std. Dev	**29.261**	**29.261**	**32.17251**	**32.172**	**29.411**	**29.411**
Std. Error	**4.647**	**3.7664**	**4.636041**	**4.468**	**4.053**	**4.274**

Table 6A. ii Individual values and Statistical analysis for TFEB overexpressing cells stimulated for 5 hours.

Fold Change	Control		Acute		Acute+ Recovery	
n	Nuclear	Cytocolic	Nuclear	Cytocolic	Nuclear	Cytocolic
1	1	1	3.354	1.288	2.981	0.680
2	1	1	1.149	0.946	1.592	0.748
3	1	1	2.289	1.731	2.733	0.473
4	1	1	0.645	0.243	0.73	0.680
Average	1	1	1.859	1.052	2.009	0.645
Std. Dev	0	0	1.048	0.543	0.905	0.103
Std. Error	0	0	0.768	0.530	0.638	0.128

Summary of Two- way ANOVA			
Source of Variation	P value	P value summary	Significant?
Interaction	0.7403	ns	No
Stimulation	0.9109	ns	No
Fractionation	0.1329	ns	No

Table 7A i. Individual values and Statistical analysis for TFEB mRNA normalized to 2 house-keeping genes.

N	GFP			TFEB		
	Control	Acute	Acute+ Recovery	Control	Acute	Acute+ Recovery
1	0.00196	0.00593	0.00281	0.00619	0.00122	0.00173
2	0.00203	0.00179	0.00153	0.0073	0.0013	0.00147
3	0.00133	0.00087	0.00114	0.00468	0.00164	0.00073
4	0.00241	0.00169	0.0014	0.00387	0.00149	0.00026
5	0.00385	0.00146	0.00154	0.00287	0.000001	0.00178
6	0.00067	0.00146	0.00228	0.00056	0.00341	0.00314
7	0.00024	0.0009	0.00122	0.00063	0.0006	0.00004
8	0.00221	0.00115	0.0031	0.00362	0.00164	0.00007
9	0.00044	0.00226	0.002257	0.0015	0.00121	0.00007
Average	**0.0016822**	**0.001945**	**0.0019196**	**0.0034688**	**0.0013901**	**0.0010322**
Std. Dev	**0.0010758**	**0.001468**	**0.0006743**	**0.0022233**	**0.0008716**	**0.0010112**
Std. Error	**0.026309**	**0.033301**	**0.0153916**	**0.0377491**	**0.023378**	**0.0314766**

Two-way ANOVA			
Source of Variation	P value	P value summary	Significant?
Interaction	0.012	*	Yes
Stimulation	0.0517	ns	No
Overexpression	0.7655	ns	No

Table 7A ii. Individual values and Statistical analysis for TFEB mRNA normalized to 2 house keeping genes

Tukey's multiple comparisons test	Significant?	Summary
control :GFP vs. control :TFEB	Yes	*
control :GFP vs. Acute :GFP	No	ns
control :GFP vs. Acute :TFEB	No	ns
control :GFP vs. Acute +Recovery:GFP	No	ns
control :GFP vs. Acute +Recovery:TFEB	No	ns
control :TFEB vs. Acute :GFP	No	ns
control :TFEB vs. Acute :TFEB	Yes	*
control :TFEB vs. Acute +Recovery:GFP	No	ns
control :TFEB vs. Acute +Recovery:TFEB	Yes	**
Acute :GFP vs. Acute :TFEB	No	ns
Acute :GFP vs. Acute +Recovery:GFP	No	ns
Acute :GFP vs. Acute +Recovery:TFEB	No	ns
Acute :TFEB vs. Acute +Recovery:GFP	No	ns
Acute :TFEB vs. Acute +Recovery:TFEB	No	ns
Acute +Recovery:GFP vs. Acute +Recovery:TFEB	No	ns

Table 7B i. Individual values and Statistical analysis for PGC-1α mRNA normalized to 2 house keeping genes.

N	GFP			TFEB		
	Control	Acute	Acute+ Recovery	Control	Acute	Acute+ Recovery
1	0.000411	0.0010516	0.00073903	0.0026484	0.0024704	0.0028845
2	0.000572	0.0008216	0.0002927	0.0043421	0.0055477	0.0042833
3	0.00077	0.00063	0.0006	0.24639	0.09892	0.02949
4	0.00075	0.00084	0.0004	0.08029	0.07092	0.08511
5	0.00152	0.00082	0.00041	0.00849	0.00044	0.02105
6	0.00038	0.00042	0.00088	0.00126	0.00103	0.00318
7	0.0015	0.00085	0.00031	0.00155	0.00182	0.00113
8	0.08724	0.0467	0.18723	0.1332	0.07991	0.13389
9	0.03603	0.04091	0.03456	0.10635	0.04875	0.03725
Average	**0.0143526**	**0.0103381**	**0.0250468**	**0.0649467**	**0.0344231**	**0.0353631**
Std. Dev	**0.0280106**	**0.0179415**	**0.0583148**	**0.0805166**	**0.0379383**	**0.0430163**
Std. Error	**0.233806**	**0.1764563**	**0.3684700**	**0.3159415**	**0.2044811**	**0.2287487**

Two-way ANOVA			
Source of Variation	P value	P value summary	Significant?
Interaction	0.4994	ns	No
Stimulation	0.6081	ns	No
Overexpression	0.0499	*	Yes

Table 7B ii. Individual values and Statistical analysis for PGC-1α mRNA normalized to 2 house keeping genes.

Tukey's multiple comparisons test	Significant?	Summary
control :GFP vs. control :TFEB	No	ns
control :GFP vs. Acute :GFP	No	ns
control :GFP vs. Acute :TFEB	No	ns
control :GFP vs. Acute +Recovery:GFP	No	ns
control :GFP vs. Acute +Recovery:TFEB	No	ns
control :TFEB vs. Acute :GFP	No	ns
control :TFEB vs. Acute :TFEB	No	ns
control :TFEB vs. Acute +Recovery:GFP	No	ns
control :TFEB vs. Acute +Recovery:TFEB	No	ns
Acute :GFP vs. Acute :TFEB	No	ns
Acute :GFP vs. Acute +Recovery:GFP	No	ns
Acute :GFP vs. Acute +Recovery:TFEB	No	ns
Acute :TFEB vs. Acute +Recovery:GFP	No	ns
Acute :TFEB vs. Acute +Recovery:TFEB	No	ns
Acute +Recovery:GFP vs. Acute +Recovery:TFEB	No	ns

Table 7C.i Individual values and Statistical analysis for LC3 mRNA normalized to 2 house keeping genes.

N	GFP			TFEB		
	Control	Acute	Acute+ Recovery	Control	Acute	Acute+ Recovery
1	0.07167	0.05075	0.05834	0.29381	0.11586	0.13585
2	0.04615	0.06044	0.10795	0.24354	0.06976	0.02949
3	0.04235	0.05113	0.03978	0.08029	0.07092	0.08511
4	0.09297	0.11637	0.13212	0.08258	0.07299	0.08138
5	0.02666	0.11828	0.04027	0.00944	0.12217	0.08419
6	0.04078	0.04309	0.04763	0.12068	0.04902	0.04411
7	0.08724	0.0467	0.16928	0.1332	0.07991	0.13389
8	0.03603	0.04091	0.03456	0.10635	0.04875	0.03725
Average	**0.055481**	**0.06595**	**0.078741**	**0.133736**	**0.07867**	**0.0789087**
Std. Dev	**0.023347**	**0.03016**	**0.0477412**	**0.0862585**	**0.02555**	**0.0382856**
Std. Error	**0.099120**	**0.11747**	**0.1701346**	**0.235872**	**0.09109**	**0.13629289**

Two-way ANOVA			
Source of Variation	P value	P value summary	Significant?
Interaction	0.0736	ns	No
Stimulation	0.4429	ns	No
Overexpression	0.0426	*	Yes

Table 7C.ii Individual values and Statistical analysis for LC3 mRNA normalized to 2 house-keeping genes.

Tukey's multiple comparisons test	Significant?	Summary
control :GFP vs. control :TFEB	Yes	*
control :GFP vs. Acute :GFP	No	ns
control :GFP vs. Acute :TFEB	No	ns
control :GFP vs. Acute +Recovery:GFP	No	ns
control :GFP vs. Acute +Recovery:TFEB	No	ns
control :TFEB vs. Acute :GFP	No	ns
control :TFEB vs. Acute :TFEB	No	ns
control :TFEB vs. Acute +Recovery:GFP	No	ns
control :TFEB vs. Acute +Recovery:TFEB	No	ns
Acute :GFP vs. Acute :TFEB	No	ns
Acute :GFP vs. Acute +Recovery:GFP	No	ns
Acute :GFP vs. Acute +Recovery:TFEB	No	ns
Acute :TFEB vs. Acute +Recovery:GFP	No	ns
Acute :TFEB vs. Acute +Recovery:TFEB	No	ns
Acute +Recovery:GFP vs. Acute +Recovery:TFEB	No	ns

Table 7D.i Individual values and Statistical analysis for LAMP2 mRNA normalized to 2 house-keeping genes.

N	GFP			TFEB		
	Control	Acute	Acute+ Recovery	Control	Acute	Acute+ Recovery
1	0.10647	0.06165	0.07526	0.24518	0.1514	0.10954
2	0.08105	0.07515	0.1243	0.17552	0.10624	0.05322
3	0.08758	0.11478	0.08736	0.14906	0.15915	0.15045
4	0.1194	0.07019	0.03306	0.10212	0.10899	0.05906
5	0.13633	0.07634	0.2562	0.19913	0.11929	0.15767
6	0.06433	0.08573	0.06583	0.15995	0.0778	0.04827
Average	**0.099193333**	**0.08064**	**0.107001667**	**0.171826667**	**0.120478333**	**0.096368333**
Std. Dev	**0.024220836**	**0.016881451**	**0.072012938**	**0.044079889**	**0.027716456**	**0.045503395**
Std. Error	**0.076903815**	**0.059447627**	**0.220148262**	**0.106339647**	**0.079851525**	**0.146580645**

Two-way ANOVA			
Source of Variation	P value	P value summary	Significant?
Interaction	0.1047	ns	No
Stimulation	0.1302	ns	No
Overexpression	0.0367	*	Yes

Table 7D.ii Individual values and Statistical analysis for LAMP2 mRNA normalized to 2 house-keeping genes.

Tukey's multiple comparisons test	Significant?	Summary
control :GFP vs. control :TFEB	No	ns
control :GFP vs. Acute :GFP	No	ns
control :GFP vs. Acute :TFEB	No	ns
control :GFP vs. Acute +Recovery:GFP	No	ns
control :GFP vs. Acute +Recovery:TFEB	No	ns
control :TFEB vs. Acute :GFP	Yes	*
control :TFEB vs. Acute :TFEB	No	ns
control :TFEB vs. Acute +Recovery:GFP	No	ns
control :TFEB vs. Acute +Recovery:TFEB	No	ns
Acute :GFP vs. Acute :TFEB	No	ns
Acute :GFP vs. Acute +Recovery:GFP	No	ns
Acute :GFP vs. Acute +Recovery:TFEB	No	ns
Acute :TFEB vs. Acute +Recovery:GFP	No	ns
Acute :TFEB vs. Acute +Recovery:TFEB	No	ns
Acute +Recovery:GFP vs. Acute +Recovery:TFEB	No	ns

Table 7E.i Individual values and Statistical analysis for Cathepsin D mRNA normalized to 2 house-keeping genes.

N	GFP			TFEB		
	Control	Acute	Acute+ Recovery	Control	Acute	Acute+ Recovery
1	0.11945	0.16174	0.11208	0.08669	0.12588	0.15055
2	0.0573	0.03902	0.00194	0.11837	0.13067	0.12018
3	0.03945	0.03667	0.06135	0.08037	0.03872	0.0209
4	0.02076	0.03387	0.03106	0.05808	0.02791	0.08351
5	0.05308	0.03	0.02985	0.05813	0.00202	0.07678
6	0.04535	0.04866	0.01914	0.03725	0.05466	0.02365
7	0.06852	0.02908	0.19495	0.07975	0.05913	0.04113
8	0.01466	0.02304	0.01545	0.06192	0.02404	0.01164
Average	**0.05232125**	**0.05026**	**0.0582275**	**0.07257**	**0.05787875**	**0.0660425**
Std. Dev	**0.030460593**	**0.042734641**	**0.060901836**	**0.022882322**	**0.043967469**	**0.047312826**
Std. Error	**0.133167823**	**0.190620157**	**0.252386612**	**0.084941815**	**0.182756106**	**0.184105658**

Two-way ANOVA			
Source of Variation	P value	P value summary	Significant?
Interaction	0.9064	ns	No
Stimulation	0.8444	ns	No
Overexpression	0.3766	ns	No

Table 7F.i Individual values and Statistical analysis for p62 mRNA normalized to 2 house keeping genes.

N	GFP			TFEB		
	Control	Acute	Acute+ Recovery	Control	Acute	Acute+ Recovery
1	0.35741	1.06036	1.35647	0.31973	0.54783	1.16356
2	0.11803	0.26007	0.32775	0.27364	0.224	0.41124
3	0.144	0.34903	0.66704	0.45373	0.34699	0.11331
4	0.10543	0.42213	0.27595	0.27635	0.45339	0.7145
5	0.25641	0.49977	0.49731	0.15272	0.33614	0.40096
6	0.06065	0.57498	0.33424	0.02481	0.54016	0.78738
7	0.19776	0.28829	0.19075	0.18847	0.40441	0.16348
8	0.23333	0.27452	0.96498	0.40099	0.50673	0.45562
9	0.09271	0.25413	0.25437	0.36301	0.29535	0.20079
Average	**0.17397**	**0.442586667**	**0.540984444**	**0.272605556**	**0.406111111**	**0.490093333**
Std. Dev	**0.089880159**	**0.243240909**	**0.369060946**	**0.125853254**	**0.107620443**	**0.323175983**
Std. Error	**0.215489767**	**0.365626323**	**0.501771167**	**0.241044428**	**0.168877714**	**0.461636012**

Two-way ANOVA			
Source of Variation	P value	P value summary	Significant?
Interaction	0.6175	ns	No
Stimulation	0.0034	**	Yes
Overexpression	0.9563	ns	No

Table 7F.ii Individual values and Statistical analysis for p62 mRNA normalized to 2 house-keeping genes.

Tukey's multiple comparisons test	Significant?	Summary
control :GFP vs. control :TFEB	No	ns
control :GFP vs. Acute :GFP	No	ns
control :GFP vs. Acute :TFEB	No	ns
control :GFP vs. Acute +Recovery:GFP	Yes	*
control :GFP vs. Acute +Recovery:TFEB	No	ns
control :TFEB vs. Acute :GFP	No	ns
control :TFEB vs. Acute :TFEB	No	ns
control :TFEB vs. Acute +Recovery:GFP	No	ns
control :TFEB vs. Acute +Recovery:TFEB	No	ns
Acute :GFP vs. Acute :TFEB	No	ns
Acute :GFP vs. Acute +Recovery:GFP	No	ns
Acute :GFP vs. Acute +Recovery:TFEB	No	ns
Acute :TFEB vs. Acute +Recovery:GFP	No	ns
Acute :TFEB vs. Acute +Recovery:TFEB	No	ns
Acute +Recovery:GFP vs. Acute +Recovery:TFEB	No	ns

Table 7G.i Individual values and Statistical analysis forBeclin1 mRNA normalized to 2 house keeping genes.

N	GFP			TFEB		
	Control	Acute	Acute+ Recovery	Control	Acute	Acute+ Recovery
1	0.05626	0.05374	0.05434	0.05159	0.03134	0.05147
2	0.02084	0.02122	0.02005	0.03993	0.02122	0.02808
3	0.03523	0.0191	0.02187	0.03004	0.02602	0.02216
4	0.02084	0.02929	0.02005	0.03993	0.02122	0.02808
5	0.0436	0.00269	0.02181	0.04054	0.03691	0.0185
6	0.04687	0.01533	0.0833	0.04875	0.03371	0.04547
Average	**0.037273333**	**0.023561667**	**0.036903333**	**0.041796667**	**0.028403333**	**0.032293333**
Std. Dev	**0.013145977**	**0.015664835**	**0.024078232**	**0.0069645**	**0.006028114**	**0.012040307**
Std. Error	**0.068091635**	**0.102052304**	**0.125340608**	**0.03406584**	**0.035768175**	**0.067000974**

Two-way ANOVA			
Source of Variation	P value	P value summary	Significant?
Interaction	0.7062	ns	No
Stimulation	0.1178	ns	No
Overexpression	0.7636	ns	No

Table 7H.i Individual values and Statistical analysis for COXIV mRNA normalized to 2 house keeping genes.

N	GFP			TFEB		
	Control	Acute	Acute+ Recovery	Control	Acute	Acute+ Recovery
1	0.00009	0.00009	0.00012	0.00122	0.00182	0.00155
2	0.00006	0.00006	0.00006	0.00138	0.00118	0.00093
3	0.00005	0.00011	0.00008	0.00008	0.0001	0.00011
4	0.00004	0.00003	0.00005	0.00007	0.00004	0.00022
5	0.00007	0.00022	0.00005	0.00026	0.00029	0.00019
6	0	0.00008	0.00001	0.00002	0.00003	0.00004
7	0.00001	0.00004	0.00006	0.00008	0.00008	0.00002
8	0.00005	0.00001	0.00011	0.00007	0.00006	0.00009
9	0.00002	0.00002	0.00004	0.00006	0.00002	0.00004
Average	**4.33333E-05**	**7.33333E-05**	**6.44444E-05**	**0.00036**	**0.000402222**	**0.000354444**
Std. Dev	**2.74874E-05**	**6.07362E-05**	**3.2356E-05**	**0.000507784**	**0.000610624**	**0.000499447**
Std. Error	**0.004175631**	**0.007092463**	**0.004030535**	**0.026762559**	**0.030446745**	**0.02652864**

Two-way ANOVA			
Source of Variation	P value	P value summary	Significant?
Interaction	0.9893	ns	No
Stimulation	0.9616	ns	No
Overexpression	0.0071	**	Yes

Table 7H.ii Individual values and Statistical analysis for COXIV mRNA normalized to 2 house-keeping genes.

Tukey's multiple comparisons test	Significant?	Summary
control :GFP vs. control :TFEB	No	ns
control :GFP vs. Acute :GFP	No	ns
control :GFP vs. Acute :TFEB	No	ns
control :GFP vs. Acute +Recovery:GFP	No	ns
control :GFP vs. Acute +Recovery:TFEB	No	ns
control :TFEB vs. Acute :GFP	No	ns
control :TFEB vs. Acute :TFEB	No	ns
control :TFEB vs. Acute +Recovery:GFP	No	ns
control :TFEB vs. Acute +Recovery:TFEB	No	ns
Acute :GFP vs. Acute :TFEB	No	ns
Acute :GFP vs. Acute +Recovery:GFP	No	ns
Acute :GFP vs. Acute +Recovery:TFEB	No	ns
Acute :TFEB vs. Acute +Recovery:GFP	No	ns
Acute :TFEB vs. Acute +Recovery:TFEB	No	ns
Acute +Recovery:GFP vs. Acute +Recovery:TFEB	No	ns

Table 7I.i Individual values and Statistical analysis for TFAM mRNA normalized to 2 house-keeping genes.

N	GFP			TFEB		
	Control	Acute	Acute+ Recovery	Control	Acute	Acute+ Recovery
1	13.40949	20.74752	26.38791	20.0545	9.934547	14.27524
2	10.1679	7.27935	11.26818	10.8374	9.46316	16.50878
3	10.27735	12.0427	8.06171	6.06398	11.24283	3.97576
4	27.45993	21.47282	21.50016	28.43396	47.59775	27.42714
5	3.32084	3.89213	2.61161	8.32227	5.38123	2.27817
6	7.28573	3.13856	24.61038	7.98224	9.58838	26.35582
7	4.22671	6.54478	6.01759	14.05121	4.11123	4.39605
8	23.14417	28.9434	14.4419	20.59801	18.82661	28.20892
9	18.82062	15.64407	10.89742	24.22522	54.63768	19.5544
Average	**13.12363778**	**13.30059222**	**13.97742889**	**15.61875444**	**18.97593522**	**15.88669778**
Std. Dev	**7.920765493**	**8.483291246**	**7.945998266**	**7.534637542**	**17.69159497**	**9.832795255**
Std. Error	**2.186452455**	**2.326102714**	**2.125371341**	**1.906510347**	**4.061303016**	**2.466949045**

Two-way ANOVA			
Source of Variation	P value	P value summary	Significant?
Interaction	0.8625	ns	No
Stimulation	0.8891	ns	No
Overexpression	0.2742	ns	No

Table 7J.i Individual values and Statistical analysis for COXI mRNA normalized to 2 house-keeping genes.

N	GFP			TFEB		
	Control	Acute	Acute+ Recovery	Control	Acute	Acute+ Recovery
1	0.00661	0.00316	0.00538	0.0062	0.00422	0.00549
2	0.00473	0.00619	0.00351	0.00521	0.00439	0.00633
3	0.004	0.00311	0.01522	0.00935	0.00706	0.0053
4	0.00363	0.00595	0.0061	0.01048	0.00554	0.00429
5	0.0065	0.00723	0.00494	0.00833	0.00797	0.01057
6	0.00343	0.00402	0.00401	0.00486	0.01456	0.00286
Average	**0.004816667**	**0.004943333**	**0.006526667**	**0.007405**	**0.00729**	**0.005806667**
Std. Dev	**0.001294548**	**0.001591139**	**0.00397958**	**0.002115079**	**0.003518181**	**0.002391071**
Std. Error	**0.018652841**	**0.022630705**	**0.049259671**	**0.024578989**	**0.041205431**	**0.031378277**

Two-way ANOVA			
Source of Variation	P value	P value summary	Significant?
Interaction	0.3160	ns	No
Stimulation	0.9987	ns	No
Overexpression	0.1592	ns	No

Table 8A Individual values and Statistical analysis mitochondrially localized LC3-II

N	Control	Acute	Acute +Recovery
1	0.693973	1.604757	1.474145
2	1.205252	0.662646	1.050846
3	0.913662	1.450247	1.303137
4	0.054958	0.681033	1.72535
5	0.455277	0.410845	0.947366
6	0.247681	1.287544	1.474081
7	0.807477	1.018719	0.362031
8	0.526879	0.514323	1.802923
Average	**0.613145**	**0.953764**	**1.267485**
Std. Dev	**0.346897**	**0.423219**	**0.44049**
Std. Error	**0.443016**	**0.433356**	**0.391259**

One-way ANOVA summary	
F	4.558
P value	0.0227
P value summary	*
Are differences among means statistically significant? (P < 0.05)	Yes

Tukey's multiple comparisons test	Mean Diff.	95% CI of diff.	Significant?	Summary
Control vs. Acute	-0.3406	-0.8871 to 0.2058	No	ns
Control vs. Acute+ Recovery	-0.6543	-1.201 to -0.1079	Yes	*
Acute vs. Acute+ Recovery	-0.3137	-0.8602 to 0.2327	No	ns

Table 8B Individual values and Statistical analysis of mitochondrially localized parkin protein western quantification

N	Control	Acute	Acute +Recovery
1	0.086618	0.288794	0.325482
2	0.324255	0.238848	0.380359
3	0.687951	0.486451	0.265719
4	0.238972	0.820984	0.574694
5	0.741185	0.413806	0.415388
6	0.307565	0.31673	0.110678
Average	0.397758	0.427602	0.345387
Std. Dev	0.237246	0.193903	0.141737
Std. Error	0.376174	0.296528	0.241174

One-way ANOVA summary	
F	0.2280
P value	0.7989
P value summary	ns
Are differences among means statistically significant? (P < 0.05)	No

Table 8C Individual values and Statistical analysis of mitochondrially localized p62 western quantification

N	Control	Acute	Acute +Recovery
1	0.620442	2.071336	1.843363
2	1.221621	0.467775	1.092925
3	0.783616	1.051727	1.039273
4	0.797234	3.06757	2.019679
5	1.843486	1.953277	1.224917
6	1.255279	1.792917	4.110478
7	1.504935	1.70728	1.199217
8	1.342031	1.132347	2.035166
Average	**1.171081**	**1.655529**	**1.820627**
Std. Dev	**0.386579**	**0.735359**	**0.949386**
Std. Error	**0.357228**	**0.571519**	**0.70361**

One-way ANOVA summary	
F	1.504
P value	0.2452
P value summary	ns
Are differences among means statistically significant? (P < 0.05)	No

Table 10A. Individual values and Statistical analysis COXI protein

N	Control	CCA
1	0.056865	0.154491
2	0.058413	0.160894
3	0.089102	0.129041
4	0.055382	0.182876
Average	**0.0649405**	**0.1568255**
Std. Dev	**0.016155133**	**0.022155583**
Std. Error	**0.063394667**	**0.055946747**

Unpaired t test	
P value	0.0005
P value summary	***
Significantly different? (P < 0.05)	Yes
One- or two-tailed P value?	Two-tailed
t, df	t=6.702 df=6

Table 10B. Individual values and Statistical analysis COXIV protein

N	Control	CCA
1	0.091465	0.255763
2	0.116663	0.575949
3	0.20215	0.281975
4	0.179249	0.301646
5	0.364593	0.441338
6	0.116858	0.634604
7	0.236096	0.214426
8	0.248062	0.198714
9	0.265848	0.376002
10	0.516502	0.23168
11	0.183582	0.642975
Average	**0.229188**	**0.377733818**
Std. Dev	**0.123362939**	**0.170164088**
Std. Error	**0.25768478**	**0.276869411**

Unpaired t test	
P value	0.0295
P value summary	*
Significantly different? (P < 0.05)	Yes
One- or two-tailed P value?	Two-tailed
t, df	t=2.344 df=20

Table 11A. Individual values and Statistical analysis for TFEB 1600 CCA luciferase activity

N	Control	CCA
1	0.294824	1.008306
2	2.623907	2.146718
3	4.374097	3.34662
4	3.129966	4.446995
5	2.915718	4.086627
Average	**2.667702**	**3.007053**
Std. Dev	**1.212398**	**1.161133**
Std. Error	**0.742295**	**0.669594**

Unpaired t test	
P value	0.7217
P value summary	ns
Significantly different? (P < 0.05)	No
One- or two-tailed P value?	Two-tailed
t, df	t=0.3691 df=8

Table 11B. Individual values and Statistical analysis for TFEB 1600 CCA luciferase activity

N	Control	CCA
1	8.190119	3.141117
2	5.577174	3.90545
3	4.116815	11.53044
4	4.715042	2.957354
5	4.084034	8.448678
6	4.251262	4.439026
Average	**5.155741**	**5.737010833**
Std. Dev	**1.45059049**	**3.173365641**
Std. Error	**0.63885056**	**1.324882245**

Unpaired t test	
P value	0.7173
P value summary	ns
Significantly different? (P < 0.05)	No
One- or two-tailed P value?	Two-tailed
t, df	t=0.3725 df=10

Table 12A. Individual values and Statistical analysis TFE3 protein following CCA

N	Control	CCA
1	0.952324	1.672928
2	0.469158	0.604159
3	0.421579	1.569987
4	0.44039	1.04987
5	0.983758	0.762327
6	0.44515	0.522196
7	0.9042	0.892735
8	1.243896	0.819786
9	1.067329	1.414164
10	0.918967	0.870842
Average	**0.7846751**	**1.0178994**
Std. Dev	**0.292581113**	**0.380876895**
Std. Error	**0.330294507**	**0.37751325**

Unpaired t test	
P value	0.1624
P value summary	ns
Significantly different? (P < 0.05)	No
One- or two-tailed P value?	Two-tailed
t, df	t=1w457 df=18

Table 12B. Individual values and Statistical analysis LAMP2 protein following CCA

N	Control	CCA
1	0.130089	0.082427
2	0.220888	0.119624
3	0.242375	0.137011
4	0.234966	0.146607
5	0.171294	0.078014
6	0.16518	0.079688
7	0.204802	0.117669
8	0.172468	0.135714
Average	**0.19275775**	**0.11209425**
Std. Dev	**0.036640234**	**0.026337749**
Std. Error	**0.08345499**	**0.078665985**

Unpaired t test	
P value	0.0003
P value summary	***
Significantly different? (P < 0.05)	Yes
One- or two-tailed P value?	Two-tailed
t, df	t=4.730 df=14

Table 12C. Individual values and Statistical analysis Cathepsin D protein following CCA

N	Control	CCA
1	1.337699	1.576306
2	0.884884	1.814647
3	0.711641	0.753558
4	0.660919	2.142446
5	0.857317	0.65289
6	0.482329	1.116006
7	0.669598	1.716608
8	0.434762	0.776689
9	0.607611	0.667147
10	0.430875	0.489096
Average	**0.7077635**	**1.1705393**
Std. Dev	**0.258122258**	**0.560357914**
Std. Error	**0.306818381**	**0.517931721**

Unpaired t test	
P value	0.0372
P value summary	*
Significantly different? (P < 0.05)	Yes
One- or two-tailed P value?	Two-tailed
t, df	t=2.250 df=18

Table 12D. Individual values and Statistical analysis TFEB protein following CCA

N	Control	CCA
1	8.21495	7.217974
2	5.74466	4.970937
3	3.103243	4.120976
4	5.654345	0.478674
5	2.863863	1.42975
6	5.41607	6.06683
7	2.084202	3.696795
Average	**4.725904714**	**3.997419429**
Std. Dev	**1.986686129**	**2.225896458**
Std. Error	**0.913874963**	**1.113307408**

Unpaired t test	
P value	0.5609
P value summary	ns
Significantly different? (P < 0.05)	No
One- or two-tailed P value?	Two-tailed
t, df	t=0.5981 df=12

Table 12E. Individual values and Statistical analysis p62 protein following CCA

N	Control	CCA
1	0.623701	0.938962
2	0.487353	1.372978
3	0.696203	0.81526
4	0.90806	0.706373
5	0.661342	1.969013
6	0.547491	0.271092
7	0.504697	0.679594
8	0.740899	0.923717
9	0.817431	0.757569
10	0.868857	0.819758
11	0.951268	1.157317
12	1.025526	1.212533
Average	**0.736069**	**0.968681**
Std. Dev	**0.171927**	**0.407366**
Std. Error	**0.200394**	**0.413899**

Unpaired t test	
P value	0.0950
P value summary	ns
Significantly different? (P < 0.05)	No
One- or two-tailed P value?	Two-tailed
t, df	t=1.745 df=22

APPENDIX B

SUPPLEMENTAL DATA

Table S1A. Individual values and Statistical analysis for 4 hour starvation nuclear and cytosolic western protein

A.U.	Control		Acute	
n	Nuclear	Cytosolic	Nuclear	Cytosolic
1	2.373583	0.052872	0.064638	0.013266
2	0.003209	0.776923	0.021371	0.5319
3	0.514495	3.217424	2.312765	1.15151
Average	**0.963762**	**1.349073**	**0.799591**	**0.565558**
Std. Dev	**0.882057**	**1.172415**	**0.926752**	**0.402957**
Std. Error	**0.898487**	**1.009401**	**1.036405**	**0.535822**

%	Control		Acute	
n	Nuclear	Cytosolic	Nuclear	Cytosolic
1	97.82101	2.178993	82.97119	17.02881
2	0.411361	99.58864	3.862642	96.13736
3	13.78633	86.21367	66.76044	33.23956
Average	**37.33957**	**62.66043**	**51.19809**	**48.80191**
Std. Dev	**37.33782**	**37.33782**	**29.5481**	**29.5481**
Std. Error	**6.110326**	**4.716852**	**4.12955**	**4.229715**

Summary of Two- way ANOVA			
Source of Variation	P value	P value summary	Significant?
Interaction	0.6278	ns	No
Stimulation	> 0.9999	ns	No
Fractionation	0.6877	ns	No

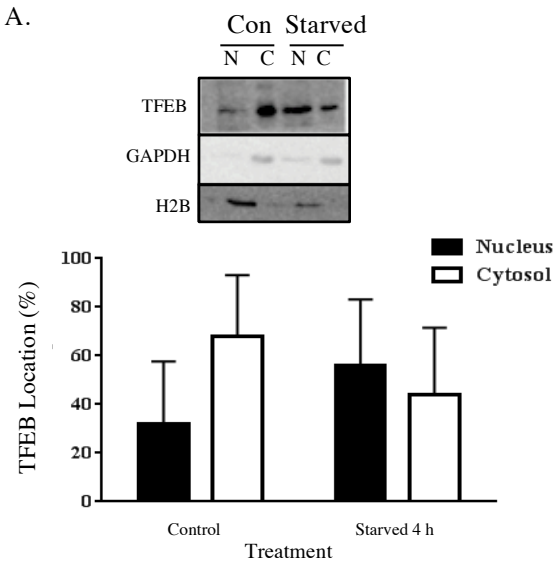

Figure S1: Graphical representations of nuclear and cytosolic cellular fractions of starved C2C12 cells demonstrated the trend of TFEB translocation from the cytosol to the nucleus following A, 4 hours of serum starvation with HBSS (n=3; X ± SEM) and the corresponding. Western blots that represent the translocation of TFEB. GAPDH and H2B were used as cytosolic and nuclear loading controls respectively.

APPENDIX C

LABORATORY METHODS AND PROTOCOLS

CELL CULTURE

Cells

C2C12 murine skeletal muscle cells (ATCC, CRL-1772)

Materials

1. Dulbecco's Modified Eagle's Medium (DMEM; Sigma D-5796/500ml)
2. Fetal Bovine Serum (FBS; Fisher Scientifitc SH3039603C/500ml)
    a. Aliquoted into 50ml sterile conical tubes and stored at -20°C
3. Penicillin/Streptomycin (P/S; Invitrogen 15140-122/100ml)
    a. Sterile aliquots of 6mls and stored at -20°C)
4. Horse Serum (HS; Invitrogen 16050-114/1000ml)
    a. Aliquoted into 50ml sterile conical tubes and stored at -20°C
    b. Heat-inactivated for 30 minutes at 56.0°C
5. 0.25% Trypsin-EDTA (1x), phenol red (Invitrogen 25200-072/500ml)
    a. Sterile aliquots of 30mls stored at -20°C
6. Dulbecco's Phosphate Buffered Saline (PBS; Sigma D-8537/500ml)
7. 15ml conical tubes, sterile (BD Falcon 352097)
8. 50ml conical tubes, sterile (BD Falcon 352098)
9. 175cm^2 canted/vented tissue cultured flasks (BD Falcon 353112)
10. 6-well sterile tissue culture dish (Sarstedt 83.1839.300)
11. Gelatin (Sigma G1890)
    a. 0.1% solution autoclaved for sterilization

Procedure

1. Allow myoblasts to proliferate in 175cm2 flask with growth medium (GM; DMEM supplemented with 10% FBS and 1% P/S) until 70% confluent.
2. Prepare six 6-well dishes for plating by coating the bottom surface with 0.1% gelatin and allow to fully dry in laminar flow hood.
3. Pre-heat GM, trypsin and PBS in 37°C water bath for 30 minutes prior to use.
4. Discard old GM from tissue culture flask and wash with 10mls of PBS to rinse off remaining GM.
5. Apply 5mls of trypsin in the flask and place in the incubator at 37°C for 3 minutes.
6. Remove flask from incubator and gently knock sides of the flask to ensure cells are lifted from flask bottom. Remove trypsin with cells and place into a sterile 15ml conical tube.
7. Rinse flask with 5mls GM and add to sterile 15ml conical tube containing the cells.
8. Spin tube for 3 minutes at 1400rpm at room temperature.

9. Discard the supernatant and add 1ml of GM for resuspension with 1ml pipette.
10. Add 3mls of GM to resuspended cell mixture for a total volume of 4mls.
11. Fill each well of tissue culture dishes with 2mls of GM and add 100μl of cell mixture to each well.
12. Rotate plate in a circular motion for 30secs and subsequently place into 37°C incubator overnight.
13. The following day remove GM from cells and replace with differentiation medium (DM; DMEM supplemented with 5% heat-inactivated HS and 1% P/S) once myoblasts are 90-95% confluent.
14. Refresh DM every other day. Mature myotubes will form after five days and be ready for contractile activity.

CYCLOSPORIN A TREATMENT OF C2C12 MYOTUBES

C2C12 skeletal muscle cells were proliferated on 6-well plates. Cells were allowed to reach 80% confluence and GM was switched to DM. DM was supplemented daily for 4d to achieve differentiated myotubes. Cyclosporin A (CsA) (Sigma-C3662) was dissolved in (DMSO) to achieve a stock 1mM solution.

On day four of differentiation, media was switched to 10nM CsA or DMSO 30 minutes pre stimulation. Cells were exposed to CsA +control, CsA + Stimulation, Vehicle + control, Vehicle + Stimulation. Immediately following stimulation whole cell extracts were collected for nuclear and cytosolic fractionation and western blotting.

ELECTRICAL STIMULATION OF MYOTUBES IN CULTURE

Cells

1. C2C12 murine skeletal muscle cells, differentiated into mature myotubes

Materials

1. Electrical Stimulator
   Gange bipolar output (+/- amplitude adjustable using one knob)

   Output voltage range = 0 to +/- 30V

   Maximum output current = 1A

   Adjustable output pulse duration from 0.001 to 0.1secs (10-1kHz)

   Adjustable output pulse repetition from 0.0005 to 0.01secs (100-2kHz)

   Adjustable polarity duration range from 1 to 100secs (0.01 to 1Hz)

   Polarity duration range = time duration for the output "pulse burst" to be positive before switching to a similar negative (amplitude) pulse burst. Positive and negative duration are of equal value except for the amplitude.

2. 6-well sterile plastic culture dishes (Sarstedt 83.1839.300 OR Biobasic SP41117) with lids modified for implantation of platinum electrode wires (see image below). Bottom of plates should be coated with sterile 0.1% gelatin.

Procedure

1. Before each bout of stimulation, electrodes are cleaned with 70% ethanol and placed in the laminar flow hood for 30mins under UV light for sterilization.
2. DM is refreshed 30mins prior to stimulation protocol.
3. Differentiated myotubes are stimulated in a parallel circuit (four 6-well dishes at once) at 5Hz, 9V for 3 hours in 2mls of DM.
4. Once the 3 hours is complete, DM should be refreshed once again.
5. The cells are allowed to rest for 21 hours until the next bout of stimulation. The total protocol lasts for 4 days and 21 hours and cells are harvested following the last 21 hour rest period.

A) Electrical Stimulator

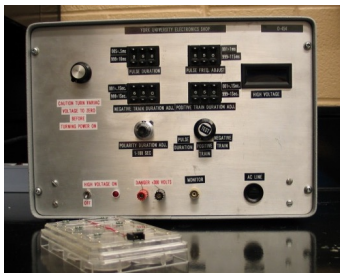

B) Modified six-well plate lid

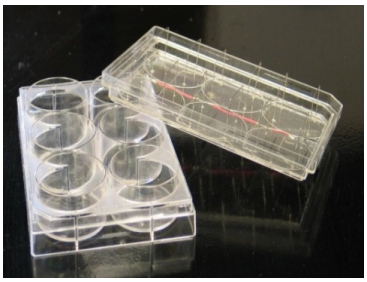

Voltage

Voltage is constant and accurate in the 6-well plates. When set at 9v the true output is 8.5v.

There is a positive train and negative train consisting of 5 repetitions each at a frequency of 5Hz.

Current

The current across a 6-well plate with 3mls and 2mls of media is 37mA and 20mA respectively.

When 6 plates (3mls) are attached to the stimulator the current is 130mA.

When 5 plates (3mls) are attached to the stimulator the current is 105mA.

When there is more contact between the wires and the media there is more current, therefore if the wires are pushed down it makes a considerable difference than if they are up or just touching the media.

Resistance

The resistance across a 6-well plate with 3mls and 2mls of media is 12 KΩ and 350KΩ respectively (direction of measurement makes no difference, see below).

The resistance in a 10cm plate with 15mls seems to be more confusing in one direction it is 1.6MΩ and the other direction it is 700KΩ. Both of these are not constant and seem to change with time in an opposite manner… Jim says it seems to act as a semiconductor … needs to be measured again.

WESTERN BLOT PROCEDURE

Part A: Protein Extraction

Reagents

1. 5X Passive Lysis Buffer diluted in ddH20 to 1X (Promega E194A)
2. Phosphate Buffered Saline (PBS; Sigma D-8537)
3. Protease Inhibtors (Complete, Roche, 1169749801; Roche diagnostics, Basel, Switzerland)
4. Phosphatase Inhibitors (Cocktails 2 and 3 Sigma, P5726 and P0044)

Procedure

1. Prepare fresh lysis buffer with protease and phosphatase inhibitors.
2. Remove media and wash cells 3X with 2mls of ice-cold PBS. Aspirate last wash.
3. Add 150μl of freshly prepared lysis buffer containing protease and phosphatase inhibitors into wells. Scrape the wells with a rubber cell scraper and place cell lysate into an eppendorf. Place eppendorf on ice. If required, combine multiple wells with a total of 150μl to increase final protein concentration.
4. Vortex sample briefly and place in liquid nitrogen. Thaw sample in water bath set to 37°C for 2 minutes. Repeat step four 2X for a total of 3 freeze-thaw cycles.
5. Spin the samples at 4°C for 5 minutes at 16.1rcf.
6. Collect the supernatant and place into a newly labeled eppendorf tube.
7. Measure the total protein concentration using the Bradford Assay.
8. Store samples at -80°C.
9. Remove the supernate and add it to a new-labelled eppendorf tube.
10. Freeze samples at -80ºC for protein quantification using the Bradford assay.

Part B: SDS Polyacrylamide Gel Electrophoresis (SDS-PAGE) – Bio-Rad Mini Protein System

Reagents:

- Acrylamide/Bis-Acrylamide, 30% Solution 37.5:1 (BioShop 10.502)
    - Store at 4°C
- Under Tris Buffer
    - 1M Tris-HCl, pH 8.8 (60.5g/500ml)
    - Store at 4°C
- Over Tris Buffer
    - 1M Tris-HCl, pH 6.8 (12.1g/100ml)
    - Bromophenol Blue (for colour)
    - Store at 4°C

- Ammonium Persulfate (APS)
    - 10% (w/v) APS in ddH_20 (1g/10ml)
    - Store at 4°C
- Sodium Dodecyl Sulfate (SDS)
    - 10% (w/v) in ddH_20 (1g/10ml)
    - Store at room temperature
- TEMED (Sigma T-9281)
- Electrophoresis Buffer, pH 8.3 (10L)
    - 25mM Tris 30.34g, 192mM Glycine 144g, 0.1% SDS 10g
    - Volume to 10L with ddH_20
    - Store at room temperature
- 2 x Lysis Buffer
- *tert*-Amyl alcohol ReagentPlus, 99% (Sigma 152463)

Procedure:

1. Prepare Mini-Protean gel caster system:
    1. Assemble glass plates as shown below:

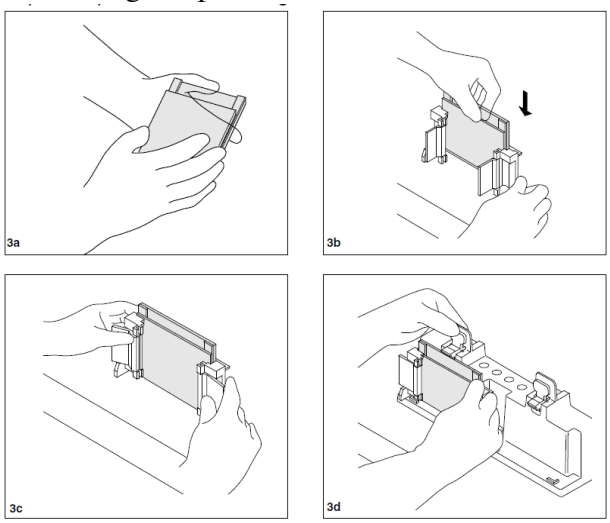

2. Check the seal by adding a small volume of ddH_20 then pour off and let dry.
3. Make a mark 2 cm below the top edge of the short plate. This will indicate how high to fill the separating gel.
4. Prepare separating gels:

Mini Protean 3 Bio-Rad System volumes

Separating Gel	**8 %**	**10 %**	**12 %**	**15 %**	**18 %**
Acrylamide	2.7 ml	3.3 ml	4.0 ml	5.0 ml	6.0 ml
Water	4.1 ml	3.5 ml	2.8 mL	1.8 ml	0.8 ml
Under Tris	3.0 ml	3.0 ml	3.0 ml	3.0 ml	3.0 ml
SDS	100 µl	100 µl	100 µl	100 µl	100 µl
APS	100 µl	100 µl	100 µl	100 µl	100 µl
TEMED	10 µl	10 µl	10 µl	10 µl	10 µl

1. Mix the contents of the separating gel without TEMED.
2. Add TEMED. Briefly stir. Immediately, pour the contents between the short and spacing plates until the volume reaches 2 cm from the top edge of the short plate
3. Coat the top surface of the gel solution with *tert*-Amyl alcohol to remove any bubbles.
4. Allow 10 - 30 minutes for gel polymerization.
5. Remove *tert*-Amyl alcohol by pouring it off and remove any remainder with a scrap piece of Whatman paper.

5. Prepare stacking gel:
    1. For a single mini gel use the following volumes:

Stacking Gel (3% Acrylamide)	**1 Mini Gel**
Acrylamide	250 µL
Water	1.875 mL
Above Tris buffer	312.5 µL
SDS	25 µL
APS	25 µL
TEMED	10 µL

2. Mix the contents of the stacking gel without adding TEMED. Stir.
3. Add TEMED. Stir and pour the stacking gel on top of the polymerized separating gel.
4. Immediately, add the appropriate comb for desired number of wells and thickness of spacer plate.

5. Allow 10 - 30 minutes for gel polymerization.
6. Gels may be used immediately or stored in a wet sealed container at 4ºC.

6. Prepare samples:
    1. Warm block heater to 95ºC.
    2. Pipette the appropriate volume of each sample into a new eppendorf. *This volume is determined by the protein concentration assessed using the Bradford assay and the required amount of protein required for the detection of the desired protein*.
    3. Add an equal amount of 2X Lysis Buffer supplemented with 5% B-Mercaptoethanol. Add 5 µL of Sample Dye to each sample.
    4. Briefly spin each sample to bring volume to the bottom of the eppendorf.
    5. Incubate each sample at 95ºC for 5 minutes in the heating block to denature the proteins.
    6. Briefly spin again to return volume to the bottom of the eppendorf.

7. Assemble Mini-Protean electrophoresis rack:
    1. See images below:

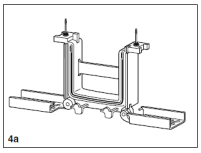

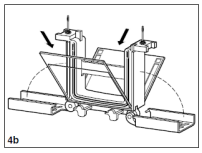

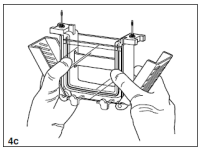

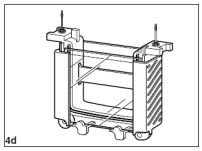

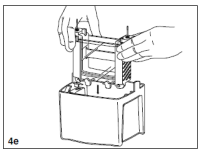

    2. If you are only running one gel a plastic rectangular pseudo plate must be clamped on the other side of the caster.
    3. Fill the middle chamber of the electrophoresis apparatus with Electrophoresis Buffer. Fill the outer chamber with Electrophoresis Buffer, until the level is approximately 2 cm above the bottom of the gels.
    4. Slowly remove the comb using both hands (one on each side) by pulling the comb straight upwards.
    5. Fix any wells that are deformed using a pipette tip.

6. Clean out the wells using a pipette tip and Electrophoresis Buffer.
7. Apply 10 µL of protein ladder to the first well.
8. Withdraw the entire volume of the sample using a gel-loading tip. Inject the solution slowly into the bottom of the well.

8. Gel Electrophoresis:
    1. After all samples are loaded, immediately, place the lid on the gel chamber.
    2. Place the positive and negative leads into the power supply.
    3. Use a power supply to apply a constant voltage of 120V across the gel. for 60 – 120 minutes until sufficient separation has been achieved as indicated by the protein ladder.
    4. Prepare for electrotransfer of proteins from the gel to nitrocellulose membrane.

<u>Part C: Western Blotting and Immunodetection</u>

Reagents:

- Transfer Buffer
    - 0.025M Tris-HCl pH 8.3 12.14g
    - 0.15M Glycine 45.05g
    - 20% Methanol 800ml
    - Make 4L with ddH_20
    - Store at 4°C
- Ponceau S stain
    - 0.1% (w/v) Ponceau S
    - 0.5% (v/v) Acetic Acid
    - Store at room temperature
- Wash Buffer
    - Tris-HCl pH 7.5 12g
    - NaCl 58.5g
    - 0.1% Tween 10ml
    - Store at room temperature
- Blocking Buffer
    - 5% (w/v) skim milk power in Wash Buffer
- Enhanced Chemiluminescence Fluid (ECL; Santa Cruz - SC-2048)
- Film Developer and Fixer

Procedure:

9. Transfer Procedure

1. Using a paper cutter cut 6 pieces of Whatman paper per gel. Each piece should measure 8.5 cm x 6 cm. Wearing gloves cut an 8.5cm x 6 cm piece of nitrocellulose membrane (GE Healthcare RPN303D). Soak Whatman paper and nitrocellulose membrane in Transfer Buffer until use.
2. Remove electrophoresis plates from chamber and separate the plates.
3. Remove stacking gel
4. Assemble Whatman paper, nitrocellulose membrane and gel as shown below, ensuring that the gel and membrane are orientated so that the gel is closer to the black surface and the membrane closer to the white plastic clamp.

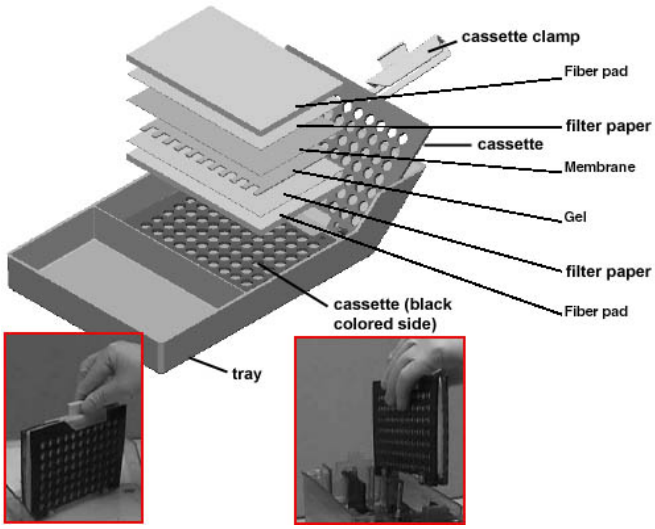

5. Close the cassette and place in the transfer chamber with the black side of the cassette facing the negative electrode (black side) of the chamber.
6. Place an ice pack and magnetic stir bar in the chamber.
7. Place the chamber in a Tupperware container. Place the container on top of a magnetic stir plate. Turn on the stir plate and ensure the magnetic stir bar is spinning.
8. Fill the chamber completely with cold Transfer Buffer. Place lid on the chamber and connect the leads to a power supply.
9. Turn on the power supply and apply a constant voltage of 120V for 1.5 hours. This can vary depending on the size of the protein of interest.
10. Removal of nitrocellulose membrane:
    1. Turn off the power supply and disconnect leads from the power supply.
    2. Remove the cassette from the chamber.
    3. While wearing gloves, carefully dispose of the Whatman paper and gel.
    4. Gently place the nitrocellulose membrane in a plastic dish and apply Ponceau S stain for 5 minutes.

5. Drain off the remaining Ponceau S and save for reuse.
6. Rinse the membrane 3-5x with ddH_2O to reduce the red background. Wrap membrane in saran wrap and scan.
7. Cut the membrane while protein bands are still visible at the desired molecular weight.
8. Rotate membrane at room temperature in Wash Buffer until remaining Ponceau S stain has been removed (~5 minutes).
9. Incubate membrane for 1 hour with rotation in Blocking Buffer at room temperature.

11. Immunodetection
    1. Primary Antibody Incubation
        i. Wrap a flat piece of glass in parafilm. Place the glass in a Pyrex dish. Arrange balls of wet tissue around the dish and cover the entire dish with saran wrap.
        ii. Place the dish in a 4ºC fridge and level.
        iii. Place nitrocellulose membrane strips face up on the flat parafilm surface.
        iv. Dilute the primary antibody raised against the protein of interest in Blocking Buffer. Gently apply ~1-1.5 mL of diluted antibody overtop of the appropriate membrane strip.
        v. Specific antibody dilutions used in this study are listed at the end of this protocol.
    2. Secondary Antibody Incubation
        i. Wash the blots in Wash Buffer with gentle rotation for 5 minutes 3X.
        ii. Incubate the blots as described in step 3.a with the following changes. Incubate the blots for 1 hour with a secondary antibody raised against the species and specific immunoglobulin molecule of the primary antibody. Incubate at room temperature.
    3. Following the incubation, wash the membrane 3X for 5 minutes with Wash Buffer.

12. Enhanced Chemiluminescence Detection

    Note: Complete the following steps in a dark room sufficient for photographic film developing.

    1. Mix ECL fluids "A" and "B" in a 1:1 ratio in a small plastic box.
    2. Place blots facedown in the small plastic box and place on a level surface. Some swirling may be required to ensure equal coverage.
    3. Following 2 minutes, remove blots and place face down on clean Kim wipes to remove excess ECL fluid.
    4. Place membrane strips on clean overhead transparency film and remove any bubbles.

5. Turn off any lights.
6. Place membrane strips face up in a film cassette.
7. Momentarily cover the strips with cardboard while cutting pieces of film to the approximate size of the membrane strips.
8. Remove the film and apply film overtop of the membrane strips. Do not move the film once it has been placed on top of the membrane.
9. Close the cassette and expose the film for the desired time.
10. After the exposure time, remove the film and place the cassette aside.
11. Attach the film to a film hanger and dip 5-6x in film developing solution.
12. Hold the film up to a red light. When bands become apparent, immediately submerge the film in water and then in the film fixing solution for a minimum of 30 seconds.
13. Following 30 seconds in the fixing solution, the film can then be submerged in water and attached to butterfly binder clips to dry. They are no longer light sensitive.

LUCIFERASE ASSAY

Part A: Cell Transfection

1. C2C12 cells are grown to 30% confluent DM was replaced with pre-transfection media (DMEM+ 10% FBS) 6 hours prior to transfection.
2. DNA was allotted into falcon tube 1 containing minimal DMEM, the volume of DNA was dependant on the concentration of DNA and desired final volume.
3. Lipofectamine 2000 (Life Technologies 11668019) reagent is deposited into a separate falcon tube 1a containing DMEM.
4. Leave both falcon tubes for 5 minutes, following which pour tube 1 into tube 1a gently and let sit for 20 minutes.
5. Following the incubation, change media on 6 well plates to minimal DMEM and pipette 500µl of DNA mix into each well.
6. Incubate at 37°C for 6 hours.
7. Following incubation remove media, wash twice with GM and change to desired media.

Part B: Cell treatment

1. Transfected cells were differentiated for 4 days (as explained previously)
2. On day 4 of differentiation myotubes were stimulated acutely or chronically.
3. Following stimulation cells were scraped with PBS and lysed as explained above.

Part C: Luciferase measurment

1. Thaw out the luciferase assay's substrate on ice or in the fridge (keep the reaction substrate on ice at all time)
2. Turn on the luminometer at least 1 hour prior of the measurement
3. Prepare the luminometer as follow:
    a. Wash the inlet:

        To wash inlet 1 (front inlet)

        Choose "others" → "oper. function" → "reagent" → "others" → "wash" → "Inj1" → check the # of wash is 5 → insert "luminometer tube into the chamber → "enter" → "repeat wash" → "exit"

        To wash inlet 2 (back inlet)

        Repeat the same step as before but choose "Inj2"

        (make sure there is enough water in the bottle)

    b. Manual unload:

        To unload inlet 1

Choose “others” → “oper. function” → “reagent” → “others” → “manual unload” → “Inj1” → repeat pressing “Inj1” 3 – 5 times

To wash inlet 2

Repeat the same step as before but choose “Inj2”

(make sure you see bubbles coming out from the inlet)

c. Prime the inlet:
Prior to priming the inlets, take the inlet out from the “water” bottle and wipe them dry with Kim Wipe. Then, put the inlet into the FFL and rLUC substrates respectively. (put the front inlet into the FFL substrate & the back inlet into the rLuc substrate)

To prime inlet 1

Choose “others” → “oper. function” → “reagent” → “prime” → “Inj1” → insert “luminometer tube into the chamber → “enter”

To prime inlet 2

Repeat the same step as before but choose “Inj2”

4. Put enough “luminometer” tube (Sarstet No 55.475) on the tube rack
5. Select protocol # 6 from the menu and follow the instructions for measurement
6. Transfer 20µl of the lysate to the bottom of the “luminometer” tube right before you are ready to measure and do a duplicate measurement for each sample

RNA EXTRACTION FROM CELLS

Reagents:

- TRIZol® Reagent
- 24:1 Chloroform:Isoamylalcohol
    - 24 parts Chlorofom
    - 1 part Isoamylalcohol
- 100% Isopropanol
- 75% Ethanol
- DEPC ddH_2O

Procedure:

1.Cell Culture:

1. Grow cells in 6 well plate
2. Pour off the medium. Wash each plate with 5 ml of ice-cold Phosphate Buffered Saline (PBS), remove all of the PBS.
3. Add 400 ul of PBS to plate and gently scrape with a rubber policeman.
4. Transfer to Eppendorf.
5. Spin the cells at 1400 RPM for 3 minutes. Remove all supernate. Resuspend in 2 mLs DPBS.
6. Spin the cells at for 3 min at 1400 RPM in a microcentrifuge. Discard the supernate with a Pasteur pipette.
7. Flash freeze and store at -80 until ready to continue

2.RNA Isolation

1. Add 1ml TRIZOL. Vortex thoroughly until pellet is completely disrupted.
2. Add 200 µL of 24:1 chloroform:isoamlyalcohol.
3. Shake vigorously for 15 seconds and leave @ room temperature for 5 minutes.
4. Spin at 14000 g for 15 minutes at 4ºC.
5. Transfer the upper phase carefully to a new eppendorf tube. Add 500 µL of 100% isopropanol and briefly shake.
6. Incubate at room temperature for 30 minutes.
7. Spin at 14000 g for 10 minutes at 4ºC.
8. Remove supernatant. Add 500 µL of 75% EtOH and wash the RNA pellet with gentle pipetting.
9. Spin at 14000 g for 1 minute at 4ºC.
10. Carefully, remove supernatant and air dry the RNA pellet.
11. Resuspend the pellet in 50 µL of DEPC ddH_2O.
12. Heat RNA samples at 65ºC for 10 minutes.

3.Quantify RNA

1. Use a spectrophotometer to measure the absorbance at 260 nm.

2. Freeze and store at -80ºC.

Part C: Reverse Transcriptase

Reagents:

- Oligo(dt) 20
- 10 mM dNTP
    - asd
- DEPC ddH_2O
- Master Mix (per sample)
    - 8 µL of 5x Buffer
    - 2 µL of 0.1 M Dithiothreitol (DTT)
    - 2 µL of RNAse Out
- Superscript III

Procedure:

1. Combine 2 µL of Oligo(dt) 20, 2 µL of 10 mM dNTP, and 4 µg of Sample RNA in a sterile 0.5 mL sterile eppendorf. Bring the volume to 26 µL with DEPC ddH_2O.
2. Heat the eppendorf at 65ºC for 5 minutes, followed by 1 minute at 4ºC in a thermocycler.
3. Make the Master Mix.
4. After the eppendorfs have been heated, add 12 µL of the Master Mix and 2 µL of Supercript III RT.
5. Incubate the eppendorf for 50 minutes at 55ºC, followed by 15 minutes at 70ºC.
6. Store samples at -20ºC.

Part D: Quantitative Polymerase Chain Reaction (qPCR) Procedure

Reagents:

- Sterile Water (MultiCell)
- Master Mix (per sample and per gene of interest)
    - Table 2 (COX IV, COXI, TFAM, LAMP2, LC3, β-Actin, Beclin1, p62)
        - 12.5 µL of PerfeCTa® SYBR® Green SuperMix with ROX™
        - 1.25 µL of 20 µM Forward Primer
        - 1.25 µL of 20 µM Reverse Primer
        - 8 µL of Sterile water
    - Table 3 (TFEB, PGC-1α, Cathepsin D, GAPDH)
        - 12.5 µL of PerfeCTa® SYBR® Green SuperMix with ROX™

- 0.625 µL of 20 µM Forward Primer
- 0.625 µL of 20 µM Reverse Primer
- 9.25 µL of Sterile water

Procedure:

1. Biochemical Assay
    1. Autoclave qPCR microtube strips and pipette tips. Sterilize pipettes with EtOH for use.
    2. Dilute gDNA or cDNA Samples appropriately with Sterile water (MultiCell) for the gene of interest:
        i. cDNA for all assessments are diluted 1:40 to obtain a 2.5 ng/µL stock.
    3. Create appropriate Master Mixes as determined during optimization. Always use a housekeeping gene to correct for difference in total cDNA amount.
    4. Add 2 µL of each diluted cDNA sample in triplicate to microtube strips.
    5. Add 23 µL of Master Mix to all wells.
    6. Close wells and place in Applied Biosystems StepOne Plus qPCR machine.
    7. Set the StepOne Plus application for a reaction volume of 25 µL, SYBR® Green Technology, Normal (~2.5 hour) Reaction Speed, and Include a Melt Curve Analysis.
2. ΔΔCt Analysis
    1. After the run is complete. Confirm that the automatically determined thresholds are in the exponential amplification phase for each gene of interest. Export all data to an Excel spread sheet.
    2. Obtain the cycle number where the sample's amplification plot crosses the defined threshold (i.e. the Ct value).
    3. Average the two closest Ct values.
    4. To determine the ΔCt take the difference between the Ct value of the gene of interest and the Ct value of your housekeeping gene. Raise this to the power of two (i.e. $2^{\Delta Ct}$) and use this to compare differences in gene expression.
    5. To determine find the fold change in the gene expression from your control samples take the ΔCt of each sample and subtract the ΔCt of the control sample. Use these values (ΔΔCt) to generate a graph of gene expression relative to your control condition

NUCLEAR AND CYTOSOLIC FRACTIONATION FROM CELLS

Reagents

1. NE-PER® Nuclear and Cytoplasmic Extraction Kit (Fisher Scientific PI78833)
    a. Contains three buffers CER I, CER II and NER
2. PBS (Sigma D-8537)
3. Protease Inhibtors (Complete, Roche, 1169749801; Roche diagnostics, Basel, Switzerland)
4. Phosphatase Inhibitors (Cocktails 2 and 3 Sigma, P5726 and P0044)

Method:

Cell Culture Preparation

1. Scrape cells with rubber policeman in ice-cold PBS and combine multiple wells. Place into a labelled eppendorf.
2. Pellet by centrifugation at 500 x g for 2-3 minutes.
3. Use a pipette to carefully remove and discard the supernatant, leaving the cell pellet as dry as possible.
4. Add ice-cold CER I to the cell pellet (table 1).

Table 1. Reagent volumes for different packed cell volumes.

Packed Cell Volume (µl)	CER I (µl)	CER II (µl)	NER (µl)
10	100	5.5	50
20	200	11	100
50	500	27.5	250
100	1,000	55	500

Cytoplasmic and Nuclear Protein Extraction

Note: Scale this protocol depending on the cell pellet volume (Table 1). Maintain the volume ratio of CER I: CER II: NER reagents at 200:11:100 µl, respectively.

1. Vortex the tube vigorously on the highest setting for 15 seconds to fully suspend the cell pellet. Incubate the tube on ice for 10 minutes.
2. Add ice-cold CER II to the tube.
3. Vortex the tube for 5 seconds on the highest setting. Incubate tube on ice for 1 minute.

4. Vortex the tube for 5 seconds on the highest setting. Centrifuge the tube for 10 minutes at maximum speed in a microcentrifuge (~16,000 x g).
5. Immediately transfer the supernatant (cytoplasmic extract) to a clean pre-chilled pre-labelled eppendorf tube. Place this tube on ice until use or storage.
6. Wash remaining pellet (DO NOT RESUSPEND) with PBS 3X and remove PBS with a pipette after brief centrifugation to sediment the pellet.
7. Suspend the insoluble (pellet) fraction produced in Step 4, which contains nuclei, in ice-cold NER.
8. Vortex on the highest setting for 15 seconds. Place the sample on ice and continue vortexing for 15 seconds every 10 minutes, for a total of 40 minutes.
9. Centrifuge the tube at maximum speed (~16,000 x g) in a microcentrifuge for 10 minutes.
10. Immediately transfer the supernatant (nuclear extract) fraction to a clean pre-chilled tube. Place on ice.
11. Store extracts at -80ºC until use.

MITOCHONDRIAL ISOLATION FROM C2C12 MYOTUBES

Adapated from: Frezza C, Cipolat S, Scorrano L. Nature Protocols 2007;2(2):287-95.

Materials

1. Cold PBS (Sigma D-8537)
2. Cell Scraper
3. Mitochondrial Isolation tubes
4. Teflon Pestle
5. Glass Potter

Mitchondrial Isolation Buffer (MIB)

1. 10ml of 0.1M Tris-MOPS
    a. Dissolve 6.05g of Tris in 250ml of ddH_20 pH to 7.4 using MOPS powder.
    b. Volume up to 500ml.
    c. Store at 4ºC.
2. 1ml of 0.1M EGTA/Tris
    a. Dissolve 19.05g of EGTA in 250ml of ddH_20 pH to 7.4 using Tris powder/HCl.
    b. Volume up to 500ml.
    c. Store at 4ºC.
3. 20ml of 1M sucrose
    a. Dissolve 171.65g of sucrose in 500ml of ddH_20. Stir until fully dissolved.
    b. Aliquot into 20ml volumes in sterile conical tubes.
    c. Store at -20ºC.
4. Volume up to 100ml with ddH_20.
5. pH to 7.4.
6. Store at 4ºC.

Method

1. Wash cells with cold PBS.
2. Add 200μl of PBS per well and scrape cells. Combine multiple wells (at least six from 6-well plates) and place in mitochondrial isolation tubes.
3. Centrifuge the cells at 600g for 10 minutes at 4ºC.
4. Pre-cool Teflon pestle and glass potter on ice.
5. Discard the supernate and resuspend the cells in 3mls of ice-cold MIB.
6. Transfer cell solution to glass potter.

7. Homogenize the cells using Teflon pestle at 1600rpm for 30 strokes in the glass potter. DO NOT USE A GLASS PESTLE, IT WILL DESTROY THE MITOCHONDRIA!
8. Transfer the homogenate from the glass potter to mitochondrial isolation tube.
9. Centrifuge at 600g for 10 minutes at 4ºC.
10. Collect the supernate (contains mitochondria and cytosol) and place into a second clean pre-chilled mitochondrial isolation tube.
11. Centrifuge the supernate at 7000g for 10 minutes at 4ºC.
12. Discard the supernate and the resultant pellet is the mitochondria.
13. Gently wash and resuspend the pellet with 200μl of MIB.
14. Transfer mitochondrial solution to a 1.5ml eppendorf.
15. Spin in a microcentrifuge at 7000g for 10 minutes at 4ºC.
16. Discard the supernate and resuspend the mitochondrial pellet with 50-100μl of MIB depending on mitochondrial yield.

ADENOVIRAL INFECTION OF C2C12 CELLS

Primary Viral Stock

1. Linearize 12.5µg of pAdEasy-Tfeb plasmid with PacI endonuclease, purify with a Qiagen column, and store @ -20^{o}C
2. Add 700µl of Solution III (MBS) to 10ml of the viral-growth media (GM), and warm it up @ 37^{o}C water bath
3. Add 10µl of stock chloroquine (25mM) to 10ml of the viral-GM, & store it @ 4^{o}C until 30 minutes before use
4. Aspirate viral growth media from the 175mm^2 flasks of AD293 cells, replace it with 10ml MBS-viral-GM, & put it back @ 37^{o}C incubator
5. After 20 minutes, add 200µl of ddH_2O to the pAdEasy-Tfeb
6. Add 62.5µl of Solution I follow by 625µl of Solution II to DNA, tap to mix & incubate @ room temp for 10 minutes
7. Gently add DNA mix to cells & incubate @ 37^{o}C for 3 hours
8. Remove MBS-viral-GM + DNA mix with 10ml pipette and discard in bleach
9. Replace media with 10ml chloroquine supplemented viral-GM & incubate @ 37^{o}C for 6 hours
10. Remove chloroquine supplemented viral-GM with 10ml pipette and discard in bleach
11. Replace media with 10ml viral-GM & incubate @ 37^{o}C for 7 – 10 days
12. Replenish media when needed until signs of cytopathogenic effect
13. Cells were trypsinized, collected in a 15ml Falcon tube, and washed once with PBS
14. Resuspend cell pellet with 1x volume of PBS and aliquot into screw-cap cryotubes
15. Subject the cell suspension to four rounds of freeze/thaw by alternating the tubes between the liquid nitrogen bath and the 37°C water bath, vortexing briefly after each thaw
16. Collect cellular debris by microcentrifugation at 12,000 × *g* for 10 minutes at room temperature
17. Transfer the supernatant (primary virus stock) to a fresh screw-cap cryotubes. Sotre viral stocks @ -80^{o}C

Secondary (and beyond) Viral Stock

1. Use 5-50µl of 1^{o} viral stock to infect each 175mm^2 flasks AD293 cells
2. Repeat steps 12 to 17 from the "Primary Viral Stock" to harvest the subsequent viruses

Infection of target cells

1. C2C12 skeletal muscle cells were proliferated on 6-well plates. Cells were allowed to reach 80% confluence and GM was switched to DM. DM was supplemented daily for 4d to achieve differentiated myotubes.
2. Thaw pAdEasy-TFEB (Quaternary virus) and p-AdEasy-GFP (Tertiary virus), spin down at 1400rpm for 3 minute
3. In a falcon tube mix 1 ml DM/well and 10 MOI of viral stock/well of pAdEasy-TFEB, in a separate tube mix 1 ml DM/well and 10 MOI of viral stock/well of pAdEasy-GFP
4. Remove media from target cells and apply 1ml of virus mix to each well
5. Incubate at 37°C for 24 hours
6. Following incubation, remove virus into a falcon tube containing bleach. Wash cells twice with DM and replenish 2ml per well
7. Replenish media daily for desired days of infection

APPENDIX D

AUTHOR CONTRIBUTIONS TO LITERATURE

Published Abstracts

1. **D. M. Brownlee**, D.A. Hood. TFEB expression and activation in contracting skeletal muscle myotubes. (2015). *Muscle Health Awareness Day*. May 22, 2015. York University, ON.

Oral Presentations

1. **D. M. Brownlee** and D.A. Hood. TFEB expression in contracting myotubes. (2015). *Biology Graduate Student Seminar Series*. February 10, 2015. York University, ON.